DEVELOPMENT OF A SCREENING MODEL FOR POLYMER FLOODING
IN MULTI-LAYER RESERVOIRS

A THESIS SUBMITTED TO
THE GRADUATE SCHOOL OF NATURAL AND APPLIED SCIENCES
OF
MIDDLE EAST TECHNICAL UNIVERSITY

BY

NEGAR ZAREPAKZAD

IN PARTIAL FULFILLMENT OF THE REQUIREMENTS
FOR
THE DEGREE OF MASTER OF SCIENCE
IN
PETROLEUM AND NATURAL GAS ENGINEERING

JANUARY 2018

Approval of the thesis:

DEVELOPMENT OF A SCREENING MODEL FOR POLYMER FLOODING IN MULTI-LAYER RESERVOIRS

Submitted by **NEGAR ZAREPAKZAD** in partial fulfillment of the requirements for the degree of **Master of Science in Petroleum and Natural Gas Engineering Department, Middle East Technical University** by,

Prof. Dr. Gülbin Dural Ünver _______________
Dean, Graduate School of **Natural and Applied Sciences**

Prof. Dr. Serhat Akın _______________
Head of Department, **Petr. and Nat. Gas Eng.**

Asst. Prof. Dr. Ismail Durgut _______________
Supervisor, **Petr. and Nat. Gas Eng. Dept., METU**

Assoc. Prof. Dr. Emre Artun _______________
Co-Supervisor, **Petr. and Nat. Gas Eng. Dept., METU NCC**

Examining Committee Members:

Prof. Dr. Serhat Akın _______________
Petroleum and Natural Gas Engineering Dept., METU

Asst. Prof. Dr. Ismail Durgut _______________
Petroleum and Natural Gas Engineering Dept., METU

Assoc. Prof. Dr. Emre Artun _______________
Petroleum and Natural Gas Engineering Dept., METU NCC

Prof. Dr. Mahmut Parlaktuna _______________
Petroleum and Natural Gas Engineering Dept., METU

Assoc. Prof. Dr. Çağlar Sınayuç _______________
Petroleum and Natural Gas Engineering Dept., METU

Date: 24.01.2018

I hereby declare that all the information in this document has been obtained and presented in accordance with academic rules and ethical conduct. I also declare that, as required by these rules and conduct, I have fully cited and referenced all material and results that are not original to this work.

Name, Last Name:

Signature:

ABSTRACT

DEVELOPMENT OF A SCREENING MODEL FOR POLYMER FLOODING IN MULTI-LAYER RESERVOIRS

ZarePakzad, Negar

M.S., Department of Petroleum and Natural Gas Engineering

Supervisor: Asst. Prof. Dr. Ismail Durgut

Co-Supervisor: Assoc. Prof. Dr. Emre Artun

January 2018, 125 pages

Polymer flooding is a chemical enhanced oil recovery method which aims to increase oil production from a water flooded oil reservoir by increase in water viscosity and reduction in water-oil mobility ratio. These changes result in significant increase in sweep efficiency of water comparing with water-only flooding technique. The objective of this study is to analyze the behavior of multilayer reservoirs under polymer flooding process, considering effects of reservoir characteristics, polymer properties and operational parameters. This research employs a commercial reservoir simulator to model the fluid flow in a polymer-flooded reservoir. A representative reservoir model is built in CMG IMEX black oil commercial simulator and an experimental design methodology is followed to include uncertainties in different parameters to create various reservoir and polymer injection (10,000) schemes. According to the performance indicators collected from the simulation runs, an optimization study is carried out to determine the optimum parameters ranges to maximize the performance of polymer flooding. To evaluate the performance of the flooding operation the performance indicators

are used to calculate efficiency and water cut for ten years of injection with two-year intervals. A data driven screening tool that utilizes artificial neural networks is trained with the inputs and outputs of the simulator. This developed tool can be used to assess a large number of scenarios within a fraction of a second. Prediction performance of the tool is inspected with numerical simulator results and an average absolute error of ±0.06 bbl/lb and ±0.02 bbl/bbl are reported for efficiency and water cut outputs. Lastly, to ease the usability of the screening tool, a graphical user interface is generated.

Keywords: Polymer, enhanced oil recovery, reservoir modeling, screening model, data-driven modeling

ÖZ

ÇOK KATMANLI REZERVUARLARDA POLİMER ÖTELEMESİ İÇİN BİR TARAMA MODELİNİN GELİŞTİRİLMESİ

ZarePakzad, Negar
Yüksek Lisans, Petrol ve Doğal Gaz Mühendisliği Bölümü
Tez Yöneticisi: Yrd. Doç. Dr. Ismail Durgut
Ortak Tez Yöneticisi: Doç. Dr. Emre Artun

Ocak 2018, 125 sayfa

Polimer ötelemesi suyla ötelenen bir petrol rezervuarında, basılan suyun akış direncinin arttırılması ve su-petrol hareketlilik oranın azaltılması ile petrol üretimini arttırmak için kullanılan bir kimyasallarla geliştirilmiş petrol çıkarma yöntemidir. Bu değişiklikler, sadece suyla karşılaştırıldığında, süpürme verimliliğinde önemli bir artışa neden olur. Bu çalışmanın amacı, çok katmanlı rezervuarların bu işlem boyunca davranışlarını rezervuar özellikleri, polimer özellikleri ve operasyonel parametreleri dikkate alarak analiz etmektir. Bu çalışmada, polimer öteleme uygulanan rezervuarlardaki akışı temsil eden bir modelin oluşturulması için CMG IMEX rezervuar simülatörü kullanılmıştır. Deneysel tasarım yönetimiyle farklı parametrelerdeki belirsizlikleri dikkate alarak birbirinden farklı rezervuar ve polimer enjeksiyon tasarıları (10,000) oluşturulmuştur. Belirlenen performans kriterleri göz önüne alarak polimer-öteleme metodunun en verimli olarak uygulanabildiği koşulların bulunması (optimizasyonu) çalışılacaktır. Öteleme

işleminin performansını değerlendirmek için performans kriterleri kullanılarak ikişer yıllık aralıklarla on yıllık verimlilik ve su üretimi değerleri hesaplanacaktır.

Veriye dayalı inceleme modeli, yapay sinir ağları kullanarak simülatörün girdi ve çıktıları ile eğitilmiştir. Elde edilen sonuçlar kullanılarak bir yapay-sinir-ağları modeli oluşturulup, bu modelin bir saniyeden bile kisa bir sürede tasarlanan işlemin değerlendirilebileceği bir tarama modeli oluşturmak amaçlanmıştır.

Anahtar Kelime: Polimer ötemesi, rezervuar modeli, yapay-sinir-ağları, optimizasyon

To my lovely parents.

ACKNOWLEDGEMENTS

I would like to express my sincere gratitude toward Dr. Emre Artun for his continuous guidance, insight and encouragement throughout the research. I am forever proud and honored to be his student.

I would like to convey my thanks to Dr Ismail Durgut for his unconditional ready support and advice. I feel need to appreciate all my committee members Dr. Serhat Akın, Dr. Mahmut Parlaktuna and Dr. Çağlar Sınayuç for allocating their invaluable time for my thesis.

I would like to give my deep acknowledgment to Prof. Dr. Salih Saner for his heartwarming encouragement, guidance and his kind generosity in sharing his knowledge. Six years studying and working with METU NCC family gave me an opportunity to grown in the best way possible and shaping my career.

A very big thank must go for Ali and Gamze for being with me in good as well as hard times. Without you this road would have been unimaginably hard to pass. Also many thanks to my new, old, nearby and faraway friends, Banfashe, Nastaran, Shima, Mahyar, Elham, Narges, Hamed and Safa.

Finally and most importantly I am indebted to my encouraging father, Habib and caring mother, Soheila for their unconditional love and endless sacrifices all my life.

TABLE OF CONTENTS

LIST OF TABLES

LIST OF FIGURES

LIST OF SYMBOLS

ρ_g	Gas Density, *lb/ft*^{3}
μ_g	Gas Viscosity, *cp*
γ_{gs}	Gas Gravity Separator Condition, *fraction*
μ_m	Polymer Mixture Viscosity, *cp*
μ_m^o	Reference Polymer Solution Viscosity, *cp*
γ_o	Oil Gravity, *°API*
μ_O	Oil Viscosity, *cp*
μ_{OD}	Dead Oil Viscosity, *cp*
μ_w	Water Viscosity, *cp*
a_{max}	Polymer Maximum Adsorption, *lb.stb*$^{-1}$
b	Langmuir Isotherm Constant, *lb.stb*$^{-1}$
B_g	Gas Formation Volume Factor, *RB/scf*
B_o	Oil Formation Volume Factor, *RB/STB*
C_g	Gas Capillary Pressure Coefficient
C_o	Oil Capillary Pressure Coefficient
C_p	Polymer Concentration, *lb.STB*$^{-1}$
C_p^o	Reference Polymer Concentration, *cp*
CPOR	Rock Compressibility, *psi*$^{-1}$
D	Reservoir Depth, *ft*
E_g	Gas Expansion Factor, *scf/RB*
f_o	Fractional Flow of Oil
k	Permeability, *mD*
k_h	Horizontal Permeability, *mD*
k_{rg}	Relative Permeability to Gas
k_{ro}	Relative Permeability to Oil

k_{rw}	Relative Permeability to Water
k_v	Vertical Permeability, *mD*
M	Mobility Ratio
M_a	Apparent Molecular Weight, *lbm/lbm.mol*
M_o	Mobility of Oil
M_w	Mobility of Water
n	Relative Permeability Curve Exponential Coefficient
P	Reservoir Pressure, *psi*
P_b	Bubble Point Pressure, *psi*
$P_{bhp(inj.)}$	Bottom Hole Pressure at Injector, *psi*
$P_{bhp(prod.)}$	Bottom Hole Pressure at Producer, *psi*
P_{cog}	Oil-Gas Capillary Pressure
P_{cow}	Oil-Water Capillary Pressure
R_s	Solution Gas Oil ratio, *scf/STB*
S_g	Gas Saturation, fraction
SG	Specific Gravity
S_o	Oil Saturation, *fraction*
S_{oi}	Initial Oil Saturation, *fraction*
S_{or}	Residual Oil Saturation, *fraction*
S_w	Water Saturation, *fraction*
S_{wirr}	Irreducible Water Saturation, *fraction*
T	Temperature, *°F* | *°R*
Z	Gas Compressibility Factor, *fraction*
γ_{gs}	Gas Gravity at Separator Condition of 100 *psig*
ρ_w	Water density, *lb/ft*^{3}
Φ	Porosity, *fraction* | *percentage*

LIST OF ABBREVIATIONS

AI	Artificial Intelligence
ANN	Artificial Neural Network
avg	Average
Conc	Concentration
eco	Economic
EOR	Enhanced Oil Recovery
GUI	Graphical User Interface
HPAM	Hydrolyzed Polyacrylamide
Inj	Injector
IPV	Inaccessible Pore Volume
MW	Molecular Weight
npv	Net Present Value
OOIP	Original Oil in Place
Poly	Polymer
Prod	Production
PVT	Pressure-Volume-Temperature
Res	Reservoir
Vol	Volume
yrs	Years

CHAPTER 1

INTRODUCTION

Nowadays, enhanced oil recovery (EOR) technology is getting more important standing in the oil industry with respect to increasing oil demand and the limited worldwide hydrocarbon resources. Difficulties in finding new productive fields lead us to further improve our current technologies in order to produce much more hydrocarbons from existing hydrocarbon reservoirs. Oil recovery has been branched out into three stages, starting from primary stage which the production depends on natural drive mechanism of the reservoir system. As the primary production ceases, immiscible gas or water may be injected as a secondary recovery stage to maintain reservoir pressure. Tertiary recovery is any method used to produce the amount of oil remained in reservoir after the economic limit of secondary stage has been achieved. Enhanced oil recovery (tertiary recovery) processes in general includes miscible gas floods, chemicals and thermal methods. All these processes aim to produce the unconventional hydrocarbon left after the primary and secondary recovery periods. Chemical methods of enhanced oil recovery use polymer, alkaline, surfactant or combination of these chemicals to alter some chemical and physical properties of the reservoir rock and fluid in a favorable manner. These alterations result in increased sweep efficiency, generally by reducing the interfacial tension, water mobility, fingering as well as alternating wettability.

Polymer flooding as one of the promising chemical EOR techniques primarily acts as a thickener in the direction of increasing the injected water viscosity (Taber et al., 1997). In addition to the increase in water viscosity, polymers can reduce relative permeability of the rock to the water, hence improving the volumetric sweep efficiency. These characteristics of polymer can boost the oil recovery compared to conventional water flooding. Polymer flooding is a mature recovery method with more than 50 years of laboratory studies and commercial scale field applications. Recovery range of 5 to 30% OOIP, applicability for wide range of reservoir conditions in addition to its low operational cost are the reasons of outnumbering polymer flood processes from other chemical EOR methods. One of the most successful and largest polymer flooding practices is implemented in Daqing field, China. It is expected that using this recovery method can achieve an ultimate recovery of more than 50% OOIP. Furthermore, it is estimated that polymer flooding could result in additional 10-12% OOIP recovery comparing with water flooding (Wang et. al., 2009).

In general, all of the oil recovery methods are expensive processes that require comprehensive analysis in order to assess the most suitable method according to a reservoir rock and fluid properties. Usually, the analysis initiate with referring to screening criteria. Although the published screening guidelines are based on real field data, they cannot provide information about production performance. Hence, laboratory studies or numerical modeling should be performed to ascertain the recovery performance. However, these analysis during appraisal stage are extremely time demanding and costly. Recently, data driven modeling approach in the petroleum engineering practices has been expanding expeditiously to assist in overcoming the aforementioned problems. The data driven modeling is used to build screening tools to facilitate the selection of suitable recovery in addition to providing the expected reservoir performance.

For the last decades, data driven modeling approach has been widely applied in diverse applications of petroleum engineering field. Some of the advantages of this method over the numerical simulations should be pointed out to answer the reason behind this growing interest. The reservoir simulators require a detailed set of physical and chemical information about the reservoir system. Even though with presence of detailed data, simulations may not give accurate predictions and they required to adjust some parameters to match the actual performance of the reservoir. Moreover, simulations are expensive, time demanding, as well as being in need of professionals and computer resources to operate. Considering large projects, it is practicable to invest on simulation studies, however, for the independent oil producers it is not the case. They demand for an inexpensive, time efficient and robust alternative. Consequently, artificial neural network based data driven models can assist in overcoming the efforts associated with the application reservoir simulations (Mabkhout et al., 2013).

In 1986, predictive model polymer flooding is developed considering a detailed economic aspects of the operation and additional oil recovery that can be achieved if polymer flooding is implanted instead of water flooding (PFPM,1986). In this model, performance of heterogeneous reservoir can be predicted assuming that no capillary pressure and cross flow exist in the system. Although the model is inclusive as it considers several reservoir, operational and economical properties, it is not practical to use in today's computers working with windows operating systems.

Since early 2000's, the literature has been enriched in various applications of data driven modelling in many reservoir engineering topics. This part of discussion is allocated to review some of the recent works published on modeling chemical EOR using artificial intelligence. Several data driven models have been developed to predict the operational and economical aspects of chemical flooding. Karambeigi (2011), predicts recovery factor and net present value for polymer-surfactant flood. Similarly, Mabkhout (2013), modeled polymer-surfactant flooding to predict the breakthrough time and the recovery factor for different amount of pore volume injection. In both of the studies, UTCHEM, a compositional chemical flood simulator is used to generate the neural network's training data set.

Concerning the application of data driven modeling approach in polymer flooding, several studies can be referred. Alghazal (2015), developed data driven models for polymer gel in naturally fractured reservoirs. Models are capable of providing forward solution for production profiles and inverse-looking solution for estimation of operational and reservoir parameters. Örs (2017), developed a data-driven model for polymer gel treatment for heavily fractured reservoirs with high water cuts. Oloo and Chon (2017), predicted the performance of the polymer flooding at different injection stages. They aimed to forecast recovery factor when two slugs of polymer are injected.

Bearing in mind all the achievements of the previously published papers regarding the chemical EOR methods and screening tools, it is intended to fill the gaps and uncovered topics related with performance prediction of polymer flooding process. Some of the features of this research that can be supplement formerly developed tools and studies are as follow:

- Diverse expectation from screening guidelines exist for different producing regions in the world. As an example, in USA the field ownership varies from one-person to large companies with low central interest in entire reserve of the country. However, in the UK all the oil reserves are owned by the government and the companies operating the fields are in partnership with each other. Hence, the screening criteria for polymer flooding should be in more detail for UK operations than in the USA (Sorbie, 1991). By the use of a data-driven based screening model numerous reservoir parameters beside wide ranges can be considered. The additional considerations namely are: relative permeabilities, capillary pressures and the wettability properties. The developed screening tool can be also beneficial for the small companies that a detailed study is not practicable as the laboratory and pilot tests are extremely costly.

- Judgment upon which reservoir parameter is more critical to consider for polymer flooding acceptance or rejection is impossible by screening guidelines. In this study, reservoir parameter's impact on polymer flooding process is sorted in the order of their importance.

- Lack of literature in having a data-driven screening tool for polymer flooding with purpose of viscosity control as an earlier data-driven screening model is developed for heterogeneity control polymer floods (polymer gel injection).

In this study, a data driven screening tool using artificial neural networks is developed for polymer flooding EOR process. The screening tool provides the expected efficiency of the flooding process for a given reservoir characteristic. The sequence of this research presentation is organized into six chapters. In Chapter 2, a summary of the previous studies conducted around polymer flood process is provided. This includes the laboratory studies, the field applications and the screening analyses. Chapter 3, presents the problem statement, objectives and the work flow of this study. In Chapter 4, characterization of the reservoir simulation model and the development of data-driven screening tool for polymer flooding is described in details. Chapter 5 is assisted to thoroughly discuss the obtained results. This section incorporates the results of the data driven model as well as the parametric study on simulation model results. Chapter 6 includes the key conclusions obtained from parametric analysis and screening tool. Lastly, Chapter 7 provides the recommendations for future work in the interest of expanding the current study.

CHAPTER 2

LITERATURE REVIEW

This chapter is dedicated to discuss the previous approaches on understanding the macroscopic and microscopic displacement behavior of the polymer flood in oil reservoir systems as well as developed of data driven models for this field of study. In the first part, the discussion mainly include: description of polymer flooding system, polymer properties, screening and field studies. The second part aims to cover the development progression of data driven models and remark the applications of these models in the petroleum industry.

2.1 Polymer-Water Flooding

Polymer flooding is an enhanced oil recovery method in which a high molecular weight water soluble polymer is added to the injected water. The main role of these particles are improving the sweep efficiency and mobility ratio of the regular water flooding through increasing the viscosity of the water. By definition, the mobility ratio is expressed as the mobility of the displacing phase divided by mobility of the displaced phase. The mobility of a fluid is the relative permeability to the fluid over its apparent viscosity (Carcoana, 1992). In polymer augmented water flooding, the mobility of the displacing fluid is reduced due to the viscosifying effect of the polymer as well as decreasing the relative permeability to the displacing fluid. In this process no alteration in oil mobility present since the physical and chemical properties of the oil is not affected by the polymer. According to the mobility ratio equation shown in Equation 2.1, reduction in displacing fluid (polymer-water mixture) alongside with an unchanged mobility of the oil, results in favorable ratio of less than unity. Mobility control, improves the efficiency of the displacement process.

$M = \frac{M_w}{M_o} = \frac{k_{rw} \cdot \mu_o}{k_{ro} \cdot \mu_w}$..Equation 2.1

Where: M_w *Mobility of water*
M_o *Mobility of oil*
k_{rw} *Relative permeability to water*
k_{ro} *Relative permeability to oil*
μ_o *Oil viscosity*
μ_o *Water viscosity*

Both areal and vertical sweep efficiencies are enhanced by polymer flooding before and after breakthrough. Improved volumetric sweep efficiency brings late breakthrough and high oil recovery at breakthrough (Sorbie, 1991). Moreover, after breakthrough polymer flood is beneficial in shifting water path toward unswept areas. Simplified Buckley and Leverett fractional flow equation given in Equation 2.2, can explain how fractional flow of the oil is increased after breakthrough due to advantageous modifications of the relative permeability and water viscosity (Carcoana, 1992).

$f_o = 1 - \frac{1}{1+\left(\frac{1}{M}\right)}$...Equation 2.2

Where: M *Mobility ratio*

2.1.1 Polymer Types

Polymer term is derived from “polys” and “meros” meaning “many parts” in Greek language. Several polymers have possess the requirements to be used in polymer augmented water flooding process. Namely these polymers are: polyacrylamides, polysaccharides, cellulosics and polyacrylates (Donaldson et al., 1989). Of the four, hydrolyzed polyacrylamide (HPAM) and polysaccharides or xanthan gum are the two types commonly used in field applications (Carcoana, 1992; Sorbie, 1991; Donaldson et al., 1989). These two types have also been utilized broadly in other industries such as paper manufacturing and drag reduction using polyacrylamide and xanthan gum as a thickener in food industry (Sorbie, 1991). In the following two sections, properties of the mentioned polymers are presented in some detail.

2.1.1.1 Hydrolyzed Polyacrylamide

HPAM as a partially hydrolyzed form of polyacrylamides is the most widely used in polymer flood applications (Manrique et al., 2006; Abidin et al., 2012; Sheng et al., 2011; Sorbie, 1991). HPAM is a synthetic polymer with a linear chain molecular structure, molecular weight (MW) in a range of $2x10^6$ to $6x10^6$ (Sorbie, 1991) and hydrolysis degree of 20% to 40% (Carcoana, 1992). HPAM is highly sensitive to several conditions which cause reduction in polymer solution viscosity when the HPAM molecules get broke down (Abidin et al., 2012; Carcoana, 1992). The presence of temperatures above 70°C, saline and hard water containing divalent ions like Ca^{2+} or Mg^{2+} cause polymer instability (Abidin et al., 2012; Sorbie, 1991).

Thermal stability of the HPAM is affected by several factors, such as brine composition, molecular weight and hydrolysis degree of the polymer. The restricted temperature for use of this polymer can be boosted to 90°C in case an alkaline brine is used. HPAM in such mixtures can be chemically stable for more than 21 months at 90°C (Sorbie, 1991). Surfactants and other chemicals used as additive fluids are the main reasons for HPAM insatiability and degradation (Abidin et al., 2012; Sorbie, 1991). The hydrolysis degree of the HPAM is a key factor to favorably change some of the physical properties of the polymer such as adsorption level, mechanical shear and thermal stability (Sorbie, 1991). However, it should be noted that high hydrolysis degree and salinity are the two factor which reduce the polymer solution viscosity at a given concentration (Donaldson et al., 1989; Taber et al., 1997).

2.1.1.2 Xanthan Gum

Xanthan gum or shortly xanthan is a polysaccharide biopolymer produced from bacterial fermentation process (Carcoana, 1992). A wide-ranging molecular weight is available from $2x10^6$ to $50x10^6$. In polymer flood applications only the biopolymers with MW near to lower limit of the stated range is commercial to use (Sorbie, 1991). The structure of this material includes side chains holding the molecule in rigid, helical form (Donaldson et al., 1989). In general, Xanthan is an expensive type of polymer which is susceptible to bacterial activities, yet high tolerance for salinity, shearing effects (Carcoana, 1992). In addition, it has been proven that the temperature stability of this polymer is only a function of temperature and the concentration of the divalent ions has no effect on stability (Sheng et al., 2011; Sorbie, 1991).

2.1.2 Polymer Solution Properties

After the discovery of first commercial oil well by Drake at Pennsylvania in 1859, Carl proposed that water injection may increase the chance on obtaining higher oil recoveries (Willhite, 1986). Starting from early 1900's, the inefficiency of the conventional water flooding methods is realized and widespread research around sweep efficiency and displacement enhancement have been commenced (Chang, 1978). In 1944, for the first time Delting introduced water soluble polymer beside several other additives to viscosify the injected water and improve the sweep efficiency (Carcoana, 1992). In 1964, Pye and Standiford conducted laboratory studies suggesting that water soluble polymers can effectively reduce the water mobility. Laboratory results are confirmed with pilot field tests and economical analyses indicated the profitability of polymer flood recovery method (Pye, 1964). Meanwhile, Standiford used HPAM in his laboratory tests, indicating low concentration of HPAM is able to enhance oil production for low to high range of oil viscosities (Sandiford, 1964). Later numerous laboratory studies on behavior of polymer solution in porous media were initiated. According to Mungan (1969), the polymer solution viscosity is affected by the molecular weight of the polymer, the shear rates, the salinity and PH of the water.

2.1.3 Flow Behavior of Polymer Solution

In the laboratory polymer flood tests, it has been commonly observed that the concentration of the polymer bank decreased due to retention of the polymer material as it propagates inside the formation. In polymer retention phenomena several mechanisms are involved, namely, adsorption, mechanical trapping and hydrodynamic retention (Sheng, 2011). Adhesion of polymer particles to reservoir rock surface is called adsorption. The film of the polymer created on rock surface during the adsorption process causing polymer loss and increasing the flow resistance (Schneider & Owens, 1982). Mechanical entrapment depends on opening size of the rock. This phenomenon happens when flow is restricted by the narrow flow channels. Hence building up of the material takes place causing the flow of the brine instead of the polymer molecules (Carcoana, 1992). Consequently, a higher polymer adsorption and entrapment occur when high polymer concentration is injected or low permeability formation exists. Hydrodynamic retention appears when a flow rate is altered. High hydrodynamic retention appears as the velocity increased. It is believed that hydrodynamic retention has a minor contribution in the total retention, its effect can be overlooked for the field applications (Sheng, 2011).

In 1972, Dawson and Lantz introduce a new cause for denudation of polymer from the solution. They have suggested that in addition to the adsorption phenomena, inaccessible pore volume (IPV) is also affecting the polymer concentration at the front (Dawson & Lantz, 1972). Inaccessible pore volume is the volume of the pores which are smaller than the polymer molecular size thus causing a barrier to polymer flow (Sheng, 2011). About 30% of the total porosity cannot be reached by polymer (Sheng, 2011; Schneider & Owens, 1982). Adsorption and the IPV influence the breakthrough time differently as the adsorption decreases the breakthrough time though IPV increases (Sheng, 2011; Dawson & Lantz, 1972). Laboratory studies on the two aforementioned processes provides that the IPV is more effective than the adsorption loss of the polymer.

In addition to the relative permeability reduction of the rock due to adsorbed polymer, relative permeability curves can be affected. This subject has been supported in a few studies. Obtained results in one of the pioneering works in 1973, indicated that the adsorption causes a minimal reduction in the oil relative permeability but decreasing the aqueous phase relative permeability considerably. Degree of the alteration in the relative permeability relations upon the adsorption is also influenced by the wettability of the rock formation (Sheng, 2011). In a water-wet rock, flooded by polymer solution, the oil relative permeability remained unaffected or increased, consequently improving oil recovery. However, the water relative permeability reduced significantly compared to its curve when rock is only water flooded. In case of oil-wet systems, both phase permeabilities affected after polymer contact. As one of the other conclusions of the experiment conducted by Schneider and Owens (1982), the various types of polyacrylamides polymers used do not notably affect the relative permeability curves.

2.1.4 Field Applications

Starting from 1970, the polymer flooding field applications have been reviewed by Jewett and Schurz (1970). In their study, 61 polymer flooding projects were investigated. These projects represent more than 95% of the polymer flood application till 1969. In this review the small volume and short-term polymer injections were excluded. About 60% of the cases started the flooding close to the end of primary depletion stage and nearly 30% and 10% corresponding to depletion stages of secondary and tertiary, respectively. Among 61 projects, 29 had sufficient information regarding the applicability of the polymer flooding method. Almost half of these 29 cases were successful projects which 9 were commercial scale field applications. This study concludes that the polymer injection process is efficacious over wide ranges of reservoir and fluid properties (Jewett, 1970).

Updated project data and the new fields which transformed from pilot test to commercial scale were reviewed by Needham and Doe (1987). Among 27 projects considered in this review, more than 90% of the polymer flooded reservoirs had sandstone lithology, 24 of them had been flooded by polyacrylamide and only two projects used biopolymers. A total of nine projects resulted in 8% or more additional OOIP recovery. After this review it was concluded that the polymer flooding is less prosperous if applied as a post water flooding application. It is beneficial in terms of oil recovery and amount of polymer usage to perform polymer flooding directly after primary production stage. Later in 1997, a similar study have been conducted by comparing the polymer injection projects inside and outside U.S. with the other EOR application. This study suggest that, the polymer flooding can improve the sweep efficiency of any water flooding operation, however, the economical limitations are the factor increasing the risk of unsuccessfulness of the polymer flooding operation (Taber et al., 1997).

The world's largest polymer flood application was implemented in China's Daqing oil field (Wang et al., 2009; Saleh et al., 2014). Daqing field is a heterogeneous, multi-layer sandstone formation. The laboratory studies began in 1960s to decide on a potential EOR method for Daqing field (Wang et al., 2009). Due to reservoir and crude oil properties of the field, it has been decided that none of the two common EOR methods, neither thermal nor miscible were suitable to apply (Wang et al., 2000). Hence polymer flooding as the only applicable method has been selected. Meanwhile in early 60's, petroleum professionals started to perform comprehensive studies, deepening their knowledge in polymer injection process. The obtained results of these studies concluded that polymer injection recovers only 2 to 5% OOIP over water flooding (Wang et al., 2009). Hence polymer flood could not be assigned as an economically feasible process among other industrial applications of EOR methods. On the contrary, the pilot test results were promising for Daqing oil field and rapidly pilot test expanded for a large spaced multi-well pattern. The obtained results from the pilot tests and the research studies from the mid 1980's confirmed that polymer injection in Daqing field can effectively improve the sweep efficiency. A field scale polymer injection in the Daqing filed was initiated in 1996. Beforehand the water flooding was practiced with an average water cut of 90% and mobility ratio of 9.4. Within two years of injection, it has been reported that the water cut decreased from 90.8 to 73.1% (Wang et al., 1998). By 2007, the polymer flood in Daqing field contributed to 22.3% of the total production and a recovery of 10 to 12% more than from water flooding. It should be also mentioned that reservoir conditions of Daqing field were in accordance with the earlier exhibited screening criteria for polymer flooding (Wang et al., 2009).

As one of the important achievements of Daqing oil field is verifying the ability of polymer to sweep residual oil. In an experimental analysis, the effect of glycerin and polyacrylamide flood on residual oil reduction was investigated. The obtained results showed that with the same displacing fluid viscosity (30 cp) the amount of displaced fluid is changed. It has been indicated that the elastic property of the polymer can mobilize all variety of residual oil. Considering the economic aspects of the field project, it has been suggested that early polymer injection can reduce the amount of injected water. This saved amount of water can fully or partially offset the cost of the polymer (Wang et al., 2000).

Going beyond the successful field projects with properties in consistency with the polymer flood screening criteria, there are some particular fields which have properties that do not follow the standard screening guides. Pelican Lake in Alberta is the first heavy oil reservoirs that polymer flooding is successfully implemented. Existence of the heavy oil in a thin formation made it inappropriate for implementation of thermal EOR due to significant heat loss (Delamaide et al., 2013). The standard screening criteria suggests that an oil viscosity above 200 cp is not suitable for polymer injection. However, with some modification in operational conditions in Pelican Lake field, the oil with a viscosity of 1000 to 1200 cp was recovered. The pioneering idea of applying polymer flood process to heavy oils was discovered as early as 1977. However, this process is applicable in the case of having horizontal wells and relatively high oil price (Wassmuth et al., 2007). Horizontal wells are used to overcome the injectivity problems of high viscosity polymer flood, in heavy oil recovery projects (Seright, 2010). By the mid 2000's, the pilot tests in Pelican Lake field have been proved to have a recovery factor of about 25% if horizontal wells are used (Delamaide et al., 2013).

In addition to the mentioned onshore applications of polymer flooding, in 2010, an offshore medium viscosity oil recovery project was practiced (Morel, 2012). Mainly two complications are associated with the offshore polymer flooding applications. Firstly and inevitably, the space limitations of offshore platform causing difficulties in installation of polymer storage, mixing and injection equipment (Sorbie, 1991). Secondly, beyond specific logistic problem, large well spacing between producer and injector is the other problem causing difficulties in flow control

All in all, polymer injection process has a wide applicability over different reservoir and operational conditions. It should be taken into account that oil price is a critical factor if the polymer flood is considered as recovery process for heavy oils or the offshore projects. As might be seen that the application of polymer in EOR extended to heavy oil recovery after mid 2000's when the oil price was exceeding $60 per barrel (MWV, 2017).

2.1.5 Screening Tools and Studies

This section is intended to discuss the progress of screening studies conducted as a guidance to select an optimum reservoir for polymer flooding. With increasing oil production from EOR projects and declining production from conventional mechanism, a vital importance of selecting the best EOR method is growing steadily. The idea behind developing a screening criteria is to set a simple range for fluid and reservoir properties to accept a recovery method for a further investigation on a specific field. By other meaning, screening criteria gives a certain rejection rather than acceptance criteria (Sorbie, 1991). Subsequently when a potential reservoir is identified for a specific EOR process, laboratory studies are initiated to further examine the rock and fluid properties. If satisfactory laboratory results are obtained, the field will undergo a pilot test before full field recovery begins (Sieberer et al., 2017).

Screening studies started in 1970 by Jewett and Schurz and later different screening works in the literature published by several other researchers. Recently, seven screening works from year 1977 till 2014 are combined and compared by Saleh et al. (2014). The comparison between the evaluated studies are shown in Figure.2.1. These data are comprised of field projects, laboratory and pilot tests. According to the graph, different screening works are in good agreement on formation depth and temperature of less than 9400 m and 98.9°C, respectively. However, the data collected by the author suggest higher upper limits for permeability as well as saturation, viscosity and gravity of oil. The applicability of polymer injection for heavy oil recovery has been considered as the reported oil viscosity and gravity ranges are representing light to heavy oil conditions. The ranges for the mentioned parameters are summarized as follow: permeability > 10 md, oil saturation > 21%, oil viscosity < 5000 cp, API gravity > 12.

A similar technical screening work is published in 2015, comparing the same works shown by Saleh et al. except including only the field and pilot tests data (Sheng et al., 2015). According to this very recent publication the range of some parameters are changed. In Table 2.1, the screening ranges proposed by Saleh et al. (2014) and Sheng et al. (2015) are conferred.

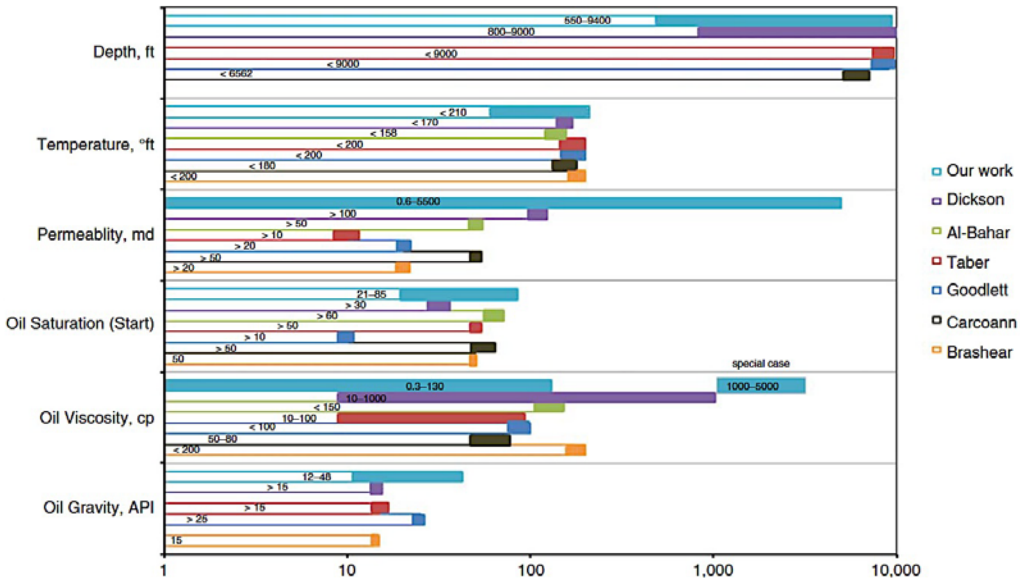

Figure 2.1. Different screening criteria for polymer injection process (Saleh et al., 2014).

Table 2.1. Comparison of some of the parameters from two recent polymer flooding screening guides.

Published by	T [°C]	Lithology	μ_o [cp]	S_o	Gravity [°API]	Depth
Saleh et al., 2014	< 98.9	Sandstone & Carbonate	< 5,000	> 0.21	> 12	<9400
Sheng et al., 2015	< 93.3	Sandstone	< 150	$(S_o$-$S_{or})$ >0.1	NC*	NC*

2.2 Overview of Data Driven Modeling Approach

Since many years ago, humans were curious to bring the idea of intelligent machines to the reality. With the evolution of the computers and 50 years of research, a new area in computational sciences called “Artificial Intelligence” have been introduced. This area of science is intending to develop machines that have an ability to think, learn and deal with new situations like a human being's brain. This ability achieved once the computer science gets along with physiology and philosophy sciences. In the last two decades, the integration of artificial intelligence (AI) with analytic tools attempt to solve challenging problems in different disciplines which previously were not possible or easy to solve (Mohaghegh, 2017). Artificial intelligence has been titled with various names such as virtual intelligence, computational intelligence and soft computing (Mohaghegh, 2000).

Artificial neural networks (ANN) are one of the paradigms of the AI, used as a data-driven modeling approach (Artun, 2016). Data driven modeling approaches have been applied in many areas such as medical, transportation, telecommunication, security, financial, manufacturing and many more. As stated by Ali (1994), "while being the first to use a new technology is hazardous, being among the last may be disaster". Remarkably, technical leadership is a necessity of the competitive oil industry. In the oil and gas industry, this technology has been used in geology, geophysics, drilling and reservoir engineering (Hagan et al., 2016).

In this study, ANN as a computational intelligence technique is used as a data-driven modeling alternative to develop a screening model for polymer flooding EOR. In the following sections, it is intended to cover the structure and mechanism of ANN, prior to reviewing the potential applications of data driven modeling in petroleum engineering field.

2.3 Historical Background

The long history of data driven modeling can be traced back to late 19th century, once a novel work by McCulloch and Pitts (1943) put an origin for neural-network field. They revealed that any arithmetic or logical operation could be processed by the network. Later Hebb (1949) showed a learning mechanism for biological neurons. A great deal of interest generated in neural network field when Rosenblatt (1958) made the first practical application of the network. In the meantime, a network similar to Rosenblatt's was introduced by Widrow and Hoff (1960), using a new learning algorithm. However, the both network's had limitations for training complex problems. Starting from 1980's, the lack of powerful computers was overcome, and new concepts were proposed. The use of statistical mechanics and backpropagation algorithm were the two concepts revivaling the field of neural networks. Since then, numerous papers have been published and many applications of neural network have been established (Hagan et al., 2016).

2.3.1 Structure of an Artificial Neural Network

The artificial neural network is an information processing system in which the brain functions and neural system are the inspiration of this development (Hagan et al., 2016). Therefore, it is prerequisite to briefly explain the biological counterparts before discussing the artificial neural network.

The basic structure of a neuron is comprising of dendrites, a cell body and an axon. A simplified schematic drawing of two bipolar neurons is shown in Figure 2.2. The dendrites are responsible to carry the information as signals (electro-chemical pulses) from other neurons to the cell body (Mohaghegh, 2017). The cell body is the processing part, which scales the incoming signals and transmits them to the next neuron via the axon (Fausett, 2004). The pathway between two consecutive neurons where the termination of axon in first neuron is close to the dendrites of the second one is called a synapse.

Artificial neural networks have several features similar to the biological neuron system, though, they are still a rough approximation of the human brain's functionality. Human brain has about 10-100 billion neurons. The interconnectivity and the parallel architecture of the neural system are the main driving force behind human's complex behavior. Although, the cycle time of biological neurons are 10 million times slower comparing with the electrical circuits, the brain can perform many task much faster than computers due to its complicated structure. Therefore, the regular simple tasks done by humans involves complicated calculations that computers are not yet able to process.

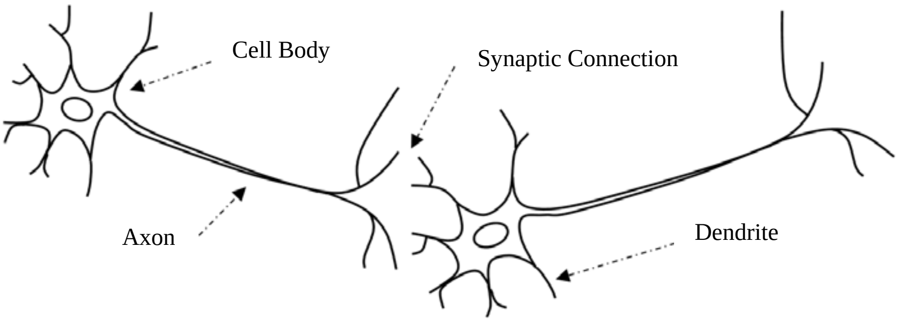

Figure 2.2. Schematic drawing of two bipolar neurons.

Figure 2.3 shows the schematic drawing of an artificial neuron. The outputs from other neurons are feed as the inputs (I_1, …, I_n) for next neuron and they are multiplied by weight factors (W_1, …, W_n). The inputs are processed in the neuron via summation and the activation function, resulting in single output.

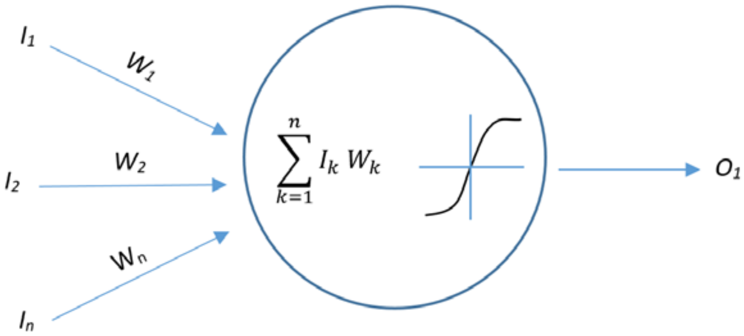

Figure 2.3. Schematic drawing of an artificial neuron.

2.3.2 Mechanism of an Artificial Neural Network

An artificial neural network is a group of neurons arranged into layers. A multi-layer network consists of an input, an output and one or more hidden layers in between. The number of neurons in the input and output layers resemble the number of parameters as an input or output to the network. Multi-layer networks are used to solve complicated problems. In data driven models, networks can be trained to generate several outputs (Fausett, 2004). Figure 2.4 is a schematic diagram of a three-layer neural net.

There are different classifications for the ANN. The most common category is the by the training methods which is subdivided into supervised and unsupervised training. In oil and gas industry the supervised training with back-propagation has more practical application as the both input and output are offered to the network. The procedure to use the artificial neural network is commenced with dividing the database into training, validation and test sets. Within the training set, both inputs and outputs are presented for the model to learn the logic of the problem. In order to check the training process, the network is calibrated with validation data. In this stage the inputs of the validation dataset are presented to the network and the obtained outputs from the model is compared with the actual outputs of the validation set. If a well prediction on validation output data are achieved, the network will be applied to a test set (Mohaghegh, 2017).

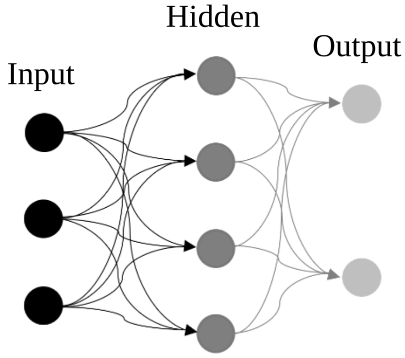

Figure 2.4. Schematic diagram of a three-layer neural network.

CHAPTER 3

STATEMENT OF THE PROBLEM

Polymer flooding as one the most common chemical EOR method is used to improve the sweep efficiency. Selection of a proper reservoir for implementation of polymer injection is a quite challenging procedure as of for any other EOR methods. Hence, use of the screening criteria is crucial in assessing field development in order to select an appropriate recovery method. Numerous polymer flooding screening guides that have been published are based on reservoir rock and fluid properties. On one hand, screening studies are incapable to provide any information about the reservoir ultimate performance. Consequently, if only the screening criteria are to be followed, the economic evaluation is not possible. On the other hand, if the economic evaluation is to be accomplished with a numerical simulator, a huge investment on computational time, complex studies and professional expertise should be considered. These drawbacks can be overcome by a screening tool which combines the recommended screening criteria with reservoir production performance. The tool-box is an artificial neural network (ANN) based data-driven model which can generate immediate results for large number of reservoir and production scenarios in a time efficient manner.

The general objective of this study is to develop a screening tool and deepening the knowledge of viscosity control polymer flooding efficiency. Several considerations are made in the tool development and parametric analysis with intention of filling the gaps of previously conducted practices on polymer flooding method. The tool is capable of estimating the polymer flooding efficiency and water cut amount for wide variety of reservoir properties for different injection duration from two to ten years of polymer injection.

CHAPTER 4

METHODOLOGY

This chapter provides the methodology followed for the construction of reservoir simulator model and the development of the screening tool for polymer flooding process. The first section of this chapter describes the reservoir model generated by a reservoir simulator to mimic the flooding process for numerous reservoir and production scenarios. In the second section, procedure of collecting the inputs and outputs of the reservoir model to develop a neural-network based screening tool for the polymer injection is discussed.

CMG IMEX black oil commercial simulator is used to build a numerical reservoir model with various reservoir and polymer injection schemes. The reservoir simulator product is used to generate the data for the training of ANN. Five ANN models are generated to estimate the additional efficiency that could be obtain if polymer flooding is practiced instead of permitting the reservoir to produce by its own natural drive mechanism. The models are presenting the efficiencies for different injection duration from two to ten years of polymer injection. All are feed forward back propagation models which estimates the efficiency for a given reservoir and operational parameters. Figure 3.1 shows the flow chart for the screening tool-box construction. The step by step procedure to build the tool-box are summarized as follow:

A.1. Constructing a reservoir model for polymer flood process using reservoir simulator.

A.2. Specifying meaningful ranges for reservoir and operational parameters.

A.3. Generating various production schemes by combination different reservoir and operational parameters.

A.4. Running the generated scenarios in reservoir simulator and recording the essential performance indicators to derive a representative efficiency value.

B.1 Feeding the neural network with the input and outputs of the simulator to train the network.

B.2. Comparing the outputs from the network to the results from the simulator to evaluate the accuracy of the network.

B.3. If the network outputs are not within an acceptable error margin:

- **i.** Evaluate the structure and topography of the network.
- **ii.** Evaluate the data set to add or remove some of the cases in order to cover diverse trends as possible.

C. Parametrically analyzing the results for a better understanding of the polymer flooding efficiency.

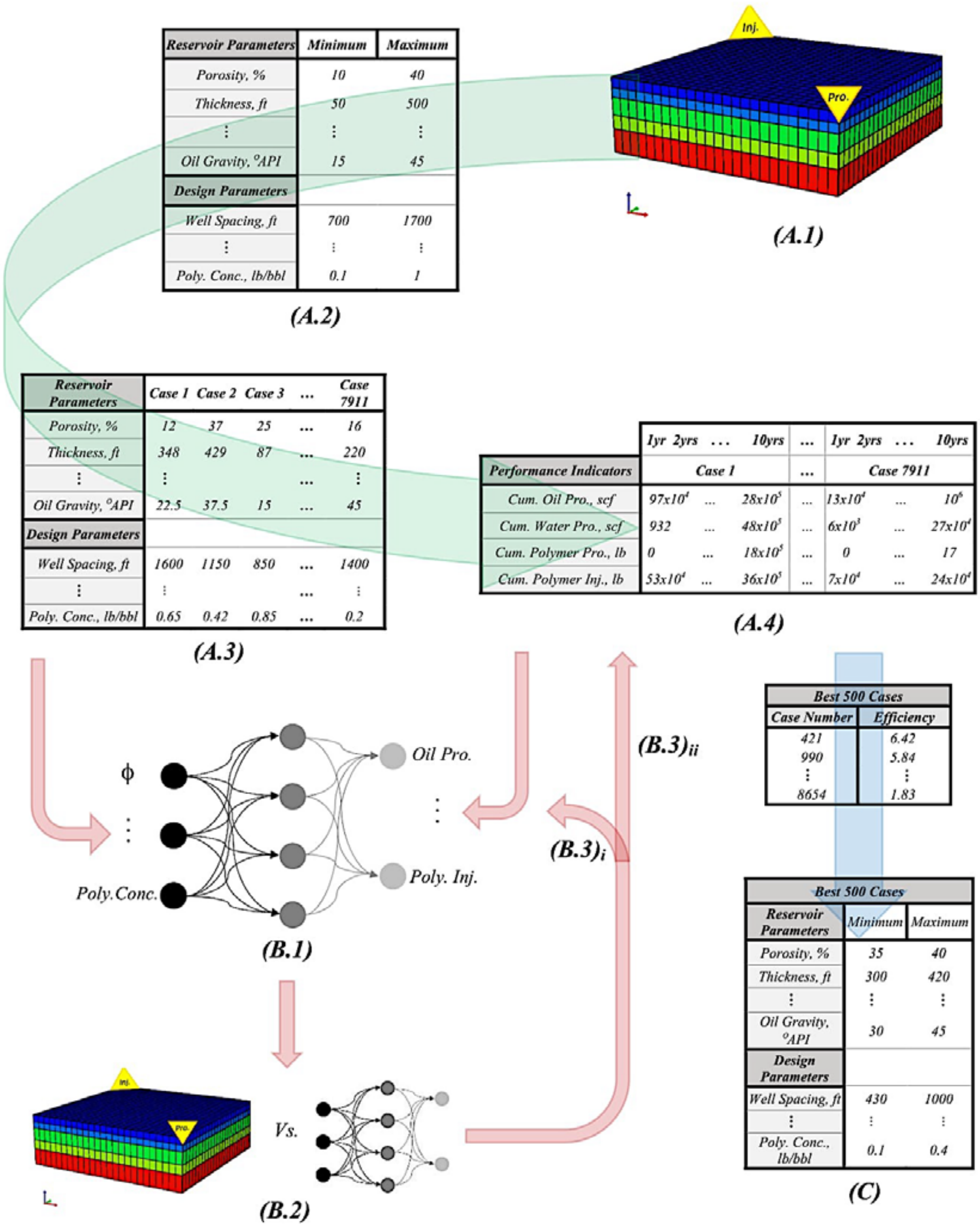

Figure 4.1. Workflow followed to achieve the objectives of the study.

A: Chapter 4 - Section 4.1
B: Chapter 4 - Section 4.2
C: Chapter 5

4.1 Reservoir Simulation Model Construction

A three dimensional single porosity, black-oil reservoir model with a Cartesian grid system is constructed using CMG IMEX (2015) reservoir simulator. In this part, general reservoir description, initial conditions, rock and fluid properties as well as the operational parameters used in the reservoir model are discussed in details. Lastly, sensitivity analyses conducted on number of grid blocks is presented.

4.1.1 General Description and Initial Conditions

A three dimensional, multi-layer reservoir with varying porosity and permeability is constructed, representing a heterogeneous system. The model has five layers in which the thicknesses are not equal and changing from 10 to 100 ft. Thus, all reservoir scenarios have a net hydrocarbon thickness of 50 to 500 ft. The layer's thickness as well as all the other parameters used in the simulator are randomly selected within a specified range to perfectly represent all the reservoir conditions exist in the nature. All the parameters are uniformly distributed between a minimum and maximum limits except for the permeability. Considering the fact that most of the reservoirs have permeability less than 200 mD and the occurrence of permeability more than 200 mD is less frequent, a combination of normal and uniform distribution utilized to generate the permeability values. To generate 10,000 random values for permeability, 8000 are selected with normal distribution having standard deviation of 1 mD and median of 4 mD. The selected median and standard deviation resulted in having 8000 values with almost all of them being less than 200 mD. For the remaining 2000 permeability values, a uniform distribution between 200 to 1000 md are used. Resulting permeability frequency distribution is shown in Figure 4.1. Porosity of the formation rock is uniformly distributed within a range of 0.1 to 0.4. Since the reservoir model represents a heterogeneous system, to characterize the degree of the pay zone heterogeneity as a single value, Lorenz

Coefficient is calculated for the given layer thicknesses, porosities and permeabilities. Lorenz coefficient varies from 0 to 1 representing a completely homogenous and heterogeneous systems, respectively. However, in the model, the porosity values are continuously modified to compensate the effect of fluid pressure rise and fall. This modification is a function of rock compressibility which varies between $3x10^{-6}$ to $1x10^{-5}$psi^{-1} at a constant reference pressure of 14.7 psi.

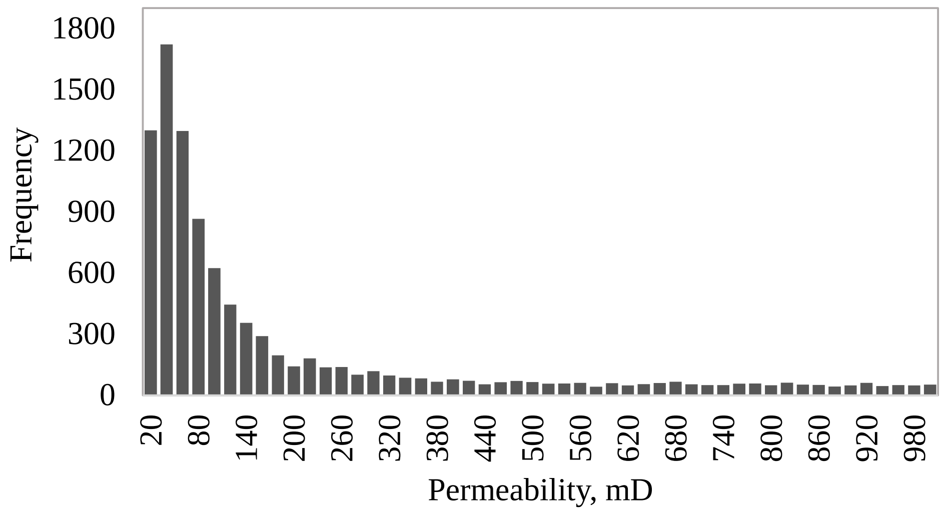

Figure 4.2. Permeability distribution.

Initial conditions are important parameters in designing the reservoir model. Reservoir pressure, bubble point pressure and water saturation are three parameters used to specify the reservoir's initial conditions. As the polymer flooding can begin after primary or secondary production stages, a wide range for the initial conditions parameters is selected. Both initial reservoir pressures and bubble point pressures are randomly selected within a range of 500 to 4,000 psi, hence, both saturated and undersaturated reservoir cases exit. Concerning the initial fluid saturations, no gas is assumed to be present at the start of the polymer flooding as the flood operation is only taking place in the pay zone. Random water saturation values are selected within a lower limit equal to irreducible water saturation which is changing from 0.1 to 0.3 and the upper limit of water saturation is 0.5. Consequently, all the reservoir cases built in this research have a minimum and maximum oil saturation of 0.5 to 0.9.

Reservoir temperature as one of the important properties of the reservoir under polymer flood, is determined as a function of reservoir depths. An average geothermal gradient of $1°\mathrm{F}/100$ft and a surface temperature of $70°$ F were used to calculate the reservoir temperature using Equation 4.1. The reservoir depths are between 500 and 10,000 ft. Consequently, the reservoir temperature is ranging from 75 to170 °F. This parameter is used in PVT calculations, which will be discussed in the rock and fluid section of this chapter.

$T = T_{surf.} + D/100$ ………………………….……………..…..... Equation 4.1

Where: T_{surf} *Surface temperature, ºF*
D *Depth, ft*

4.1.2 Rock and Fluid Properties

This part of the discussion is framed by a brief explanation on the methods and assumptions used in generating the PVT, polymer adsorption and relative permeability data sets. In order to create 10,000 reservoir scenarios with different rock and fluid properties a number of Matlab codes are developed.

4.1.2.1 Fluid Properties

Pressure-volume-temperature (PVT) relation consideration is an essential stage to understand the behavior of reservoir fluid in porous media. As the reservoir cases under investigation are all operating for ten consecutive years, it is expected to have many cases in which the reservoir pressure drop below the bubble point pressure. Consequently, the PVT calculations are necessary to perform in order to accurately considering the effect of pressure drop on gas evolution. The defined PVT properties in the simulator as function of reservoir pressure includes: solution gas ratio, oil formation volume factor, oil viscosity, gas expansion factor and gas viscosity. These factors are calculated using different methods and correlations. The calculated PVT properties are compared with the CMG Builder PVT Generator. In the Table 4.1 the methods available in CMG Builder for PVT calculation and the methods selected for this study are summarized.

Table 4.1. PVT calculation methods.

	CMG Builder	In this study
Solution Gas Ratio, [scf/STB]	− Standing − Vazquez and Beggs − Glaso − Lasater	− Vazquez and Beggs
Oil Formation Volume Factor, [RB/STB]	− Standing − Vazquez and Beggs − Glaso − Lasater	− Vazquez and Beggs
Oil Viscosity, [cp]	Dead Oil: − Beggs and Robinson − Beal and Chew − Glaso Live Oil: − Beggs and Robinson − Beal and Chew	Dead Oil: − Beggs and Robinson Live Oil: − Beggs and Robinson
Gas Critical Properties, Gas Viscosity [cp]	− Standing − Sutton	− Sutton (Critical gas properties) − Lee - Gonzalez – Eakin (Gas viscosity)

In calculation of solution gas ratio, R_s, and the oil formation volume factor, B_o, Vazquez and Begss (1980) correlations given in Equations 4.2 and 4.3 are used. R_s is a function of temperature, pressure, oil gravity and imperial constants depending on oil API gravities. B_o is calculated for below bubble point pressure as the simulator uses only saturated oil in the PVT table. The simulator automatically uses a variable substitution technique to calculate the PVT properties for under saturated conditions (IMEX User Guide, 2015). In Figure 4.2, the thick lines show the PVT data introduced to the simulator, dash lines show the modifications simulator makes if pressure is above the bubble point pressure.

$$R_s = C_1 \gamma_{gs} P^{C_2} e^{\left(C_3\left(\frac{\gamma_o}{T+460}\right)\right)} \text{...Equation 4.2}$$

$$C_1 = 0.0362\ (\gamma_o \leq 30), 0.0178\ (\gamma_o > 30)$$

$$C_2 = 1.0937\ (\gamma_o \leq 30), 1.1870\ (\gamma_o > 30)$$

$$C_3 = 25.7240\ (\gamma_o \leq 30), 23.9310\ (\gamma_o > 30)$$

Where: γ_{gs} *Gas gravity at separator condition of 100 psig*
γ_o *Oil gravity, °API*
P *Reservoir pressure, psia*
T *Reservoir temperature, °F*

$$B_o = 1 + C_1 R_s + C_2 (T - 60)\left(\frac{\gamma_o}{\gamma_{gs}}\right) + C_3 R_s (T - 60)\left(\frac{\gamma_o}{\gamma_{gs}}\right) \text{.............. Equation 4.3}$$

$$C_1 = 4.677x10^{-4} (\gamma_o \leq 30), 4.670x10^{-4}\ (\gamma_o > 30)$$

$$C_2 = 1.751x10^{-5}\ (\gamma_o \leq 30), 1.100x10^{-5}\ (\gamma_o > 30)$$

$$C_3 = -1.811x10^{-8}\ (\gamma_o \leq 30), 1.337x10^{-9}\ (\gamma_o > 30)$$

Where: R_s *Dissolved GOR, scf/STB*
γ_{gs} *Gas gravity at separator condition of 100 psig*
γ_o *Oil gravity, °API*
T *Reservoir temperature, °F*

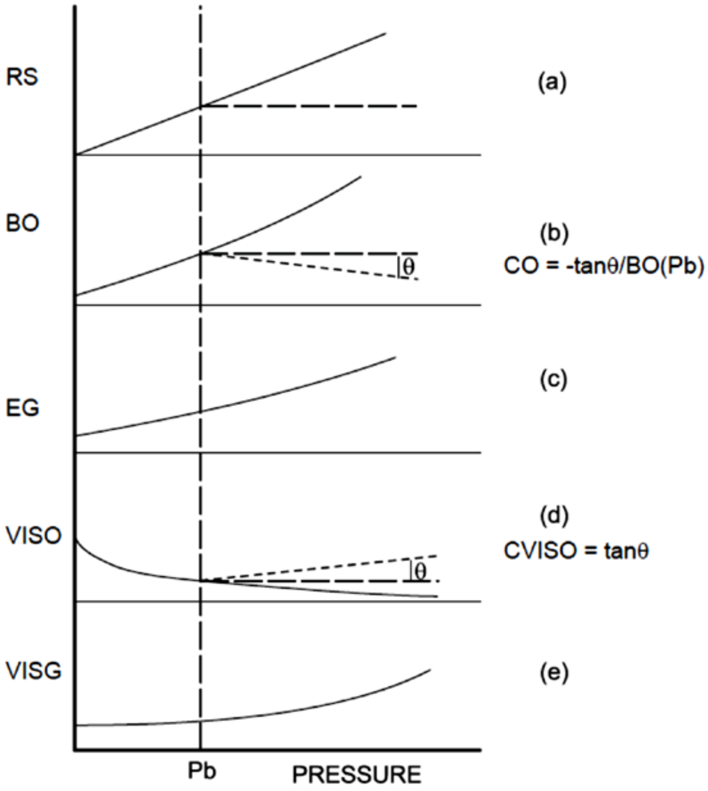

Figure 4.3. PVT data curves (IMEX User Guide, 2015).

The oil viscosity at pressures below bubble point requires two calculation steps. First step is to obtain dead oil viscosity when no dissolved gas exists using Equation 4.4. Second step is to use the previously obtained dead oil viscosity and solution gas oil ratio in Equation 4.5 to calculate the live oil viscosity.

$$\mu_{OD} = 10^{X} - 1 \quad \text{Equation 4.4}$$

$$X = Y\,T^{-1.163}$$

$$Y = 10^{Z}$$

$$Z = 3.0324 - 0.02023\,\gamma_o$$

Where: T Temperature, °F

γ_o Oil gravity, °API

$$\mu_o = A\,\mu_{OD}^{B} \quad \text{Equation 4.5}$$

$$A = 10.715\,(R_s + 100)^{-0.515}$$

$$B = 5.44(R_s + 150)^{-0.338}$$

Where: μ_{OD} *Dead oil viscosity, cp*

R_s *Dissolved GOR, scf/STB*

Oil density is calculated as a function of oil API gravity and taking a water density of 62.4 lb.ft^{-3} using Equations 4.6 and 4.7.

$$SG = \frac{141.5}{131.5 + \gamma_o} \qquad \text{Equation 4.6}$$

$$\rho_o = \frac{\rho_w}{SG} \qquad \text{Equation 4.7}$$

Where: γ_o *Oil gravity, °API*

ρ_w *Water density, lb/ft*^{3}

SG *Specific gravity*

Some of the parameters are constant for all the property calculations. These parameters are, gas specific gravity of 0.8, separator temperature and pressure of 80°F and 115 psi, respectively. The pseudo critical properties of the gas phase are calculated by Sutton (1985) correlation. Compressibility of gas is calculated by Dranchuk and Abou-Kassem (1990) equation of state (Aniemena, 2013). The obtained compressibility value is used to calculate the gas expansion factor using Equation 4.8. Gas viscosity is estimated by Equation 4.9 (Lee et al. 1966). Viscosity using this method is a function of reservoir temperature, apparent molecular weight and density of the gas.

$$E_g = \frac{1}{B_g} = 198.6\ \frac{P}{z.T} \qquad \text{Equation 4.8}$$

Where: *P* *Pressure, psia*

z *Gas compressibility factor*

T *Temperature, °R*

Bg *Gas formation volume facto, ft*^{3}*/scf*

$$\mu_g = Ae^{(B\rho_g^C)}10^{-4} \qquad \text{Equation 4.9}$$

$$A = \frac{(9.379 + 0.0160M_a)T^{1.5}}{209.2 + 19.26M_a + T}$$

$$B = 3.448 + \left(\frac{986.4}{T}\right) + 0.01009M_a$$

$$C = 2.447 - 0.2224B$$

Where: ρ_g *Gas density, lb/ft*^{3}
M_a *Apparent molecular weight, lb/lb.mol*
T *Temperature, ºR*

The parameters in PVT generated by the simulator is compared with the PVT data calculated using the above mentioned methods and all are shown in Figure 4.3 to Figure 4.7. The graphs represent a reservoir case with 30 °API oil at temperature of 122.5°F.

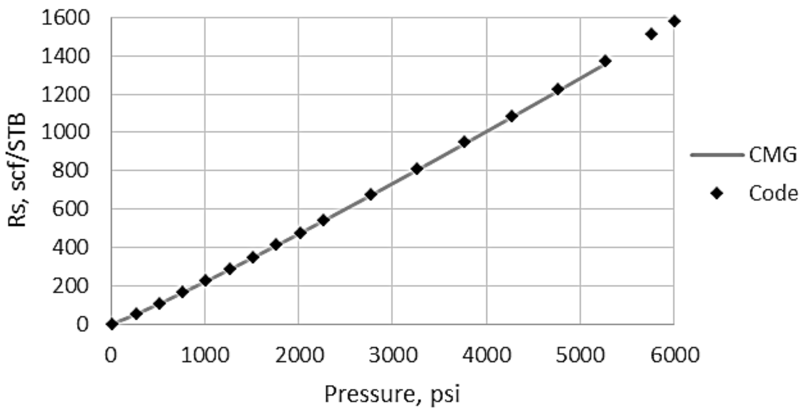

Figure 4.4. R_s vs. pressure obtained from CMG and calculation.

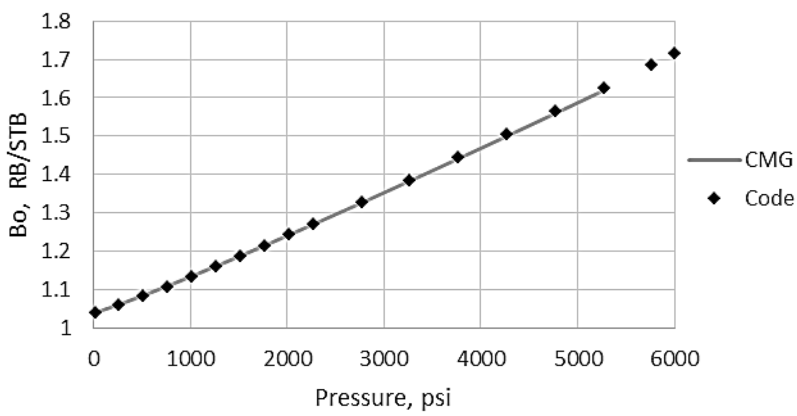

Figure 4.5. B_o vs. pressure obtained from CMG and calculation.

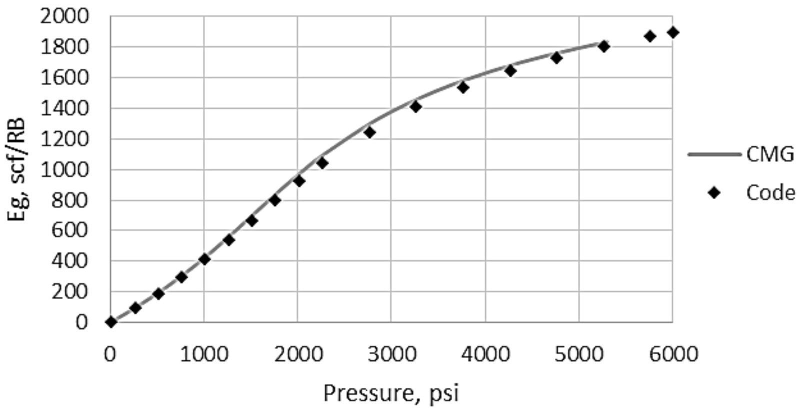

Figure 4.6. E_g vs. pressure obtained from CMG and calculation.

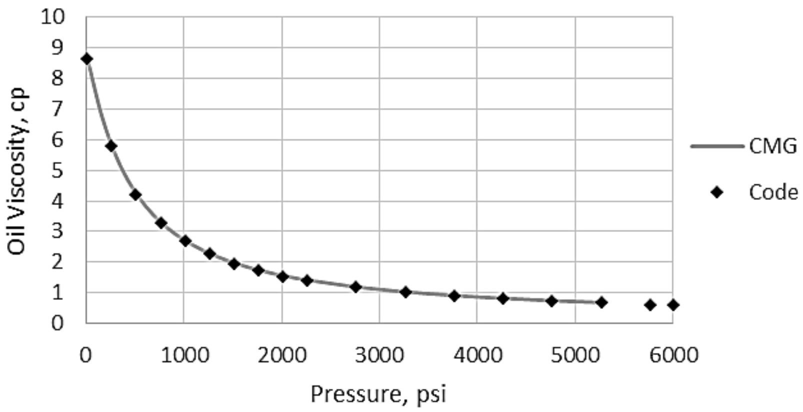

Figure 4.7. Oil viscosity vs. pressure obtained from CMG and calculation.

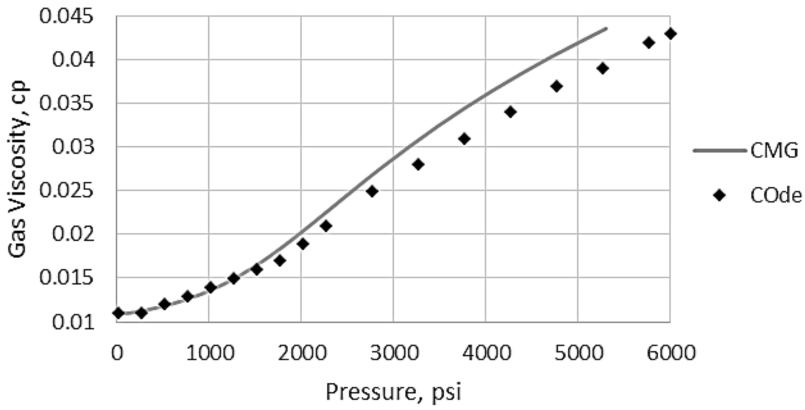

Figure 4.8. Gas viscosity vs. pressure obtained from CMG and calculation.

Some physical properties of the polymer as an additional component of the reservoir after the injection, is included in the model. CMG uses a nonlinear mixing model to modify the polymer solution viscosity accounting for the mixing of water and polymer. As shown in Equation 4.10, the mixture viscosity is a function of polymer viscosity, water viscosity and "α" which is a polymer concentration dependent parameter given in Equation 4.11. The reference polymer concentration in α is used to weight the polymer concentration for the viscosity mixing and it is assumed to be one. The new form of the nonlinear mixing model for solution viscosity is shown in Equation 4.12. The polymer concentration values, C_p, are randomly selected between 0.1 to 1 $lb.STB^{-1}$ to represent low to high polymer concentrations floods (Denney, 2009; Yang et al., 2006). A constant water viscosity of 0.3 cp was considered. This low water viscosity value is selected in order to taking account the high salinity and high temperature effect on water viscosity. (Sharqawy et al., 2012).

$$\mu_m = \mu_p^{o\alpha} + \mu_w^{(1-\alpha)} \quad \text{Equation 4.10}$$

$$\alpha = \frac{C_p}{C_p^o} \quad \text{Equation 4.11}$$

$$\mu_m = \mu_p^{oC_p} + \mu_w^{(1-C_p)} \quad \text{Equation 4.12}$$

Where: μ_p *Polymer viscosity, cp*

μ_w *Water viscosity, cp*

C_p *Polymer concentration, lb.STB*$^{-1}$

4.1.2.2 Rock-Fluid Interaction

Relative permeability and capillary pressure are the two essential factors to be considered when flow mechanics in the porous media is assessed. In addition, these factors have a great importance in reserve and recovery estimation. The chemical properties of both fluid and rock, as well as the structure of the rock are the main reasons altering the relative permeability and the capillary pressure.

Effective permeability and absolute permeability are two terms that are needed to be defined prior to starting relative permeability concept. Conducted laboratory studies confirm that the effective permeability to a fluid is influenced by the fluid saturation and wetting property of reservoir rock. The absolute permeability is a rock property, determining the capability of the formation fluid flow. As in the real reservoirs more than one fluid exists, relative permeability should be defined for each of the phases. Relative permeability of a fluid is the ratio of its effective permeability to the absolute permeability at a given fluid saturation (Ahmed, 2010). In this study, two relative permeability data sets are used. First relative permeability data set is for the water-oil system and the second one is for liquid and gas phases. Both of the data sets are accounting for two-phase flow of the wetting and non-wetting phases. In the model, as the initial condition of the reservoirs are gas free, the oil-water relative permeability data is used. Later, when the reservoir pressure drops below the bubble point pressure, the liquid-gas relative permeability curves are considered in the calculations. Two phase relative permeability data in this study were generated using Corey's correlations. The relative permeability calculations for oil-water system are calculated with Equations 4.13 and 4.14. In the liquid-gas relative permeability data set, Equations

4.15 and 4.16 are used to generate the relative permeabilities (Corey, 1954; Sun & Ertekin, 2017).

$$k_{rw} = \left(\frac{S_w - S_{wirr}}{1 - S_w - S_{wirr}}\right)^n \text{..................................} \quad \text{Equation 4.13}$$

$$k_{row} = \left(\frac{1 - S_{or} - S_w}{1 - S_{or} - S_{wirr}}\right)^n \text{..................................} \quad \text{Equation 4.14}$$

$$k_{rg} = \left(\frac{S_g}{1 - S_{wirr}}\right)^n \text{..................................} \quad \text{Equation 4.15}$$

$$k_{rog} = \left(\frac{1 - S_g - S_{wirr}}{1 - S_{wirr}}\right)^n \text{..................................} \quad \text{Equation 4.16}$$

Where: *n* *Relative permeability exponential coefficient*
S_w *Water saturation, fraction*
S_{wirr} *Irreducible water saturation, fraction*
S_{or} *Residual oil saturation, fraction*
S_g *Gas saturation, fraction*

Capillary pressure in the reservoir system is a function of several reservoir rock and fluid properties. These parameters are namely: surface tension of rock and fluid, interfacial tension between fluids, pore size, pore geometry and wetting properties of the formation. Any two combination of the reservoir fluids namely, oil, gas and water result in immiscible mixture that a discontinuous pressure presents between them. The pressure difference between the wetting and the non-wetting phase is called capillary pressure (Ahmed, 2010). Corey's method is utilized for generating the capillary pressure data as a function of fluid saturation. Equations 4.17 and 4.18 are used to calculate capillary pressures for oil-water and liquid-gas systems, respectively. Water saturation (S_w), residual oil and irreducible water saturations (S_{or}, S_{wirr}), relative permeability curve exponential coefficient (n) and the capillary pressure coefficient for oil and gas (C_o, C_g) are the five variables used to generate relative permeability and capillary pressure as function of saturation.

$$P_{cow} = \frac{C_o}{\sqrt{\frac{S_w - S_{wirr}}{1 - S_{or} - S_{wirr}}}} \text{..................................} \quad \text{Equation 4.17}$$

$$P_{cog} = \frac{C_g}{\sqrt{\frac{1-S_g-S_{wirr}}{1-S_{wirr}}}} \qquad \text{Equation 4.18}$$

Where: C_o *Oil capillary pressure coefficient*
C_g *Gas capillary pressure coefficient*
S_w *Water saturation, fraction*
S_{wirr} *Irreducible water saturation, fraction*
S_{or} *Residual oil saturation, fraction*
S_g *Gas saturation, fraction*

The mechanism effecting the polymer injection process in the model accounts for the mobility control, polymer retention and dispersion, inaccessible pore volume, apparent viscosity and resistance factor. However, it should be noted that among all the mentioned factors, the mobility ratio and viscosity alteration due to polymer adsorption. Adsorption of polymer on the rock surface during flooding is introduced to the simulator as a function of polymer concentration. In Figure 4.8, three common adsorption isotherms, Langmuir, Freundlich and Linear adsorption isotherms are shown. In polymer adsorption studies generally Langmuir isotherm is used. Langmuir adsorption isotherm, given in Equation 4.19 is used to generate polymer concentration and adsorption table. This type of isotherm indicates that at low polymer concentration the adsorption level rapidly rises to its maximum value and then becomes plateaus for higher concentrations.

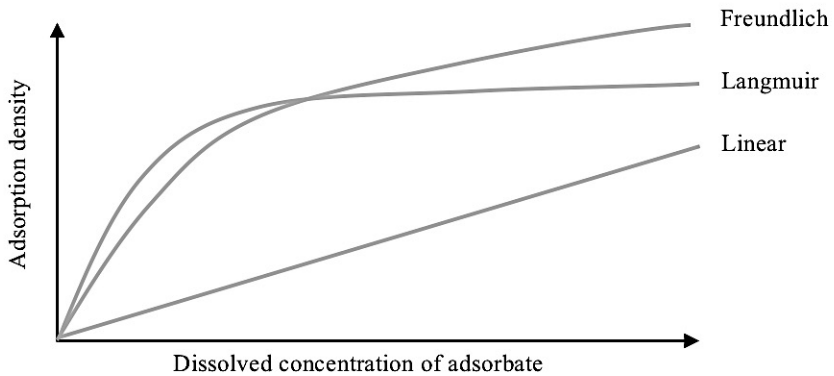

Figure 4.9. Commonly reported adsorption isotherms.

The coefficient of a_{max} and b values are adjusted to fit the function with the default concentration and adsorption data provided in the simulator. With a_{max}, maximum adsorption capacity equal to 0.15 $lb.STB^{-1}$ and b, a constant (function of enthalpy of adsorption and temperature) equal to 4 the curve fits perfectly with the concentration and adsorption graph of the simulator as shown in Figure 4.9 it has been observed that several factors can significantly alter the adsorption level of the polymer. These parameters namely are polymer type, surface area and type of the rock, pH, salinity, hardness of the solvent water (Sorbie, 1991). In order to take account the mentioned effects, wide ranges for a_{max} from 0.01 to 0.3 and b from 1 to 20 are selected.

$$a = a_{max} \frac{b.C}{1+b.C} \qquad \text{Equation 4.19}$$

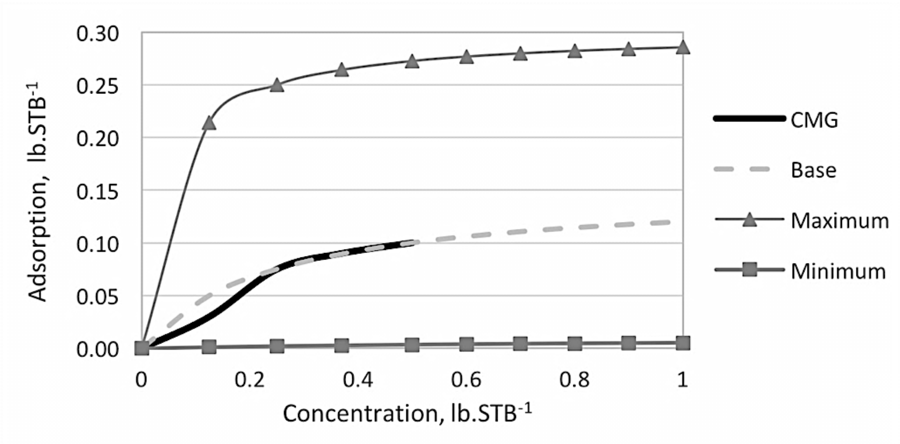

Figure 4.10. Polymer adsorption isotherms.

4.1.3 Operational Conditions

Several operational parameters and constraints can be defined in CMG IMEX reservoir model undergoing polymer flooding process. Namely, wellbore's location and geometry, wellhead and bottom hole pressures, fluid injection duration and its polymer concentration are the parameters controlling the operational aspects of the flooding process. In this study, one injection and one producer wells are indicated in the model. The well spacing in different production scenarios are between 565 to 1697 ft. Both wells are restricted by a maximum bottom hole pressure values. Flow rates of the wells are considered to be extremely high in order to letting the wells injecting and producing with any flow rate and having bottom hole pressure as the only controlling operating factor. For each of the reservoir cases, injection and production bottom hole pressures are a function of initial reservoir pressure, P. Using the fact that injector bottom hole pressure, $P_{bhp\ (inj.)}$, should be higher that reservoir pressure, this pressure is taken randomly between a minimum pressure of P+1500 psi and a maximum pressure of P+3000 psi. In order to have the flow toward the producer, the bottom hole pressure at the producer, $P_{bhp\ (prod.)}$, is selected below the reservoir initial pressure. $P_{bhp\ (prod.)}$ is a pressure value between 5% and 95% of the reservoir initial pressure for lower and upper limits of the random value selection, respectively.

4.1.4 Grid Sensitivity

Model sensitivity analysis is a very crucial preliminary step for numerical models. Sensitivity of the reservoir model was necessary to perform to determine the minimum number of grids which could result in accurate outputs in an acceptable computational time. In general, simulation time and accurate results both are directly related with the number of grids. Considering 20,000 simulation cases of this research practice, grid block sensitivity is an important stage to minimize the total computational time of the simulations. A base polymer flood scenarios having average of all the reservoir and operational parameters is used for grid sensitivity analysis. The CMG's template for polymer flood process (mxspr005) using the base values is shown in Appendix A. Cumulative oil production, Cumulative water production and the average reservoir pressure are the parameters selected to compare the total simulation elapse time. Using the base values for all the input parameters, seven models are generated with different number of grid blocks from 5x5 to 35 x 35. In Figures 4.10 through 4.12 the simulation elapse time shows a sharp increase when the grid number is 30x30 or more. In Table 4.2 the relative change percentages of two consecutive grid number gives information on how fast we can approach to a stable value while increasing the grid number. Cumulative oil production has the least relative change percentage as the grid number increased. This relative change percentage is so small that one can say that the accuracy of this parameter is not affected by the grid number as the relative change is not more than 1%. In addition, average reservoir pressure value is perfectly stabilized for grid number 15x15 or more with relative change of less than 0.5%. However, cumulative water production is greatly sensitive to the number of the grids. Considering the results of the most sensitive parameter, the cumulative water production and the elapsed time, it can be logical to decide on a model with 25x25 grids. This is firstly due to computational time that it is hugely increasing for 35x35 grids. Furthermore, the cumulative water production relative change for different grid numbers is dropping to less than 10% for the grid number of 25x25 and more.

Table 4.2. Relative change percentages of successive grid numbers.

Grid Number	Oil Production	Water Production	Reservoir Pressure
5x5 & 10x10	0.9 %	24.5 %	4.7 %
10x10 & 15x15	0.8 %	16.1 %	2.2 %
15x15 & 20x20	0.8 %	14.2 %	0.5 %
20x20 & 25x25	0.7 %	11.1 %	0.2 %
25x25 & 30x30	0.5 %	7.6 %	0.3 %
30x30 & 35x35	0.3 %	5.9 %	0.4 %

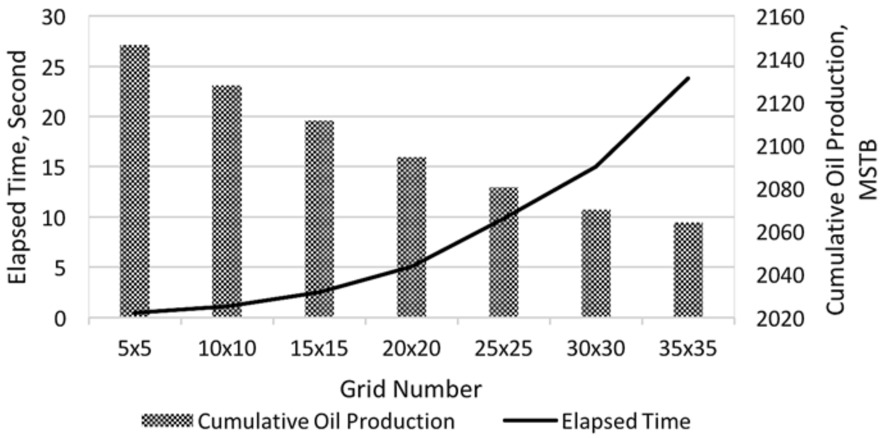

Figure 4.11. Cumulative oil production sensitivity to the model grid number.

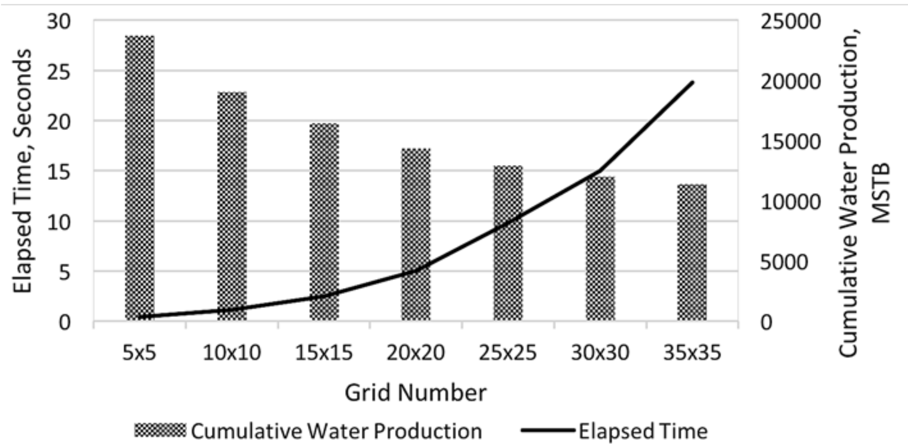

Figure 4.12. Cumulative water production sensitivity to the model grid number.

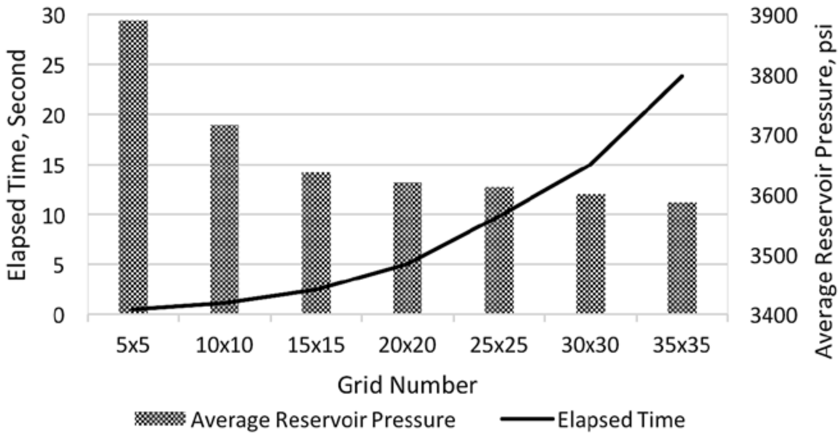

Figure 4.13. Cumulative oil production sensitivity to the model grid number.

4.1.5 Generation of the Data Set for the Data-Driven Model

In order to compute the efficiency of the polymer flooding process, the performance of a reservoir when reservoir is flooded by polymer should be compared with the performance when the reservoir is producing by its natural drive mechanism. In this study 20,000 production scenarios are generated by combination of the parameters randomly selected within a specified range as shown Table 4.3. These scenarios include 10,000 no injection reservoir cases in which all the parameters are kept the same as 10,000 polymer flooding scenarios except shutting down the injector well.

The performance indicators for ten years of production for 20,000 simulation runs are summarized in Table 4.4. Among total 20,000 simulator runs 7,200 are omitted as they could not normally terminate the run process due to convergence problem. This is due to some reservoir cases that the random parameter combination may not be logical. Among the converged cases, material balance error for 3,000 random polymer injection and no injection cases are checked. Almost all the case are resulting in a material balance error of one, which is indication of logical flow behavior in the reservoir system. The material balance error frequency for both production scenarios are presented in Figures 4.14 and 4.15, respectively.

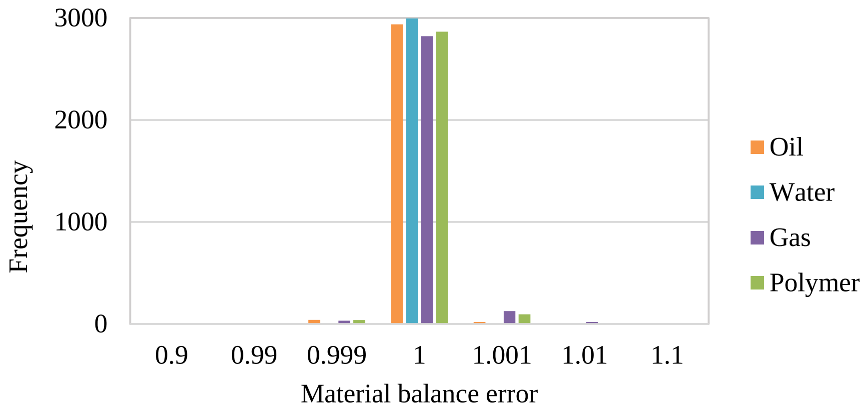

Figure 4.14. Polymer injection cases material balance error frequencies.

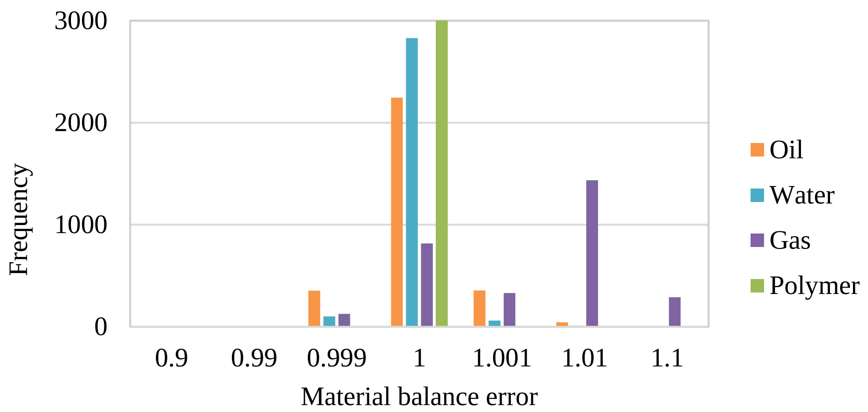

Figure 4.15. No injection cases material balance error frequencies.

Table 4.3. Range of model input parameters.

Parameters	**Minimum**	**Maximum**
Well Spacing, *ft*	565	1,697
Layer Thickness, *ft*	2	100
Reservoir Depth (D), *ft*	500	10,000
Permeability Anisotropy Ratio (k_V/k_H)	0.01	1
Porosity (ϕ),*fraction*	0.1	0.4
Permeability (k), *mD*	1	2,000
Pore Compressibility (CPOR), psi^{-1}	3×10^{-6}	1×10^{-5}
Oil Gravity (γ_o), *°API*	15	45
Bubble Point Pressure (P_b), *psi*	Less than reservoir pressure	
Reservoir Pressure (P), *psi*	500	4,000
Adsorption Coefficient (b)	1	20
Maximum Polymer Adsorption (a_{max}), $lb.STB^{-1}$	0.01	0.3
Reference Polymer Solution Viscosity (PVISC), *cp*	1	5
Irreducible Water Saturation (S_{wirr})	0.1	0.3
Residual Oil Saturation (S_{or})	0.1	0.3
Relative Permeability Coefficient (n)	2	4
Oil Capillary Pressure Coefficient (C_o)	0.5	4
Gas Capillary Pressure Coefficient (C_g)	0.1	0.3
* Water Saturation (S_w)	S_{wirr}	0.5
Polymer Concentration (C_p), $lb.STB^{-1}$	0.1	1
**Injector Bottom Hole Pressure ($P_{bhp\ (inj.)}$), *psi*	P + 1,500	P + 3,000
**Producer Bottom Hole Pressure ($P_{bhp\ (prod.)}$), *psi*	0.05P	0.95P

* *Lower limit is S_{wirr} dependent*

** *Reservoir pressure dependent*

Table 4.4. Performance indicators collected from runs.

Performance Indicators	Scenario Type	Injection/Production	Term
Cumulative Oil	Polymer Flood	Production	$N_{p\ (poly)}$
	No Injection	Production	$N_{p\ (no.\ inj)}$
Cumulative Water	Polymer Flood	Production	$W_{p\ (poly)}$
		Injection	$W_{i\ (poly)}$
	No Injection	Production	$W_{p\ (no.inj)}$
		Injection	$W_{i\ (no.inj)}$
Cumulative Polymer	Polymer Flood	Production	P_p
		Injection	P_i

In order to evaluate the efficiency of the polymer flooding process, the performance indicators collected from polymer flood and no injection scenarios are used to derive a single efficiency value. As the performance indicators are generated for every year of production for a time span of 10 years, it is a necessity to create a single value output which could represent large number of performance indicators, hence, could be fed into neural network for the training process. Yearly cumulative oil production from polymer injection and no injection scenarios and the cumulative polymer injection are the performance indicators used in calculation of efficiency value. Steps I through IV are followed to generate the efficiency value. Five data sets containing efficiencies and water cuts at different injection durations of two to ten years are calculated using Equation 4.30 and 4.31 to feed the five ANN models. A volumetric efficiency term, is also defined using Equation 4.32. The volumetric efficiency is used to parametrically evaluate the polymer flooding method as the division of the efficiency value by the reservoir volume can eliminate the effect of reservoir size and provide net effects of the reservoir and operational parameters. The process of feeding and training the data driven screening tool and the parametric studies on the reservoir simulator results are presented in the following chapters.

a) Yearly oil and water productions of polymer injection and no injection scenarios for $n = 1,2,\dots,10$ years of production:

$N_{p(poly)_n} = N_{p(poly)_n} - N_{p(poly)_{n-1}}$ ……..........………….........Equation 4.20

$W_{p(poly)_n} = W_{p(poly)_n} - W_{p(poly)_{n-1}}$ ....……….……………........Equation 4.21

$N_{p(no.inj)_n} = N_{p(no.inj)_n} - N_{p(no.inj)_{n-1}}$ ....……………...…......Equation 4.22

$W_{p(no.inj)_n} = W_{p(no.inj)_n} - W_{p(no.inj)_{n-1}}$ ....…………...…......Equation 4.23

b) Yearly polymer injection, oil and water production increments ($n = 1,2,\dots,10$):

$P_{p_n} = P_{p_n} - P_{p_{n-1}}$ ....…………………...…………...……...Equation 4.24

$N_{p_n} = N_{p(poly)_n} - N_{p(no.inj)_n}$ ....……………...….................Equation 4.25

$W_{p_n} = W_{p(poly)_n} - W_{p(no.inj)_n}$ ....………………..................Equation 4.26

c) 10 % discounted net present value (*npv*) for two years increments ($n = 2, 4, 6, 8, 10$) of polymer injection, oil and water productions:

$N_{npv\,(n)} = N_{npv}\left({N_{p_n}}/{N_{npv}}, 10\%, n\right)$…......………..…...…Equation 4.27

$P_{npv\,(n)} = P_{npv}\left({P_{pn}}/{P_{npv}}, 10\%, n\right)$………………..……Equation 4.28

$W_{npv\,(n)} = W_{npv}\left({W_{pn}}/{W_{npv}}, 10\%, n\right)$…...………….……Equation 4.29

d) Efficiency value for two years increments ($n = 2, 4, 6, 8, 10$):

a) $Efficiency_n = \frac{N_{npv\,(n)}}{P_{npv\,(n)}}$....………...……………..……...Equation 4.30

b) $Water\ cut_n = \frac{W_{npv\,(n)}}{N_{npv\,(n)} + W_{npv\,(n)}}$....………...…....……...Equation 4.31

c) $Volumetric\ efficiency_n = \frac{N_{npv\,(n)}}{P_{npv\,(n)}\ X\ V_{res}}$……………....Equation 4.32

4.2 Screening Tool Development

This part provides the methodology followed for the development of the screening tool, which is a neural-network based model. MATLAB Neural Network Toolbox (2013) is utilized to construct and train the network with a data set generated by the reservoir simulator's inputs and outputs.

4.2.1 Optimization of Neural Network's Design Parameters

The structure of the neural network depends on the data set comprised of the simulator input and output data, namely reservoir properties, operational parameters and the performance indicators. Referring to the fact that a huge data set necessitates a large amount of computation, a complex problem such as reservoir performance prediction with large number of inputs and outputs may decrease the accuracy of the model. Consequently, to enhance the accuracy, the complexity of the polymer flooding performance prediction problem is reduced by creation of five different ANN models, representing two, four, six, eight and ten years of polymer injection. ANN model for two years polymer injection is presented in Appendix B. All models are fed with similar input and functional links components which are tabulated in Table 4.5. Though, the outputs defer according to the injection period and the optimum topography varies for each ANN model. In order to develop a reliable and accurate model, several design components are optimized individually for each of these five ANN models. A systematic trial and error approach is utilized to obtain the optimum network structures. A set of guidelines and procedures are taken into account to create and optimize the screening models. In order to validate the network's performance, regression plots are evaluated to ensure perfect fits. The regression plot displays the network outputs with respect to training targets. In a perfect fit, network outputs should lie along a 45 degree line which represents where the outputs are equal to targets.

Table 4.5. Input and output components of the ANN models.

Input	Reservoir Properties	Well Distance Net Thickness Thickness-Weighted Average Porosity Thickness-Weighted Average Permeability Lorenz Coefficient Permeability Anisotropy Ratio Pore Compressibility Oil Gravity Reservoir Depth Reservoir Pressure Bubble Point Pressure Water Saturation Irreducible Water Saturation Residual Oil Saturation Relative Permeability Coefficient Oil Capillary Pressure Coefficient Gas Capillary Pressure Coefficient Adsorption Coefficient Maximum Polymer Adsorption Reference Polymer Solution Viscosity
	Operational Parameters	Polymer Concentration Injector Bottom Hole Pressure Producer Bottom Hole Pressure
	Functional Links	f_1: *Oil Density* f_2: *Oil Saturation* f_3: *Poly. Conc.* / S_w f_4: *Side* ^{2} *x Thickness* f_5: *Poly. Conc.* / $P_{bhp\ (prod.)}$ f_6: *Reservoir Temperature* f_7: *Res. Pressure* / $P_{bhp\ (inj.)}$ f_8: *Res. Pressure* / $P_{bhp\ (prod.)}$ f_9: (*Res. Vol.* x S_{oi} x ϕ) / 5.615
Output	Performance Indicators	$^{*}Efficiency_{(n)} = \frac{N_{npv\ (n)}}{P_{npv\ (n)}}$ $^{*}Water\ cut_{(n)} = \frac{W_{npv\ (n)}}{N_{npv\ (n)} + W_{npv\ (n)}}$

** n=2, 4, 6, 8, 10 for ANN(2.yrs), ANN(4.yrs), ANN(6.yrs), ANN(8.yrs), ANN(10.yrs), respectively.*

During the optimization procedure, it has been observed that the efficiency output was more complex for the network to be predicted accurately. Therefore, the models were primarily optimized by considering the accuracy of the prediction of the efficiency parameter, as the network was capable of precisely predicting water cut output without getting significantly influenced by different network structures. In the following sections, the optimization procedure is discussed in details and step by step structure selection for two years polymer injection model (*2.yrs*) is presented.

Size of the dataset is an important design component as the optimum number of cases should be fed to train the network. Providing the network with unnecessary and extra data cause memorization and over fitting problems. On the other hand, not sufficient data cause under fitting which the network fail to predict a requisite trend regardless of the structure being used. In this study, after experimenting the models with different number of datasets, the use of total 6400 available cases offered the best product. It should be noted that normalization of the data set is a very important stage prior to feeding to the network when the input and the output variables are in different ranges (e.g. $3\ x\ 10^{-6}$ <CPOR< 10^{-5} psi^{-1} and 500 < P < 4,000 psi). In feedforward backpropagation of multi-layer network training, the most commonly used activation functions are sigmoid functions. It is a necessity to normalize the data set between 0 to 1 for binary sigmoid function and -1 to 1 for bipolar sigmoid function. Considering that the generated data set contains negative and positive values, the normalization is performed with a range of -1 to 1.

Division of dataset is the number of cases subdivided into training, validation and testing sets. In addition to the optimum total number of data being used for the network, sufficient number of cases in the training set has high importance in order to prevent over-fitting or under-fitting problems. Training data set as the first subset, is used to updating and arriving at optimum weights. Second subset is the validation set which is used to evaluate the performance of the network on new patterns and stop the training process when the best generalization is achieved. In the testing set as the last subset, the overall performance of the network is generated. The division percentage of data set for the validation and testing sets should be also evaluated to be confident that the sets are covering a wide variety of patterns. Different data division percentages are selected for each of the models. Table 4.6 shows the dataset division for training, validation and testing sets of two years polymer injection model. The model is tested with 50% to 90% division for the training set and the remaining data are equally divided for the validation and the testing sets. In *2.yrs* model the optimum division is selected as 70%, 15% and 15% for the training, validation and testing sets, respectively. In this selection the priority is given for the testing set regression following by training and overall regressions. It should be noted that the cases within the sets are randomized prior to feed the network to ensure that relatively same cases are not piled up in any of the subsets. Hence, “divideint” function is used instead of commonly used “dividerand” (Matlab, 2013). This procedure results in training, validating and testing same cases for each of the sets as trial and error method is used for the optimization.

Determination of number of neurons, layers and functional links is the most important and significant step in ANN structure design. In this study, once the number of data and their division into training, validation and testing sets are optimized, the next step is to decide upon number of neurons within the hidden layer(s). First, Neuroshell rule-of-thumb formula suggested for the selection of optimum number of neurons is used. This experimentally derived equation is dependent on number of input and output variables as well as the total number of the dataset used in the training data set given in Equation 4.33 (Neuroshell, 1998). It should be noted that the equation is not derived on theoretical basis, hence it can be used only to have a rough estimation on the optimum neuron number when starting to the optimization process (Artun, 2008). Neuroshell equation recommended to start to the optimization with 95 neurons, as 32 input neurons (N_i), 2 output neurons (N_o) and average of 5760 dataset in the training set are used in the model. 75, 85, 95, 105, 115 neurons are adjusted to the single hidden layer model during optimization process. This neuron number optimization results for two years polymer injection model is summarized in Table 4.7. It can be seen that the highest regression for the testing set is 0.931 when 85 neurons is selected. However, this neuron number is considerably reducing the training performance. Consequently, the total of 95 neurons results in acceptable regressions for both testing and training sets.

$$N_n = \frac{N_i + N_o}{2} + \sqrt{Total\ number\ of\ dataset\ in\ traning\ set} \quad \text{.........Equation 4.33}$$

Table 4.6. Data set division optimization for *2.yrs* polymer injection model.

Divisions Training, Validation, Testing	Efficiency Regression			
	Training	Validation	Testing	Overall
50%, 25%, 25%	0.901	0.834	0.798	0.856
60%, 20%, 20%	0.945	0.924	0.896	0.928
***70%, 15%, 15%**	**0.950**	**0.939**	**0.923**	**0.941**
80%, 10%, 10%	0.946	0.941	0.863	0.932
90%, 5%, 5%	0.960	0.923	0.898	0.949

* *Selected data division*

Table 4.7. Neuron number optimization for *2.yrs* polymer injection model.

# Neurons	Efficiency Regression			
	Training	Validation	Testing	Overall
75	0.944	0.937	0.898	0.932
85	0.911	0.908	0.931	0.891
***95**	**0.950**	**0.939**	**0.923**	**0.941**
105	0.921	0.910	0.838	0.902
115	0.930	0.915	0.846	0.909

* *Selected neuron number*

When the optimum neuron in one hidden layer structures is achieved, the model is evaluated with two hidden layers by dividing the total neuron number in different distribution of neurons in the first and the second layer. The different neuron division in two layer model is made in such a way that the number of neurons in first layer is higher than the next layer. The optimization results of neuron division within two layer structure for *2.yrs* model is presented in Table.4.8. Referring to the table, it can be observed that a configuration with 60 neurons in the first hidden layer and 35 neurons in the second hidden layer results in the best regression of the testing set. Moreover, the performance of the model is evaluated using different functional links and different combinations of these functions. It has been observed that using nine functional links which previously presented in Table 4.5 results in the best performance. Furthermore, during the training process, it has been detected that the network is sensitive to low polymer concentrations values, thus in four functional links, concentration is included. The regression results for *2.yrs* model with and without functional links are shown in Table 4.9.

Table 4.8. Neuron division optimization in two layer structure for *2.yrs* polymer injection model.

# Neurons	Efficiency Regression			
Layer 1, Layer 2	Training	Validation	Testing	Overall
50 + 45	0.979	0.941	0.898	0.956
55 + 40	0.968	0.935	0.874	0.943
***60 + 35**	**0.972**	**0.915**	**0.928**	**0.953**
65+ 30	0.937	0.911	0.872	0.919
70 + 25	0.969	0.923	0.921	0.953

* *Selected neuron number in the hidden layers*

Table 4.9. Function optimization for *2.yrs* polymer injection model.

Functions	Efficiency Regression			
	Training	Validation	Testing	Overall
***Nine Functions**	**0.972**	**0.915**	**0.928**	**0.953**
No Function	0.980	0.918	0.912	0.956

* *Selected functional link*

The regression plots of the testing, validation, training sets and overall data for efficiency and water cut values are shown in Figures 4.16 and 4.17. The same optimization procedure used for the two years polymer injection model is also implemented for generating the optimum models for four to ten years of injection models. The optimum network structure for the five ANN models are summarized and presented in the results chapter of this study.

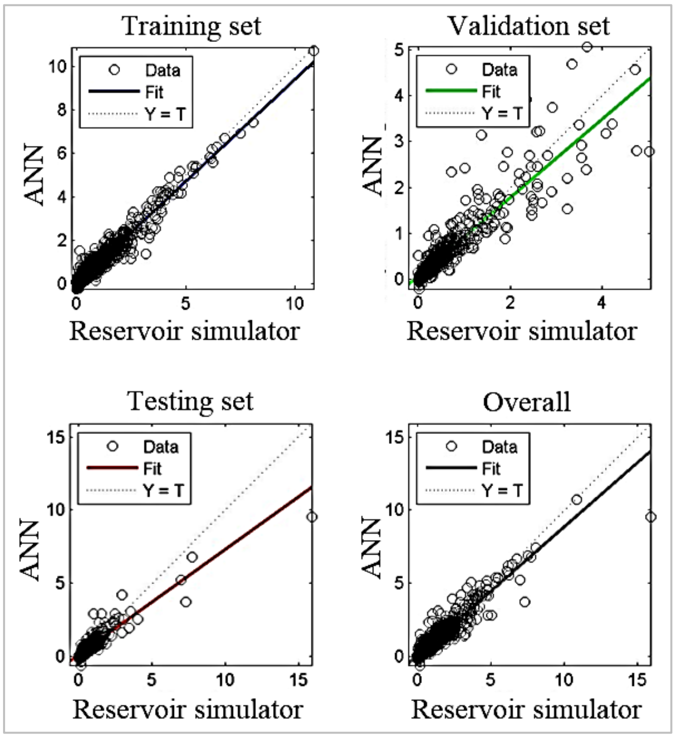

Figure 4.16. Regression plots for the efficiency output.

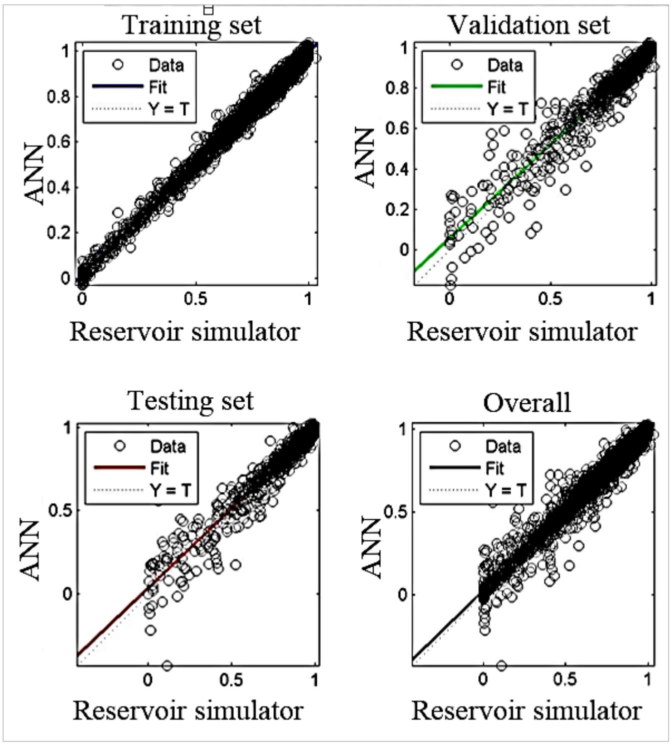

Figure 4.17. Regression plots for the water cut output.

CHAPTER 5

RESULTS AND DISCUSSIONS

In this chapter, the results obtained from reservoir simulation and screening tool developed for polymer flooding process are discussed in detail. In the first part, the results of the reservoir simulation are investigated to understand how the reservoir and operational parameters work against or in favor of the polymer injection process. Second part is aiming to evaluate the performance of the developed polymer flooding screening tool, ensuring that the tool is sufficiently capable of generalizing the relation among the parameters. Ultimately, the developed Graphical User Interface (GUI) for the polymer flooding screening tool is introduced.

5.1 Parametric Study of Reservoir Simulator Results

In this part the polymer flooding performance is assessed to have a better understanding of the optimum ranges of reservoir and operational parameters in favor of the polymer flooding process. A screening guideline is offered, which suggest the optimum variable ranges as well as accounting their order of significance. Furthermore, the practical implementations of the data-driven polymer flooding screening model is presented.

5.1.1 Evaluation of High Performance Polymer Flooding Scenarios

The parametric study is conducted on the best 500 efficiency cases out of 6400 total polymer injection scenarios. For the selection of the most successful ones, both of the defined unit efficiency and the water cut values are considered by dividing the two outputs as shown in Equation 5.1. The reason behind defining such an indicator to select the efficient cases are: (1) the unit efficiency is the ratio of the incremental oil production over incremental polymer injection which is divided by the reservoir volume to eliminate the effects of the reservoir size, (2) the unit efficiency value is divided by the water cut value to eliminate the cases which have high efficiency as well as very high water cuts.

$$Efficiency_{normalized,n} = \frac{Volumetric\ efficiency_n}{Water\ cut_n}$$ ……………………..Equation 5.1

$Where\ (n = 2, 4, 6, 8, 10)$

In order to analyze the effect of the reservoir and operational parameters on the performance of the polymer flood, histograms of all the parameters are plotted to visually observe the number of occurrences of successful cases within a different range of the parameters. The provided histograms are intended to illustrate two distinctive information: 1) the thick bars represent the frequency percentage of the total scenarios for a specific parameter, 2) the line bars show the number of occurrences successful cases for different injection duration. These data are presented on the same graph, to conveniently decide whether a non-uniform distribution of the efficient cases is resulted by the original distribution type of the all the cases or it should be considered as the parameter's own effect on the flooding performance.

Distribution of the total and 500 most efficient cases for different reservoir depth intervals is shown in Figure 5.1. The graph suggest that the performance of the polymer flooding is not effected by the reservoir depth as the successful cases show similar distribution profile as all the cases. Likewise, in Figure 5.2 the distribution of the total and efficient cases with different injection duration indicates that the thickness of the reservoir is not affecting the polymer flooding performance. This is an expected distribution as the reservoir volume effect on the unit efficiency ($E_{(u)n}$) value is ignored. Thickness weighted average porosity histogram is shown in Figure 5.3. The plot indicates that higher porosity can positively affect the efficiency of the process. Figure 5.4 shows the histogram of the thickness weighted average permeability. The permeability distribution graph suggest that the permeability is a critical parameter as the histogram of the best 500 cases deviates notably from the histogram of the total 6400 cases. About 65% and 25% of the best performance cases have permeability of less than 80 and 160 mD, respectively. However, the distribution of the permeability in all the cases shows a frequency percentage of around 50 for permeability values less than 160 mD. Regarding higher permeability values, almost no successful case is observed for permeability above 400 mD. Though, these high permeabilities contribute to 16% of the all the cases under investigation. Considering the effect of the porosity and the permeability, it should be emphasized that the porosity of the formation has a marginal effect on the polymer flooding efficiency comparing with the permeability. The combinational effect of the thicknesses, porosities and permeabilities can be observed from Lorenz value histogram. As shown in Figure 5.5 the low Lorenz values representing more homogeneous reservoirs, are in favor of polymer flooding application. The Lorenz coefficient distribution within successful cases is denser for the coefficients less than 0.5. For more homogeneous reservoirs the distribution of normalized efficiency and all the cases are 80% and 50%, respectively. Hence, the homogeneity or heterogeneity level of the reservoir has significant importance for polymer flooding process as it directly contributes to high fingering and resulting in high water cuts.

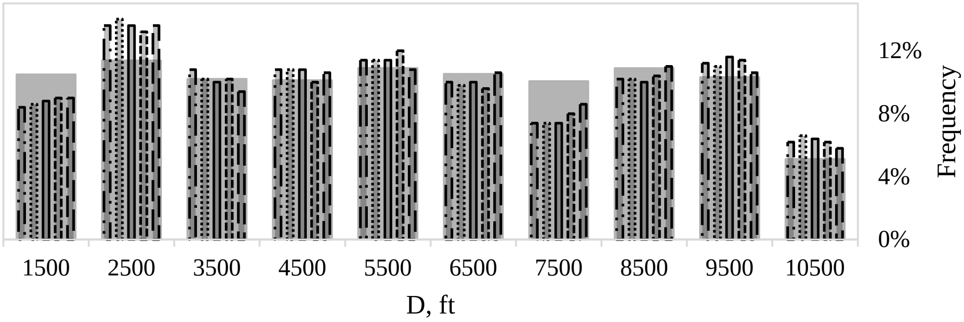

Figure 5.1. Reservoir depth distribution in best 500 and all the cases.

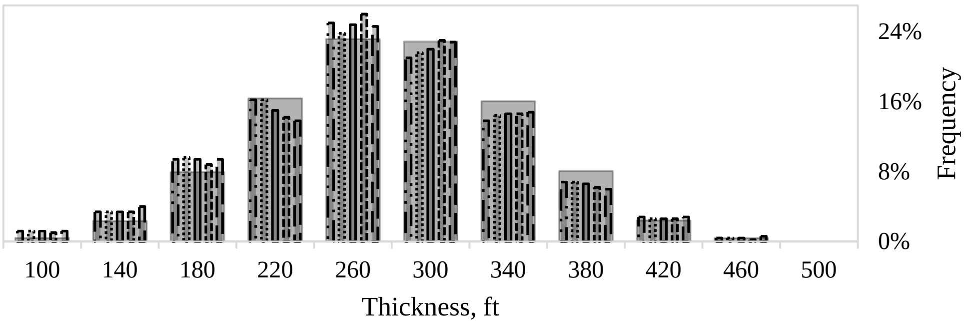

Figure 5.2. Reservoir thickness distribution in best 500 and all the cases.

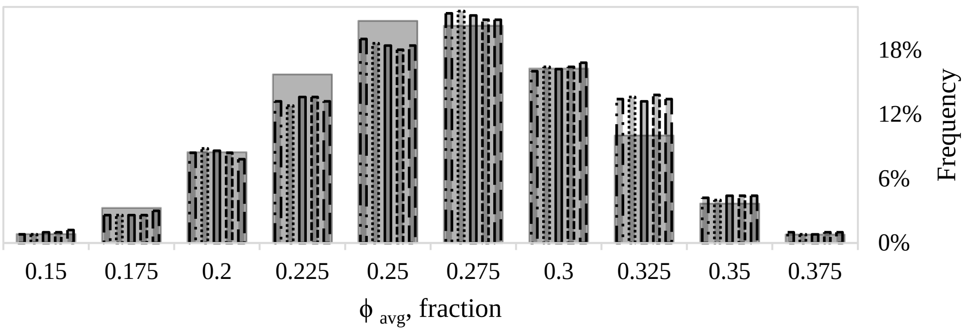

Figure 5.3. Thickness weighted porosity distribution in best 500 and all the cases.

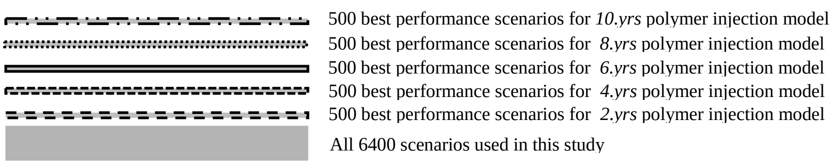

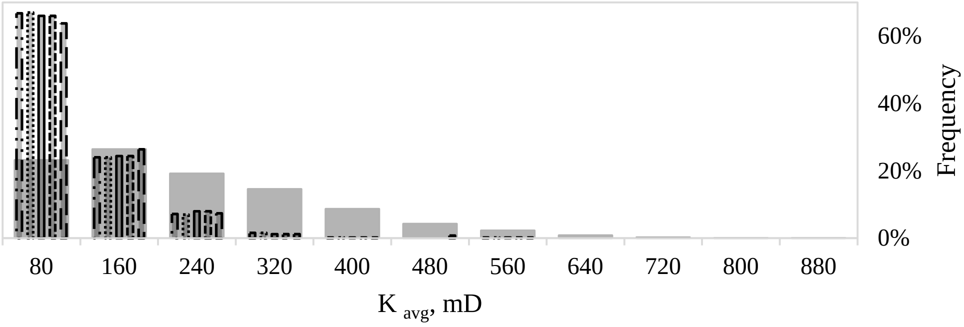

Figure 5.4. Thickness weighted permeability distribution in best 500 and all the cases.

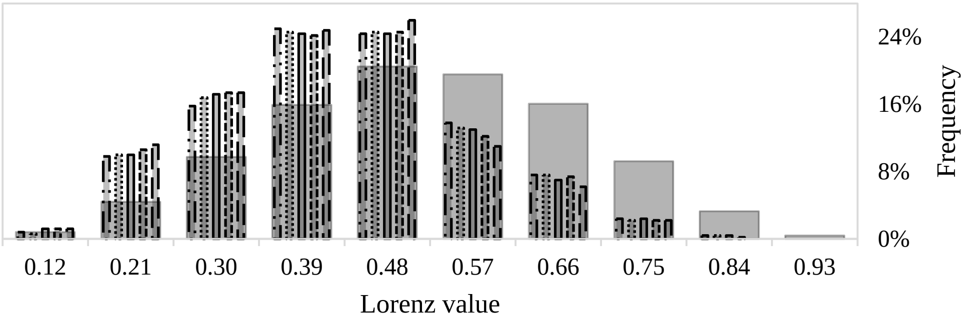

Figure 5.5. Lorenz coefficient distribution in best 500 and all the cases.

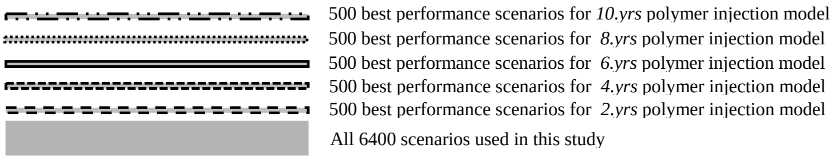

Anisotropy ratio distribution shown in Figure 5.6 indicates that the flooding performance is not affected by this ratio as the distributions for all the cases and the best 500 performance cases are alike. Due to the fact that, injection and production is applied for each of the five layers, it can be assumed that the reservoir fluids are forced to flow in horizontal direction from the injection perforation to production perforation of a single layer. In Figure 5.7 pore compressibility (CPOR) distribution plot is also another reservoir rock property which does not have any remarkable influence on the performance of the polymer flooding process.

Distribution of reservoir pressure and bubble point pressure as two of the most important initial reservoir conditions are plotted in Figures 5.8 and 5.9, respectively. Results suggest both low reservoir and bubble point pressures are in favor of the polymer flooding practice. The intention of the flooding system to low reservoir pressures can be clarified by referring to the injection bottom hole pressure and the permeability distributions. The low permeability of the successful cases can directly affect the injection bottom hole pressure as in tight systems high pressure cause injectivity problems. Consequently, the reservoir pressure is affected by as the injector bottom hole pressure is defined to be a function of reservoir pressure. Also, the efficiency of the different polymer injection duration is affected inversely by the reservoir initial pressure as the high initial reservoir pressures prefer lower duration of polymer injection operation. This is confirming that when the reservoir pressure at the start of the flooding operation is low, the energy of the system is not sufficient to continue the injection process.

Concerning the bubble point pressure, an expected behavior is observed higher efficiency flooding scenarios have low bubble point pressures. This can be explained by the fact that lower bubble point pressure cause late evolvement of gas out of oil. Reservoir water saturation (S_w = 1-S_o) distribution, as the third initial condition of the production scenarios is presented in Figure 5.10. A significant alteration of initial water saturation distribution for both of the total and the best 500 performance polymer flooding scenarios is an indication of high influence of the water saturation on the flooding process. Hence, higher oil saturation or by other meaning starting the polymer flooding application in early stages of the production marks for effective operations. In addition, different injection durations for the best performance cases show different distribution of water saturation. Shorter polymer injection duration works in favor of reservoirs with low water saturation (high oil saturation). On the contrary, low initial water saturation reservoir require longer injection duration process to achieve a high performance operation.

Oil °API gravity distribution as one of the important outcomes of this part of analysis, reveal that low gravity values are resulting in higher polymer flooding efficiencies. The distribution of the oil °API gravity is presented in Figure 5.11. This performance suggests that, high °API gravity oils may sweep effectively by the reservoir natural drive mechanism. Consequently, if polymer is injected for a low °API gravity oil, the additional oil that can be produced by polymer injection instead of no injection scenario is insignificant. As a result, opposing to the general belief that polymer flooding is much suitable for medium to light oils, this outcome strongly recommends to perform the polymer flooding application for heavy oils with acceptable recovery and water cut.

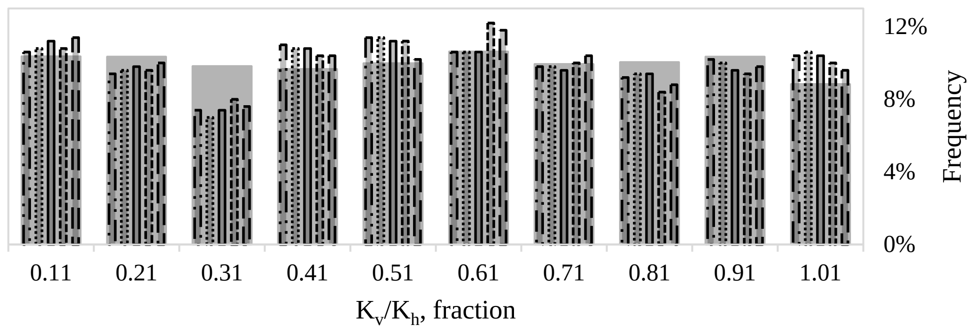

Figure 5.6. Anisotropy ratio distribution in best 500 and all the cases.

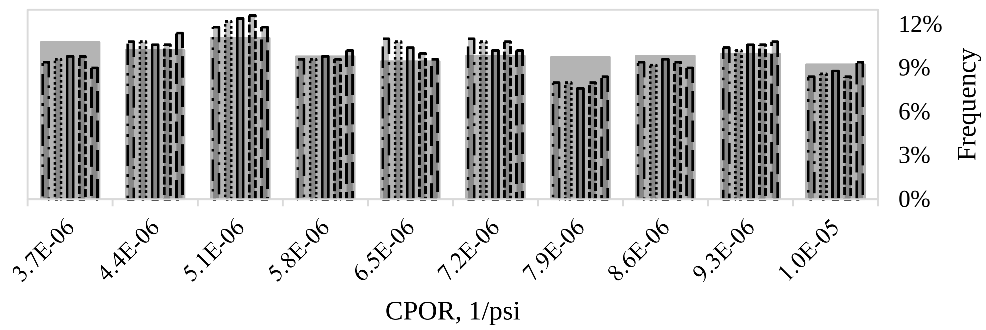

Figure 5.7. Pore compressibility distribution in best 500 and all the cases.

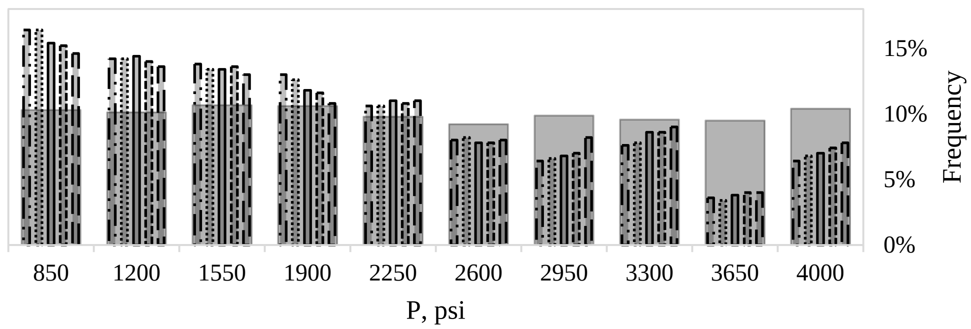

Figure 5.8. Reservoir pressure distribution in best 500 and all the cases.

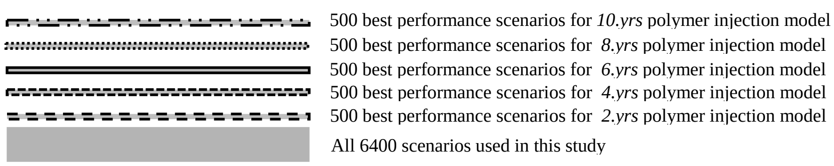

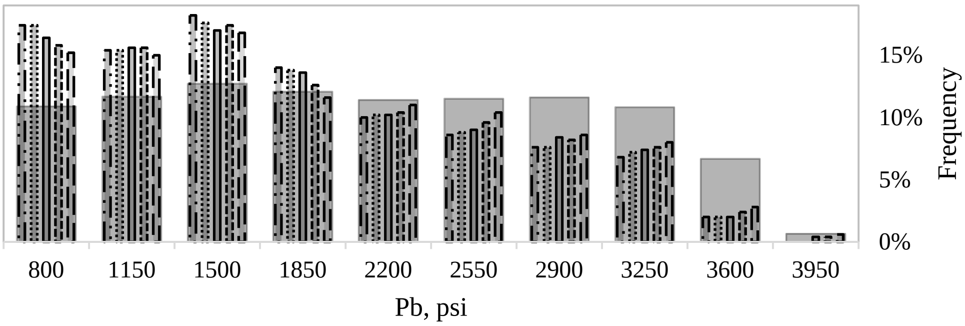

Figure 5.9. Reservoir bubble point pressure distribution in best 500 and all the cases.

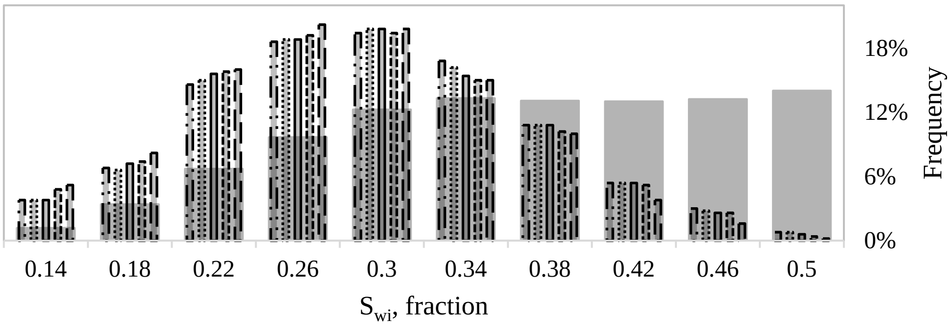

Figure 5.10. Initial water saturation distribution in best 500 and all the cases.

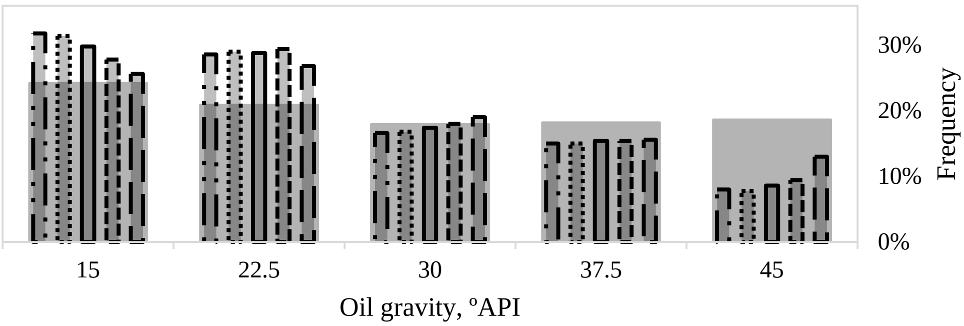

Figure 5.11. Oil ºAPI gravity distribution in best 500 and all the cases.

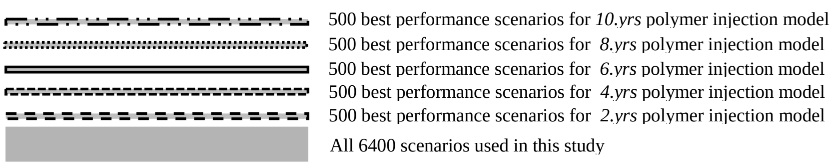

Polymer maximum adsorption level and adsorption coefficient distributions are shown in Figures 5.12 and 5.13. The two polymer related rock properties exposed no significant impact on the flooding efficiency. Yet the negligible influence, low values for polymer maximum adsorption do increase the flooding performance. This is an acceptable outcome as the high adsorption results in decrease in concentration of the polymer solution, hence, decreasing the sweeping performance of the flooding process. Moreover, high reference polymer solution viscosity (PVISC) as one of the polymer properties increases the polymer solution viscosity. This behavior can be perceived from PVISC distribution graph shown in Figure 5.14 as the PVISC increases the higher polymer solution viscosity can be obtained, henceforth, increasing the polymer flooding performance.

Two phase relative permeability data of the scenarios were generated using Corey's correlation in which the residual oil saturation (S_{or}), irreducible water saturation (S_{wirr}) and relative permeability coefficient (n) are the variables. Residual oil saturation distribution within best 500 and total scenarios is presented in Figure 5.15. Denser accumulation of successful cases for low residual oil saturations is not far from what should be expected. The lower residual oil saturation (higher mobile oil saturation) is an advantageous property of a reservoir in all kinds of the production methods. Residual water saturation distribution is shown in Figure 5.16. The frequency graph of efficient and all the cases do not show any specific behavior with different intervals of the water saturation. Comparing the effect of residual oil and irreducible water saturation, it can be assumed that the efficiency of the polymer flooding application is substantially influenced by the residual oil saturation.

Moreover, the relative permeability coefficient distribution which is a parameter that specifies the sorting level of the pores is presented in Figure 5.17. High value corresponds to well sorted pore system that assist the fluid flow within porous media. Consequently, the sweep efficiency is improved as the sorting level increases. The distribution graph obtained from this set of data reveals the improvement of the polymer flooding process with increase of the relative permeability coefficient value. The capillary pressure coefficient for oil and gas distributions are plotted in Figures 5.18 and 5.19, respectively. The similarities of the total and the best 500 cases distribution for different intervals of capillary pressure coefficients, indicated an insignificant effect of these parameters on the efficiency of the polymer flood process.

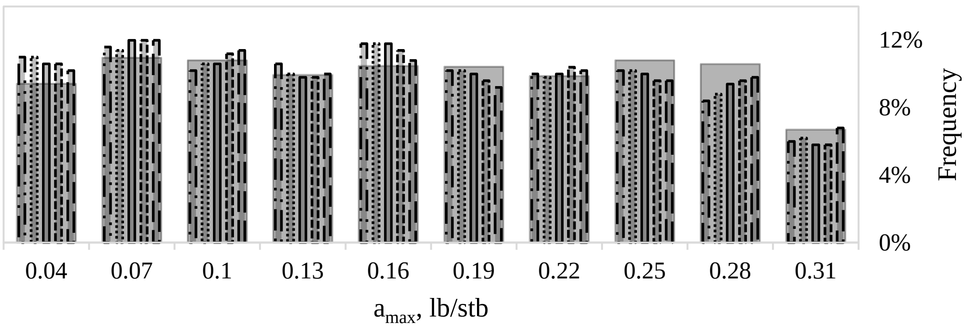

Figure 5.12. Maximum polymer adsorption distribution in best 500 and all the cases.

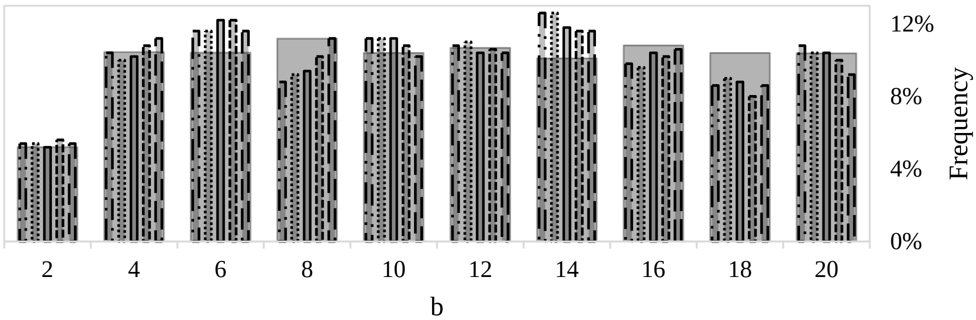

Figure 5.13. Polymer adsorption coefficient distribution in best 500 and all the cases.

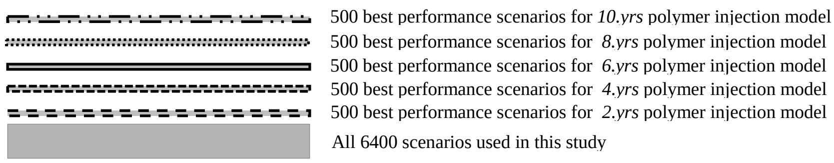

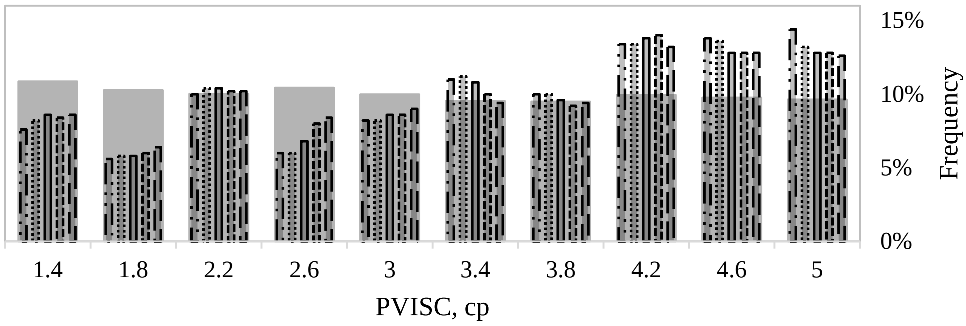

Figure 5.14. Reference polymer viscosity distribution in best 500 and all the cases.

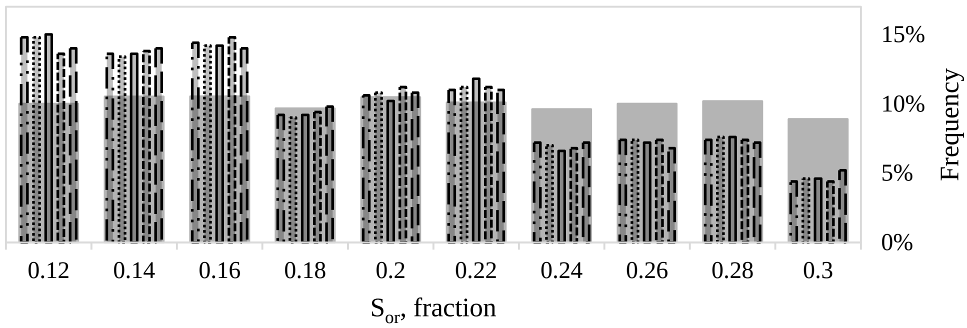

Figure 5.15. Residual oil saturation distribution in best 500 and all the cases.

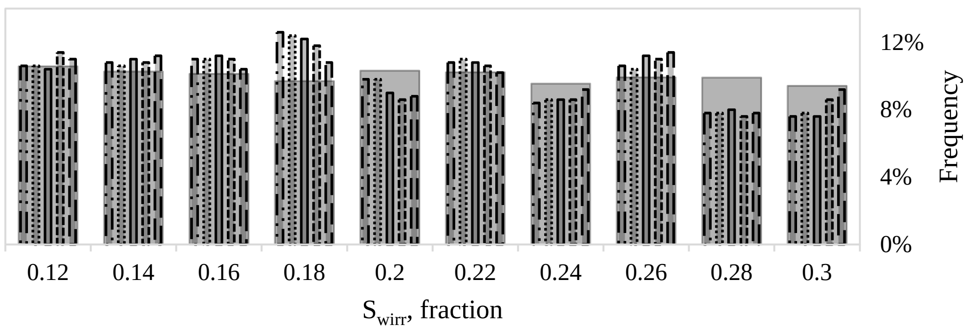

Figure 5.16. Irreducible water saturation distribution in best 500 and all the cases.

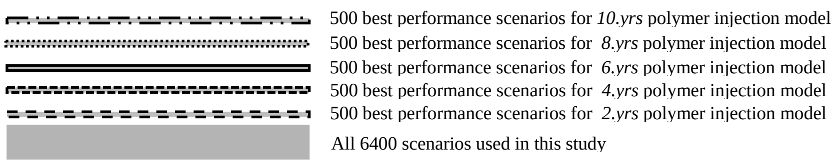

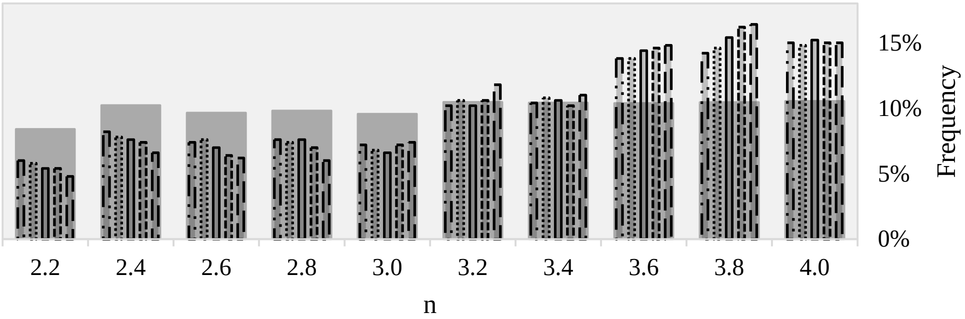

Figure 5.17. Relative permeability coefficient distribution in best 500 and all the cases.

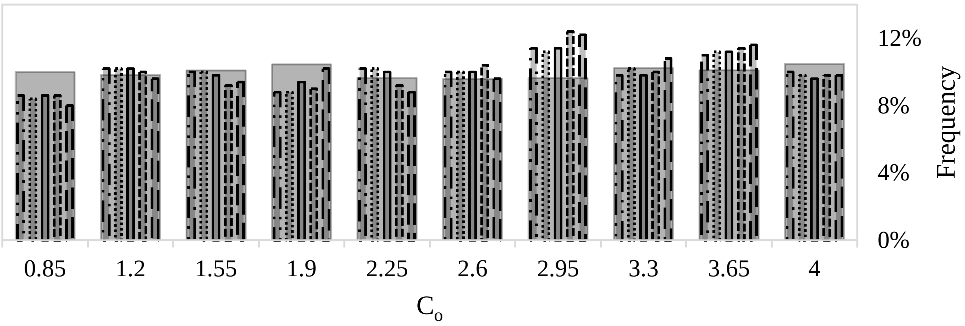

Figure 5.18. Oil capillary pressure coefficient distribution in best 500 and all the cases.

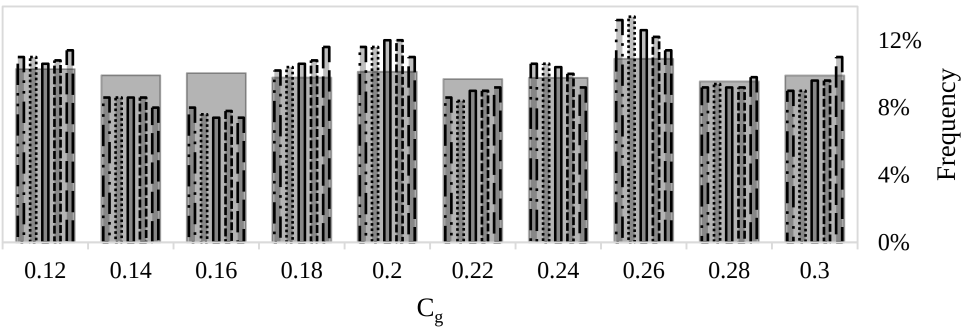

Figure 5.19. Gas capillary pressure coefficient distribution in best 500 and all the cases.

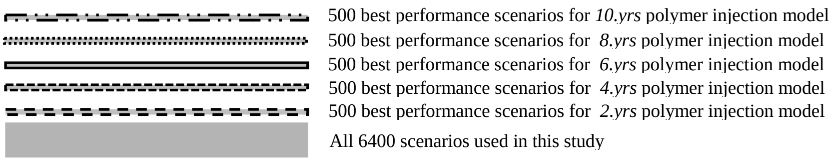

As one of the most important stages of process optimization, the effect of the operational parameters should be evaluated. Polymer mixture concentration and the injection pressure of the mixture are critical points for the polymer injection method. The polymer concentration distribution is shown in Figure 5.20. Approximately 45% of the successful flooding scenarios have concentration of less than 0.25 $lb.bbl^{-1}$. This output suggest that low concentrations lead to more efficient flooding operation. Moreover, considering the concentration distribution for different injection duration, it can be observed that, for short injection duration high concentrations provide better productivity. In contrary, for long injection periods the concentration should be kept low. Distribution of the injector bottom hole pressure for the 500 efficient cases indicates that low injection pressure values are in favor of the process as shown in Figure 5.21. This behavior can be explained by the fact that these successful cases mostly have low permeabilities (less than 100 mD). Therefore, practically very high injection pressures cannot be applied to a low permeability formation and the injectivity problem is the limiting factor. Additionally, the distribution of the injection bottom hole pressure varies for different injection durations. Low injection bottom hole pressure showed better flooding performance in long injection durations. Likewise, for short injection processes the high injection pressures should be applied. On the contrary, the bottom hole pressure at the producer does not show a notable effect on the performance of the flooding operation, as shown in Figure 5.22. However, extremely low production bottom hole pressures (less than 400 psi) results in less efficient cases. Lastly, the well space as another significant factors in designing the polymer flooding operation should be evaluated. The production and injection wells spacing distribution is presented in Figure 5.23. Opposing to the common belief that, for polymer injection, low well spacing should be considered, the outputs of the successful cases is conflicting with this idea. Well spacing shows a substantial impact in the efficiency of the successful scenarios. High well spacing should be preferred for polymer injection process to delay the water break though time as much as possible, hence, reducing the water cut.

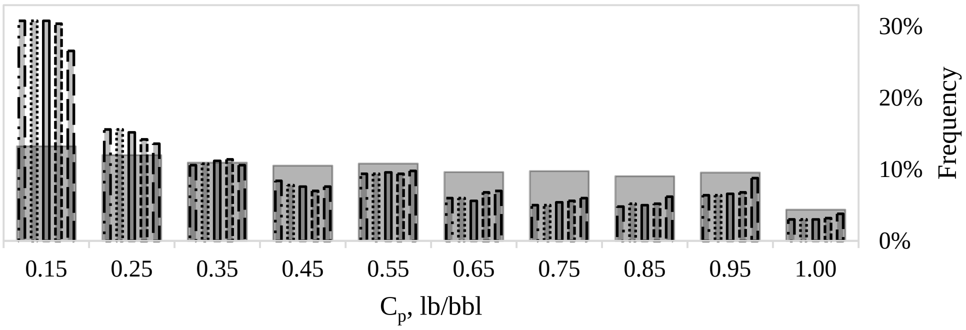

Figure 5.20. Polymer concentration distribution in best 500 and all the cases.

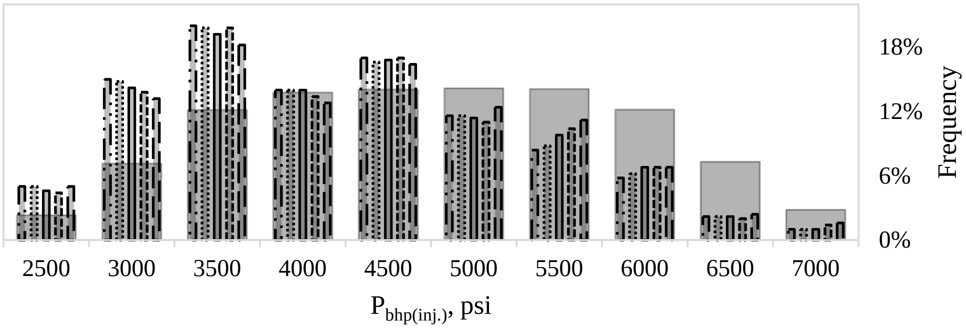

Figure 5.21. Injector bottom hole pressure distribution in best 500 and all the cases.

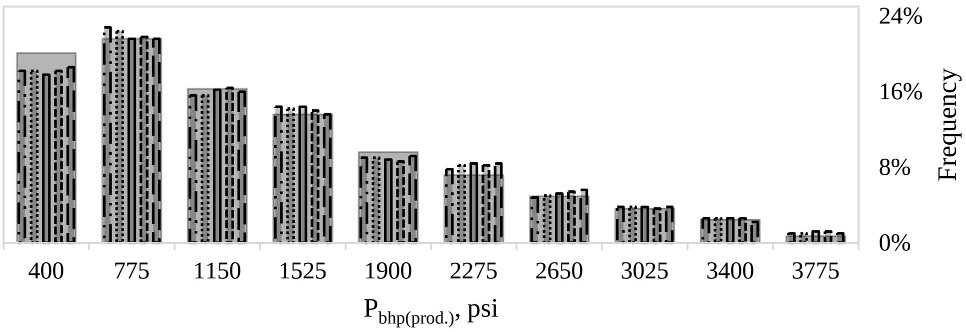

Figure 5.22. Producer bottom hole pressure distribution in best 500 and all the cases.

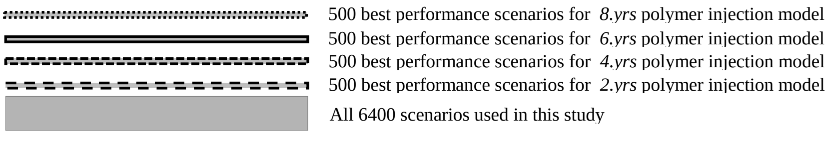

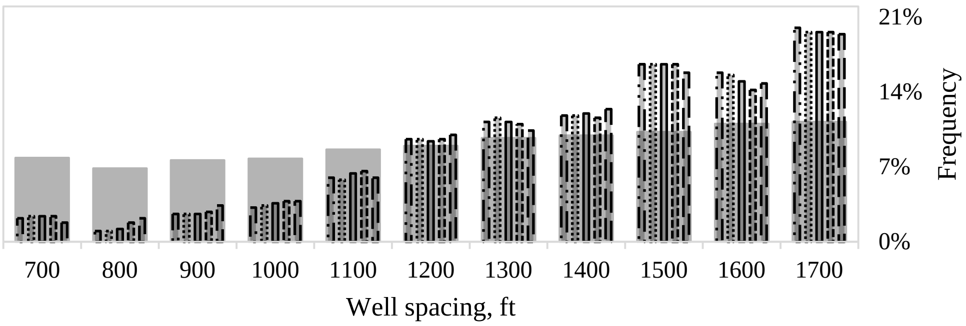

Figure 5.23. Well spacing distribution in best 500 and all the cases.

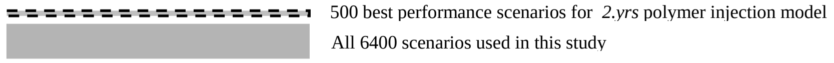

5.1.2 Parameter Sensitivity Analysis

For further evaluation of the reservoir and operation parameters effects on the polymer flooding operation, a sensitivity analysis is performed, which aims to sort the parameters in order of their influence. The procedure to achieve a representable sensitivity analysis was completed by assigning a base value, a minimum and a maximum for each of the parameters. In this study the base is the average, the minimum and maximum is the calculated by taking 95% and 105% of the base value.

Sensitivity to the following two parameters: 1) efficiency and 2) water cut are studied. This work would be a supplement to the previous study, as a complex efficiency term ($E_{Best,n}$) is defined for finding the distribution of parameters in best-performance cases. Henceforth, the parameter sensitivity is supplemented to compare the effects of the parameters separately on efficiency (E_n) and water cut. Tornado charts is used as graphical demonstration of the sensitivity analysis results. Figure 5.24 and Figure 5.25 show the sensitivity to the efficiency and water cut for each of the parameters from two to ten years of polymer injection. The x-axis represent the efficiency values, bars expresses the impacts while parameter value change from minimum to maximum and in the y-axis the parameters are sorted in order of their impacts.

In general, it should be stated that both polymer injection efficiency and its water cut are prominently and commonly affected by oil API gravity, well spacing, initial water saturation, bottom hole pressures at the injector and the producer wells. Moreover, for short period polymer injection scenarios the order of the parameters are differing as the injection time increase. Four to ten years of injection processes indicate same behavior to the change of the parameter values. Considering the common rank parameters, the most 15 influencing ones for efficiency and water cut value are summarized in Table 5.1.

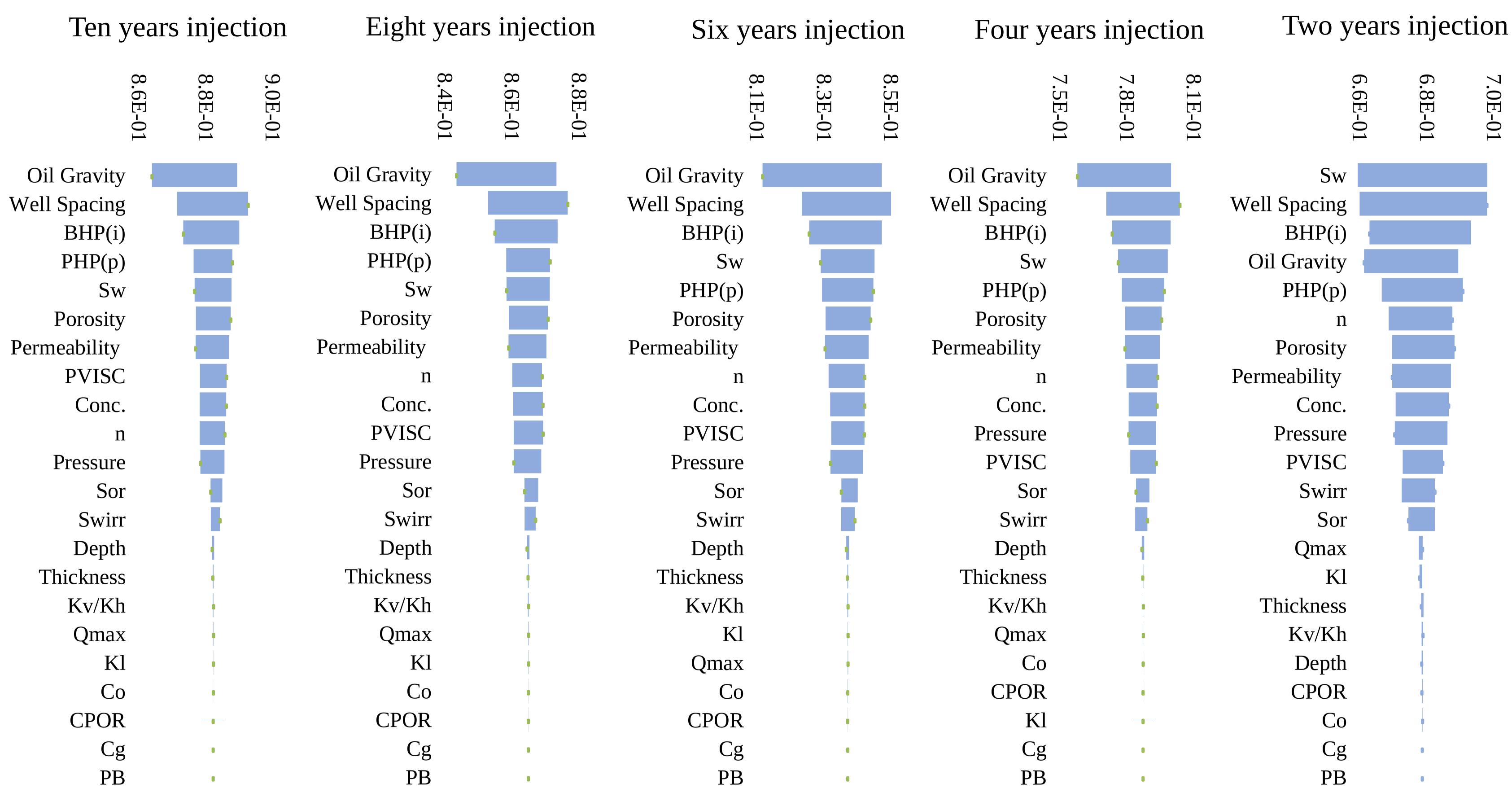

Figure 5.24. Parameter sensitivity of the water cut for different injection durations.

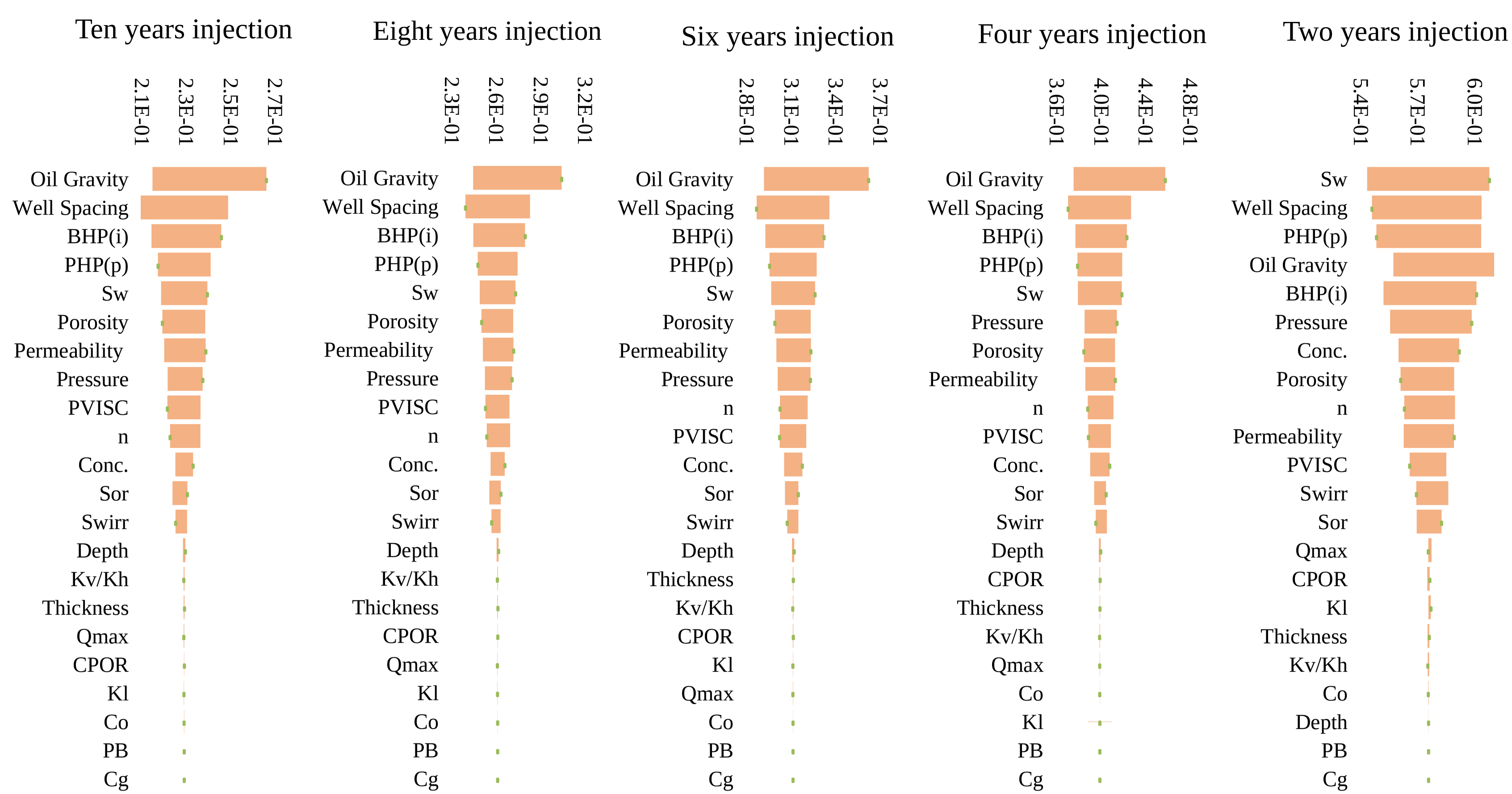

Figure 5.25. Parameter sensitivity of the efficiency value for different injection durations.

Table 5.1. Parameter sensitivity order for efficiency value and water cut.

Rank of importance	Efficiency	Water cut
1st	Oil gravity	Oil gravity
2nd	Well spacing	Well spacing
3rd	BHP(i)	BHP(i)
4th	BHP(p)	Sw
5th	Sw	BHP(p)
6th	Porosity	Porosity
7th	Permeability	Permeability
8th	Reservoir pressure	n
9th	PVISC	Poly. concentration
10th	n	PVISC
11th	Poly. concentration	Reservoir pressure
12th	Sor	Sor
13th	Swirr	Swirr
14th	Reservoir depth	Reservoir depth
15th	CPOR	Reservoir thickness

5.1.3 Economic Analysis of Polymer Flooding Operation

With the aim of having a rough knowledge on feasibility of the polymer injection operation, two considerations should be made. In the first step, it is to be decided whether the polymer injection process can result in additional oil production comparing with without injection production plan. In this study, the decision upon profitability of the polymer flooding over no injection scenario can be made by referring to the sign of the defined efficiency value. Meaning that, the negative sign is suggesting a production by the reservoir's natural derive mechanism. And positive sign is an indication of productive scenario if polymer flood is chosen. In the second step, economic feasibility of the process should be questioned. Among total scenarios under investigation, the polymer injection is always resulting in oil production above the production could be attained without the injection. Statistically 99.9% of the case resulted in a positive efficiency, implying that almost for all the scenarios, polymer injection has priority over no injection scenario. Yet, particularly by having the positive efficiency value, it is not possible to ascertain the selection of the polymer flooding as a production scheme.

Accordingly, in order to have a rough idea on economic feasibility of the polymer injection operation, a simple economic efficiency value is defined. As shown in Equation 5.2, the economic efficiency is considering the income achieved from incremental oil production and the cost generated by the injection of the profile. It should be mentioned that the capital, operational and etc. are not considered. Hence, the oil price and polymer price are the income and cost aspects of this feasibility study. This equation, though simple, can suggest if a polymer injection is feasible for different operation efficiencies, oil and polymer prices. An economic efficiency above 1 is the indication of a feasible injection scenario and below 1 is the clue of higher cost than income.

$$Efficiency_{eco} = Efficiency_n x \frac{\$/bbl\ oil}{\$/kg\ polymer} \quad \text{…...……..…………..Equation 5.2}$$

Where $Efficiency_n = \frac{N_{npv\,(n)}}{P_{npv\,(n)}}$

A quick feasibility study is conducted on 6339 efficient cases (additional oil production over no injection scenario) assuming oil and polymer price uncertainty of 20 to 100 $/bbl and 1 to 3 $/kg, respectively. Due to the uncertainty in the costs, Monte Carlo simulation is assessed to observe the impact of cost variabilities. The 6339 random price values for the oil and polymer price are generated within the specified range of uncertainty. In Figure 5.26, the economic efficiency probability of the total available scenarios in this study is presented. The graph shows that almost with 90% probability, the economic efficiency is above one. This means that the polymer injection application for the scenarios generated in this study is economically feasible for more than 90%. The proved, probable and the possible probabilities of economic efficiency for different injection durations are summarized in Table 5.2. It can be seen that the proved probability is more than one for injection duration of two to six years. For injection duration of six to ten years the economic efficiency may not be feasible with the uncertainties defined for polymer and oil prices. Hence, to conclude this section of the analysis, polymer flooding can be assertively applied for six years regardless of the price fluctuations of 20 to 100 $/bbl of oil and 1 to 3 $/kg of polymer.

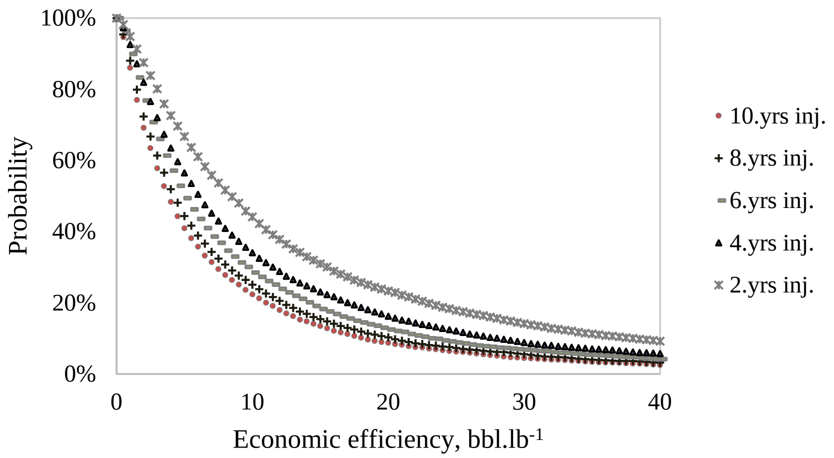

Figure 5.26. Probability of the economic efficiency.

Table 5.2. Probability of the economic efficiency.

Injection duration	90 %	50 %	10 %
2 years	1.6	8.5	38
4 years	1.3	6.1	28
6 years	1.1	5.9	23
8 years	0.9	4.3	20.5
10 years	0.8	3.7	18.4

5.2 Performance Evaluation of Polymer Flooding Screening Tool

To evaluate the performance of the ANN models the outputs should be compared with numerical model results to be assured that the models is sufficiently capable of generalizing the relation among the inputs and the outputs. Primarily, the neural network structure optimization summaries for the five ANN models are presented. In addition, to graphically illustrate the capability of the tool in predicting the polymer flooding performance, regression plots, overlapping graphs and model's sensitivities to the parameters are compared with numerical simulator. Secondarily, the implementations that mark the data-driven screening tool to be superior to reservoir simulators are demonstrated.

5.2.1 ANN Models Structure Optimization's Results

The structure of the five ANN models for each two consecutive years of polymer injection are decided using the same methodology followed and described in chapter 4 for two years polymer injection model. The optimization results of the five ANN models representing different injection durations are summarized in Table 5.3. In Table 5.4 and 5.5 training, validation, testing and overall data regressions after the optimization process are presented. The graphical view of testing set regressions for all five ANN models are shown in Figure 5.27. Regression plots can also indicate that predicting the output of efficiency is less accurate than the water cut output.

Table 5.3. Optimum structures for the five ANN models.

Model Name	Network Structure Design Components			
	Divisions	Neuron	Hidden Layer	Neuron Division
2.yrs	70%,15%,15%	95	2	60 + 35
4.yrs	90%, 5%, 5%	85	2	55 + 30
6.yrs	90%, 5%, 5%	85	2	50 + 35
8.yrs	90%, 5%, 5%	105	1	105
10.yrs	90%, 5%, 5%	95	1	95

Table 5.4. Efficiency regression for the optimum structure selected for the ANN models.

Model Name	Efficiency Regression			
	Training	Validation	Testing	Overall
2.yrs	0.972	0.915	0.928	0.953
4.yrs	0.982	0.944	0.942	0.971
6.yrs	0.991	0.951	0.971	0.984
8.yrs	0.986	0.956	0.987	0.985
10.yrs	0.988	0.961	0.985	0.986

Table 5.5. Efficiency regression for the optimum structure selected for the ANN models.

Model Name	Water Cut Regression			
	Training	Validation	Testing	Overall
2.yrs	0.995	0.960	0.963	0.985
4.yrs	0.996	0.979	0.970	0.994
6.yrs	0.997	0.981	0.974	0.995
8.yrs	0.998	0.981	0.969	0.996
10.yrs	0.997	0.981	0.979	0.995

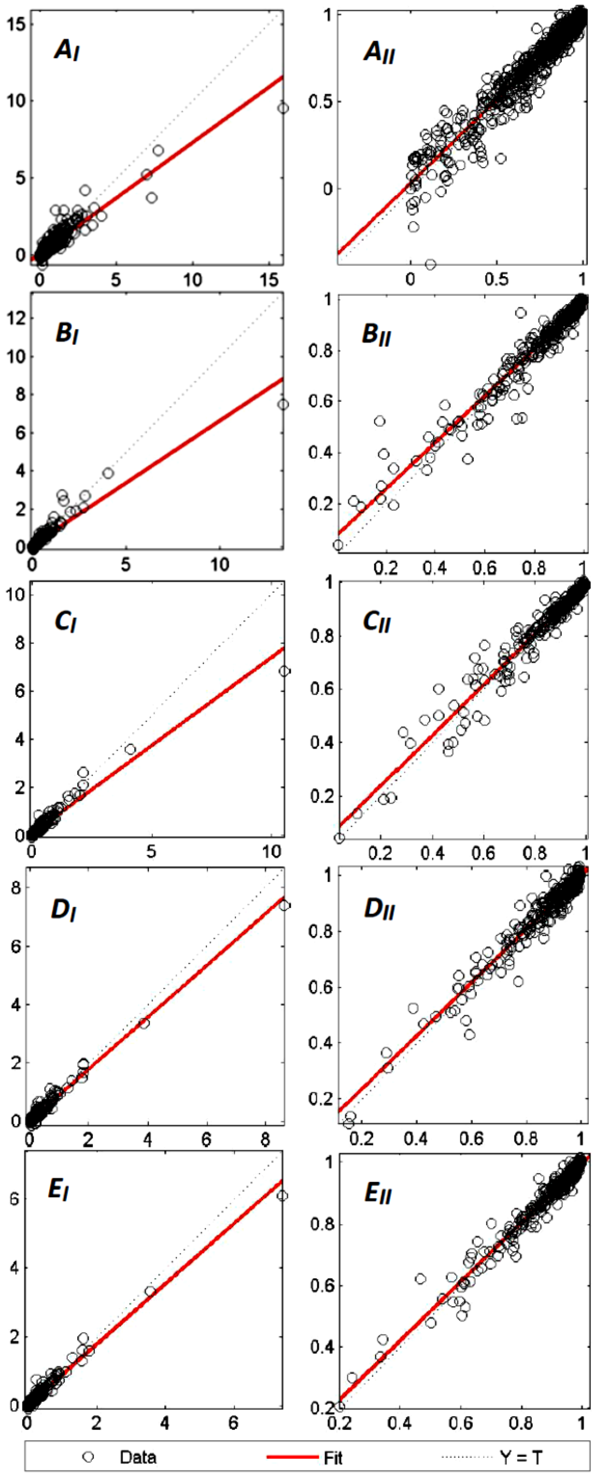

Figure 5.27. Testing set regressions. **(A)** *2.yrs* model, **(B)** *4.yrs* model, **(C)** *6.yrs* model, **(D)** *8.yrs* model, **(E)** *10.yrs* model. **(I)** Output 1: Efficiency, **(II)** Output 2: *Water cut*. **X-axis**: target output (numerical model results), **Y-axis**: ANN. results.

5.2.2 Training Performance Evaluation

The performance of the ANN models should be compared with numerical model results to be assured that the models is capable of accurately predicting the polymer flooding performance. Accordingly, the testing set results obtained from reservoir simulator are overlapped against the ANN results for two years injection model, as shown in Figure 5.28. Remarkably, some extreme cases are predicted sufficiently well (e.g cases 51 and 159 for efficiency output and cases 13, 55, 115 and 223 for water cut output). The comparison of the simulator results with ANN models for four to ten year of injections are presented in Figures 5.29 through 5.32. It can be noticed that the network can effectively predict the performance of the polymer flooding efficiency for different injection durations.

The model sensitivity to the input parameters can also be used to check if the physics of the problem is understood correctly by the network. This includes examining the both reservoir simulator and ANN model to recognize the input influence on the outputs. For the parameter sensitivity, a base value for each of the parameters are selected and a minimum and maximum values are assigned for each by multiplying the base value with 1.05 and 0.95, respectively. Tornado charts are utilized as a graphical output of the sensitivity analysis. The x-axis of this chart shows the value of our primary objective which is the efficiency or water cut. The horizontal line represents the objective value of the base case. Each parameter has its own bar. Width of the bar expresses the impact weight of the parameter on the objective while changing through the range from minimum to maximum. In Figures 5.33 through Figure 5.37 the sensitivity analysis conducted for efficiency value of two to ten years of polymer injection models are presented. The figures illustrate that even if the order of parameters sensitivities are not exactly matching, the orders are moving very closely. Comparing the five models of different injection durations, *2.yrs* model shows higher inconsistency in order of parameters sensitivity. This inconsistency is reduced significantly as the injection duration increases (*4.yrs,…, 10.yrs*). Figures 5.38 through Figure 5.42 represent the sensitivity of the numerical simulator and the ANN model to the water cut. Similar with the decreasing mismatching trend observed for sensitivity analysis with efficiency value objective from 2*.yrs* to *10.yrs* injection models, the water cut sensitivity shows the same behavior. Hence, it can be concluded that the physics of the problem is perfectly understood for *10.yrs* model as the order of the parameter sensitives are almost the same for both ANN and simulator models and this performance is marginally reduced when injection duration decreased. Moreover, comparing the sensitivity analysis conducted with different objectives, the efficiency and the water cut, it can be seen that the order of the parameters are more alike when water cut is intended. Ultimately, the results obtained from the parameter sensitivity is in agreement with the regression values. Both approaches suggest that the accuracy of the model is increasing from *2.yrs* to *10.yrs* injection duration models and, water cut output is predicted more precisely comparing with the efficiency output.

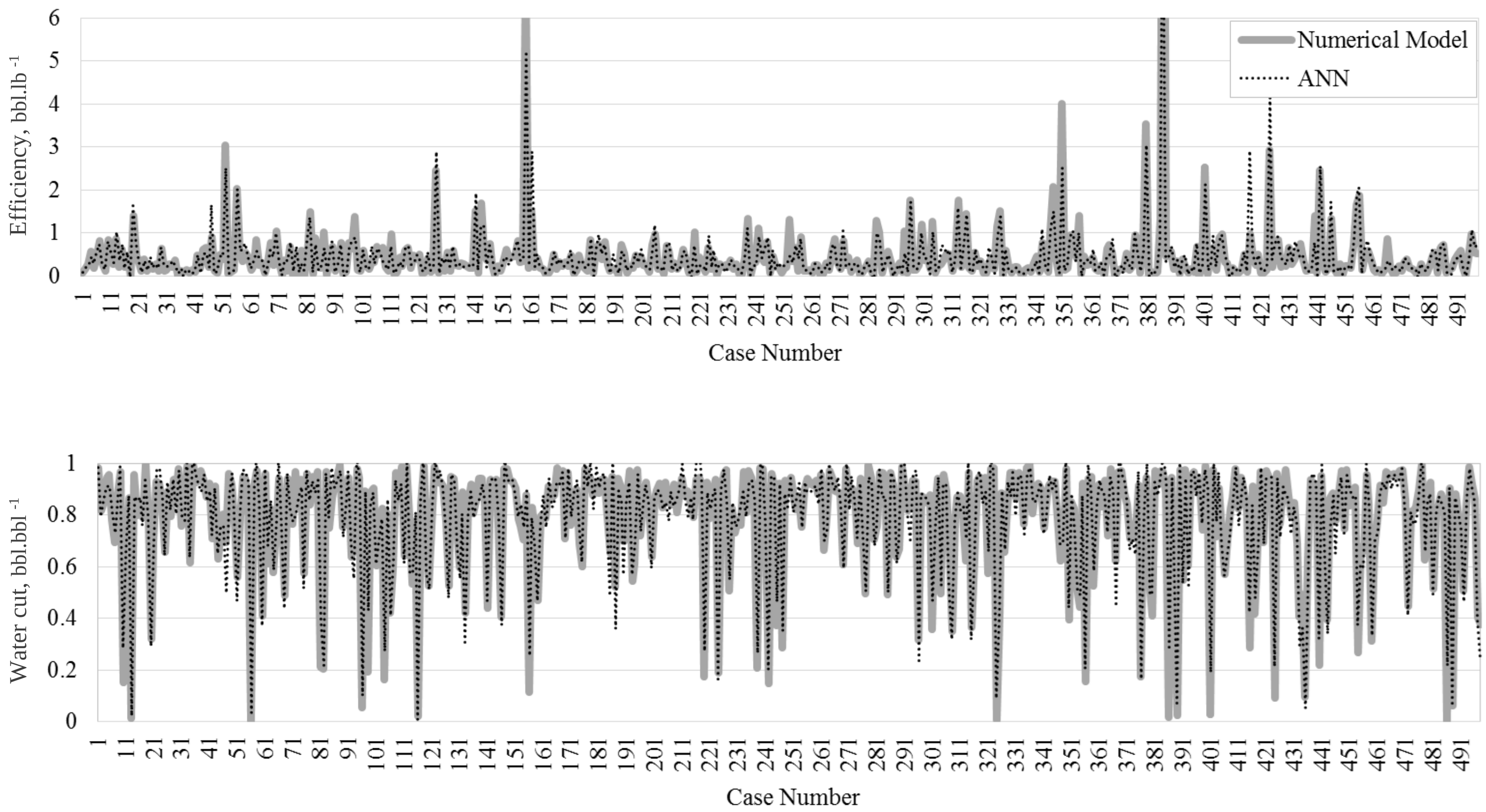

Figure 5.28. Numerical model and ANN testing set comparison for *2.yrs* model.

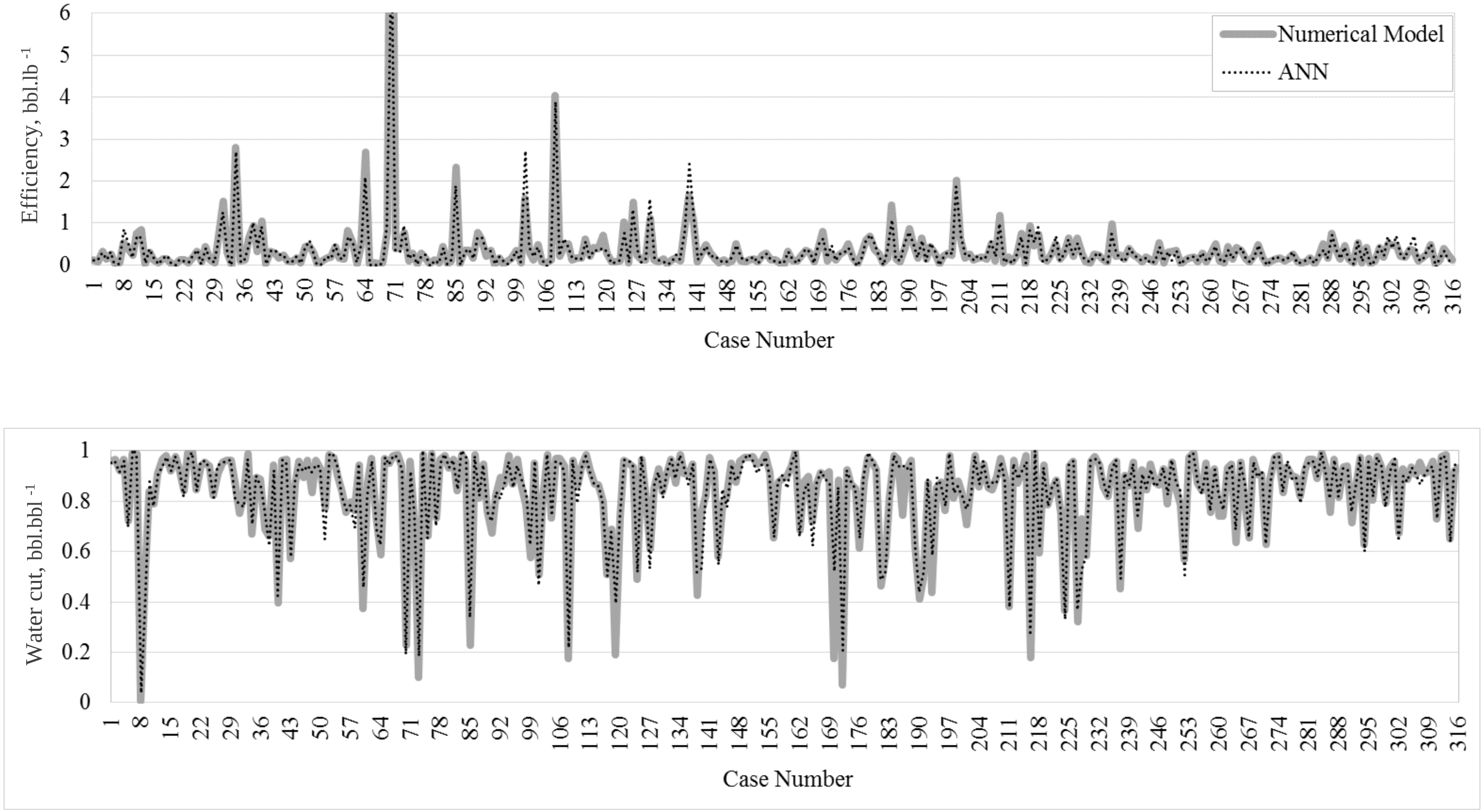

Figure 5.29. Numerical model and ANN testing set comparison for *4.yrs* model.

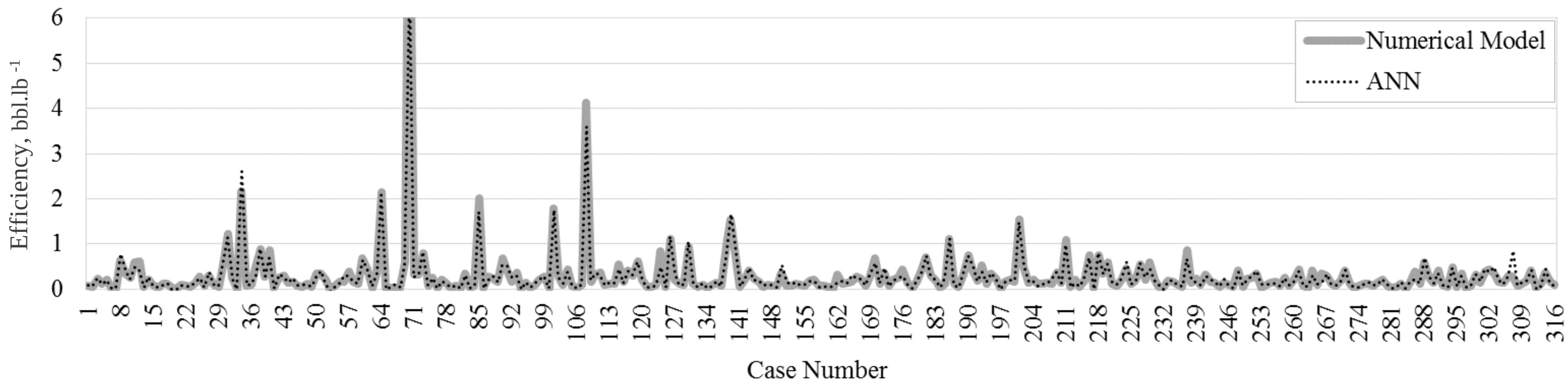

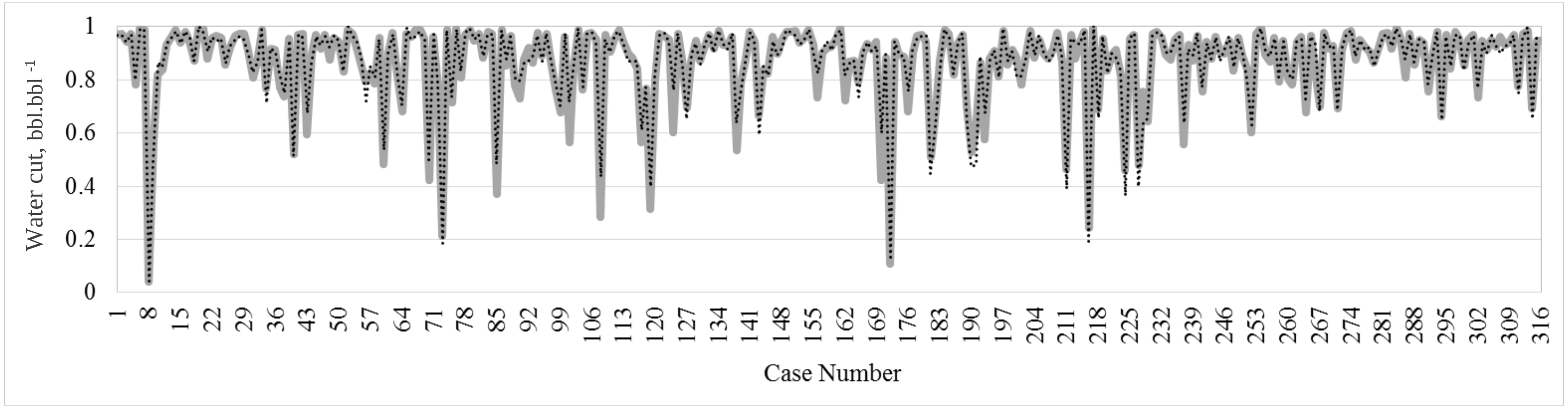

Figure 5.30. Numerical model and ANN testing set comparison for *6.yrs* model.

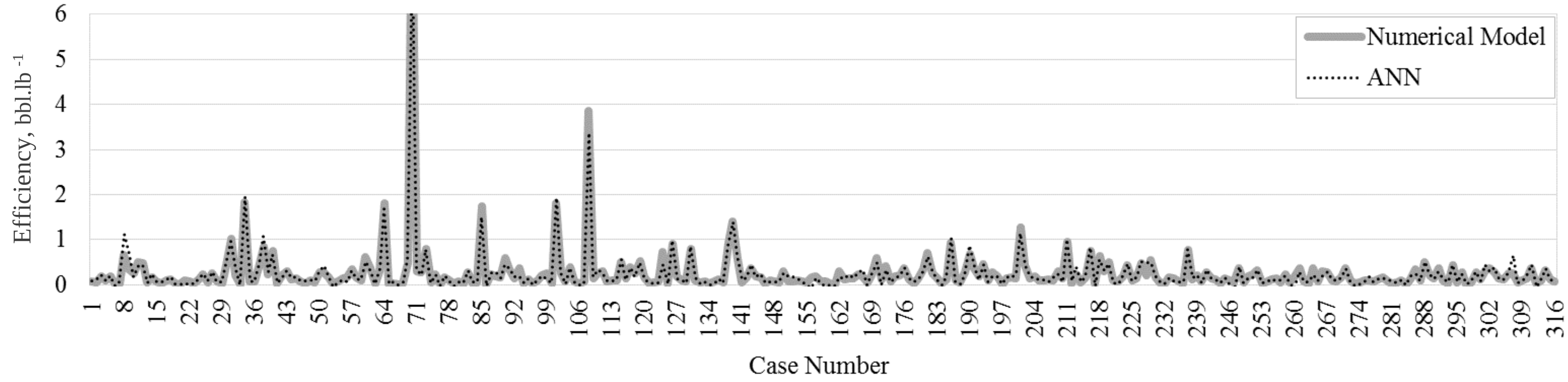

Figure 5.31. Numerical model and ANN testing set comparison for *8.yrs* model.

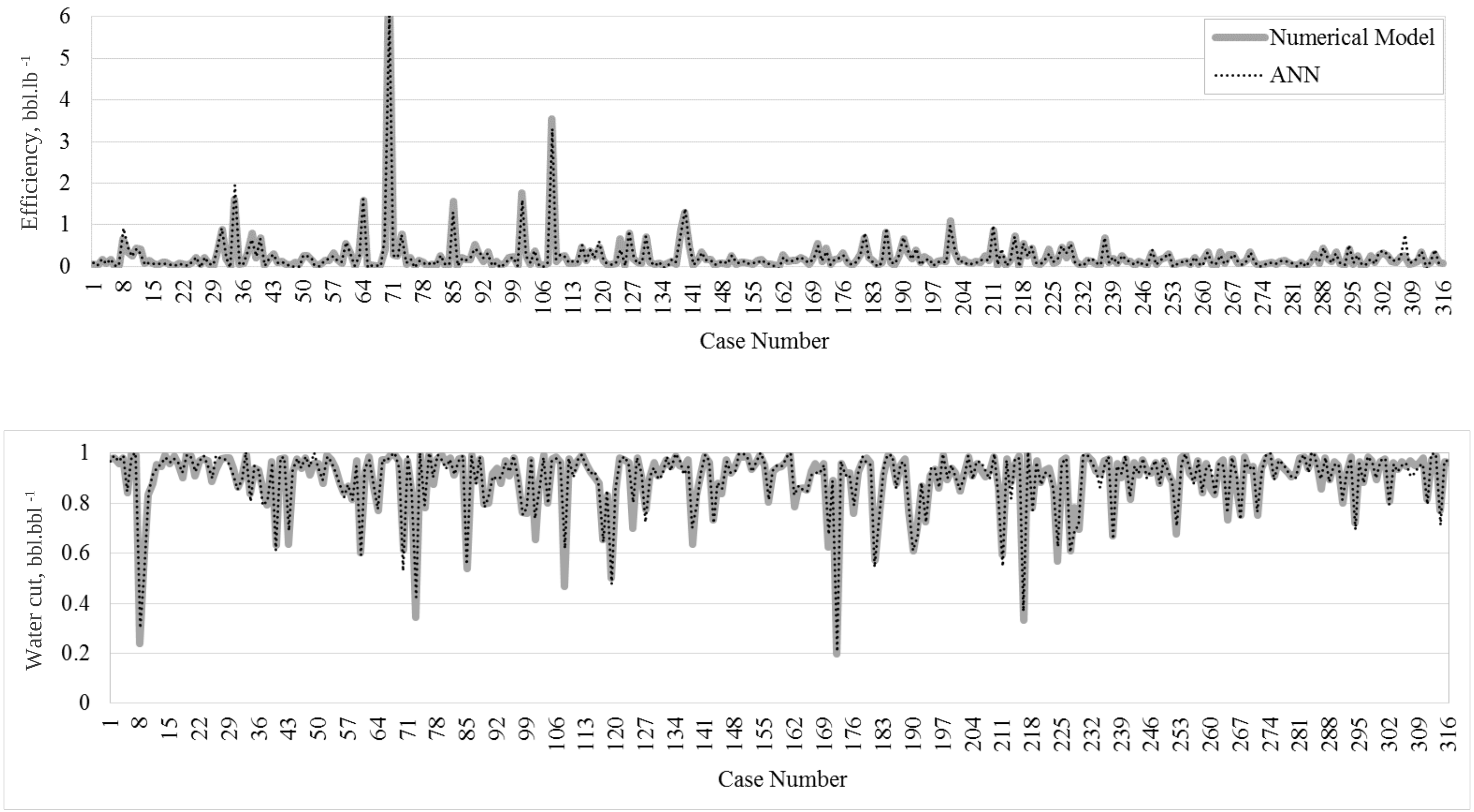

Figure 5.32. Numerical model and ANN testing set comparison for *10.yrs* model.

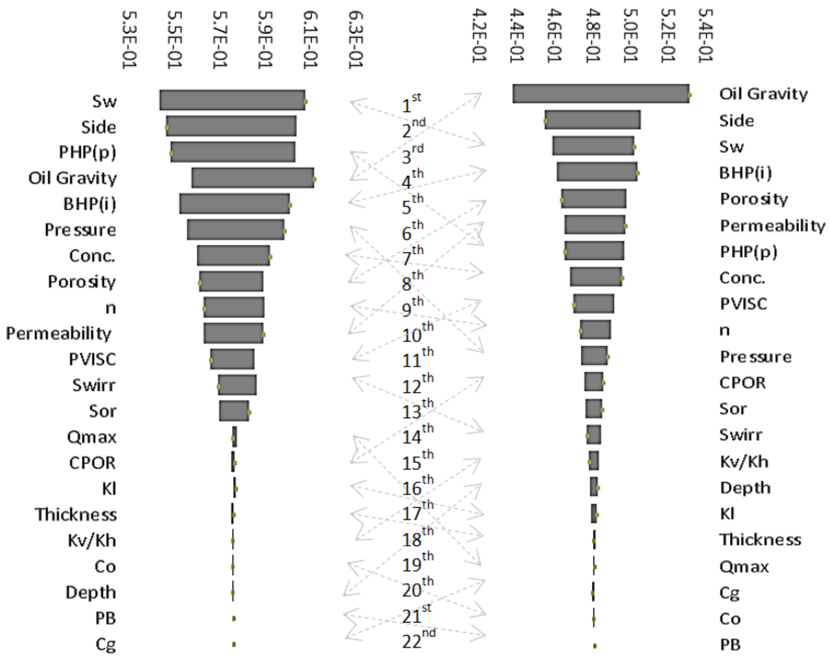

Figure 5.33. Parameter sensitivity of numerical model (left) and ANN model (right) to efficiency for *2.yrs* polymer injection model.

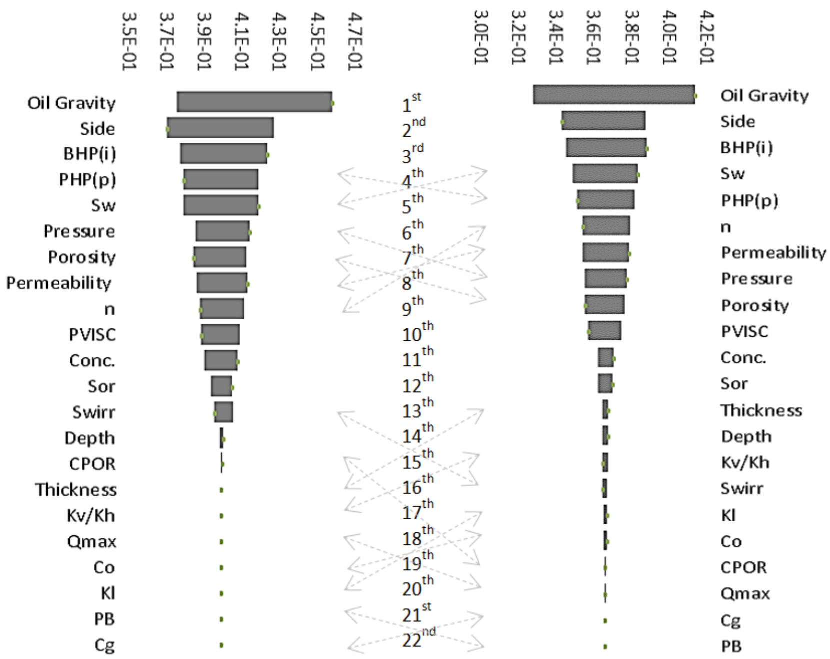

Figure 5.34. Parameter sensitivity of numerical model (left) and ANN model (right) to efficiency for *4.yrs* polymer injection model.

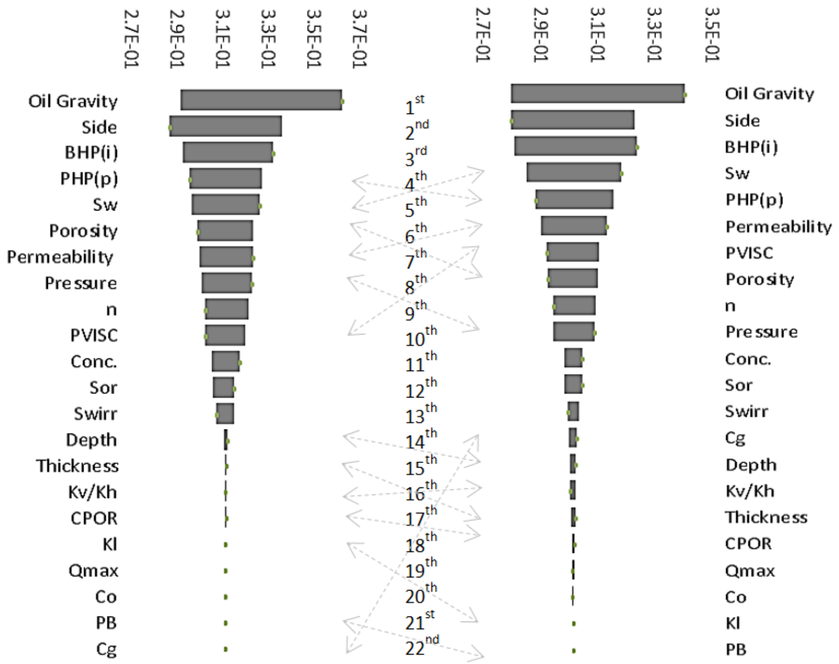

Figure 5.35. Parameter sensitivity of numerical model (left) and ANN model (right) to efficiency for *6.yrs* polymer injection model.

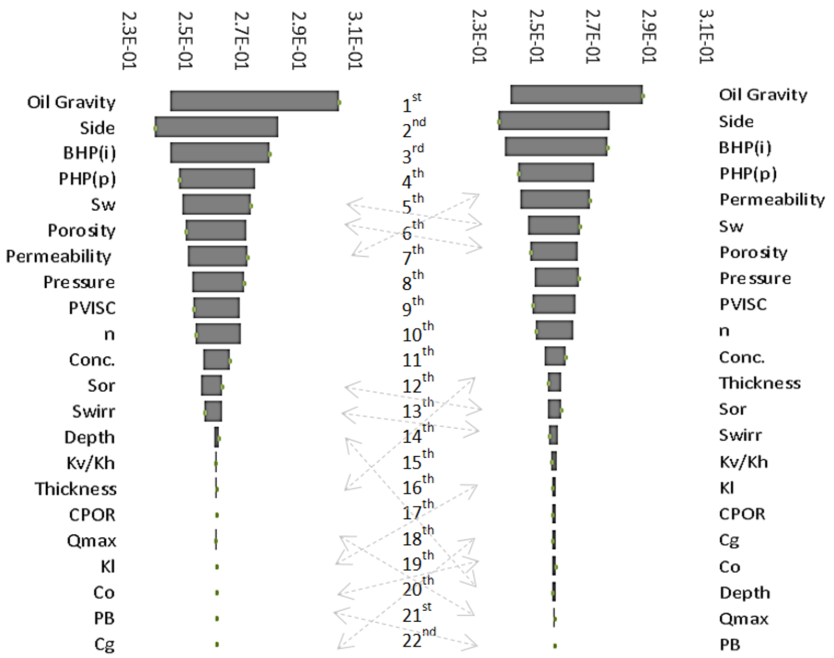

Figure 5.36. Parameter sensitivity of numerical model (left) and ANN model (right) to efficiency for *8.yrs* polymer injection model.

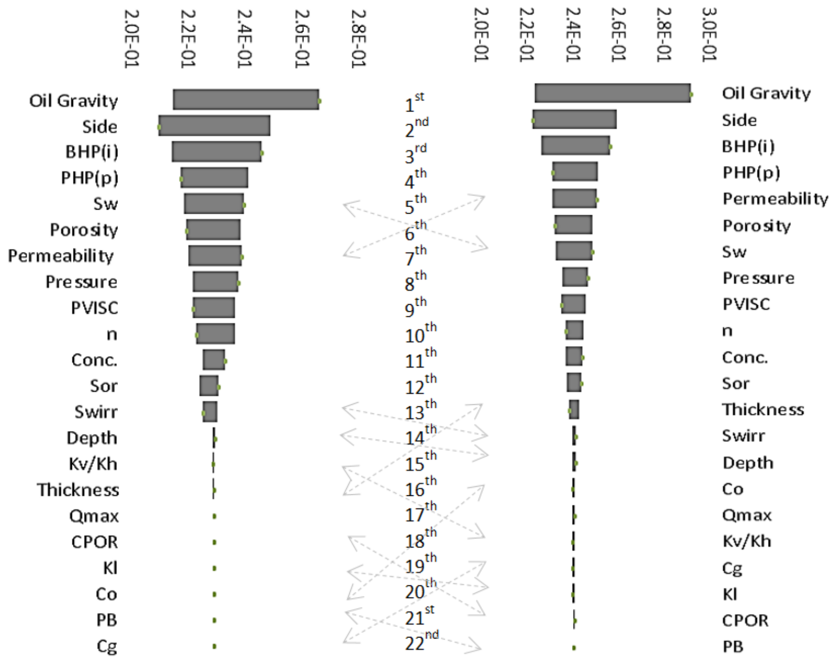

Figure 5.37. Parameter sensitivity of numerical model (left) and ANN model (right) to efficiency for *10.yrs* polymer injection model.

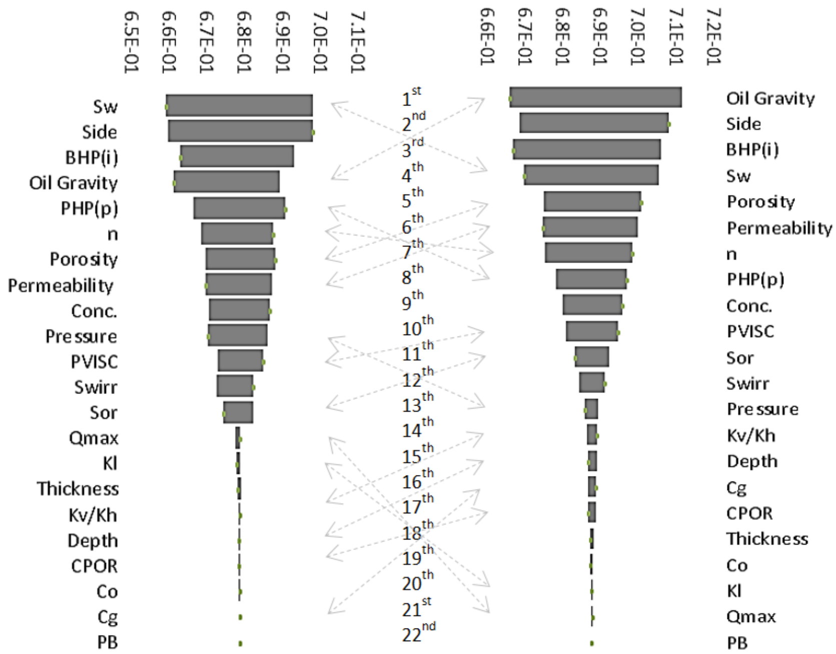

Figure 5.38. Parameter sensitivity of numerical model (left) and ANN model (right) to water cut for *2.yrs* polymer injection model.

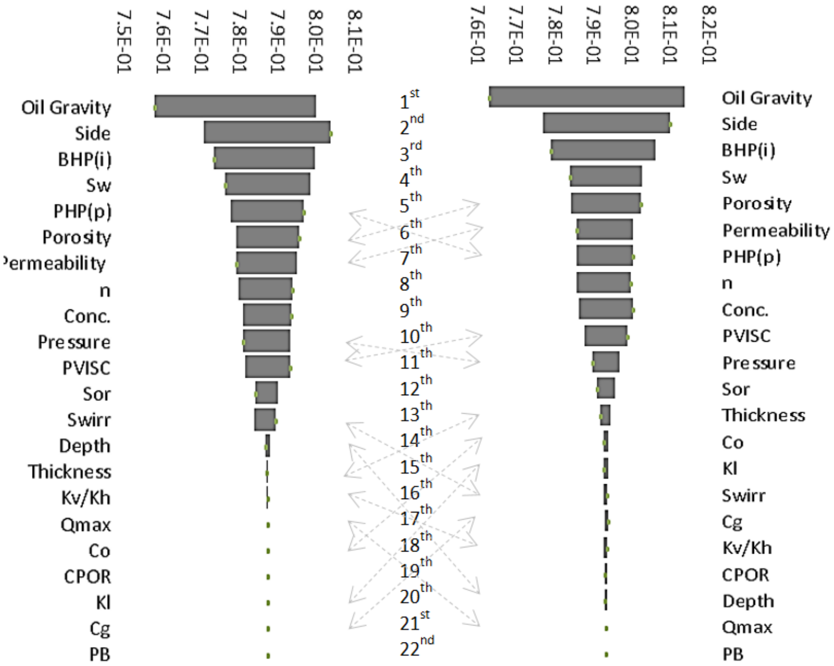

Figure 5.39. Parameter sensitivity of numerical model (left) and ANN model (right) to water cut for *4.yrs* polymer injection model.

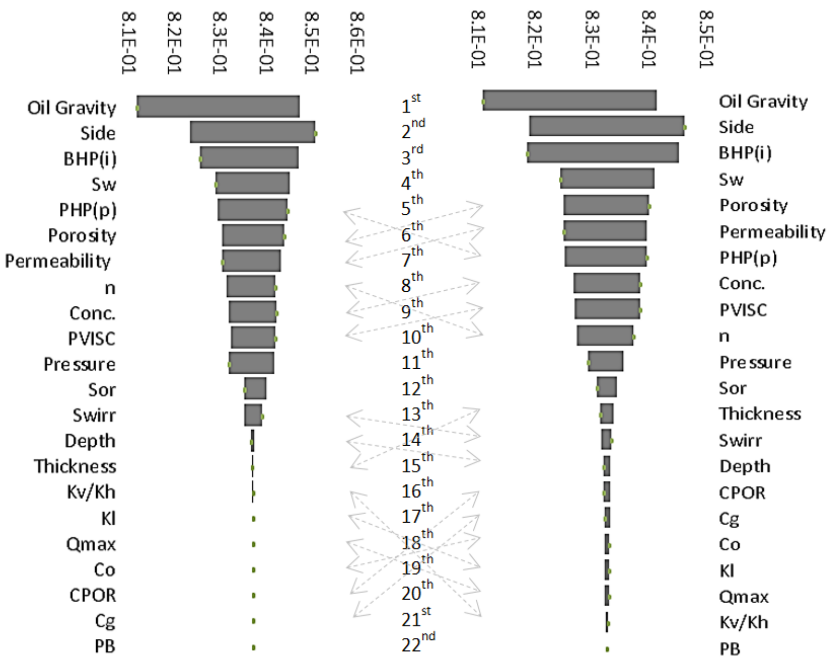

Figure 5.40. Parameter sensitivity of numerical model (left) and ANN model (right) to water cut for *6.yrs* polymer injection model.

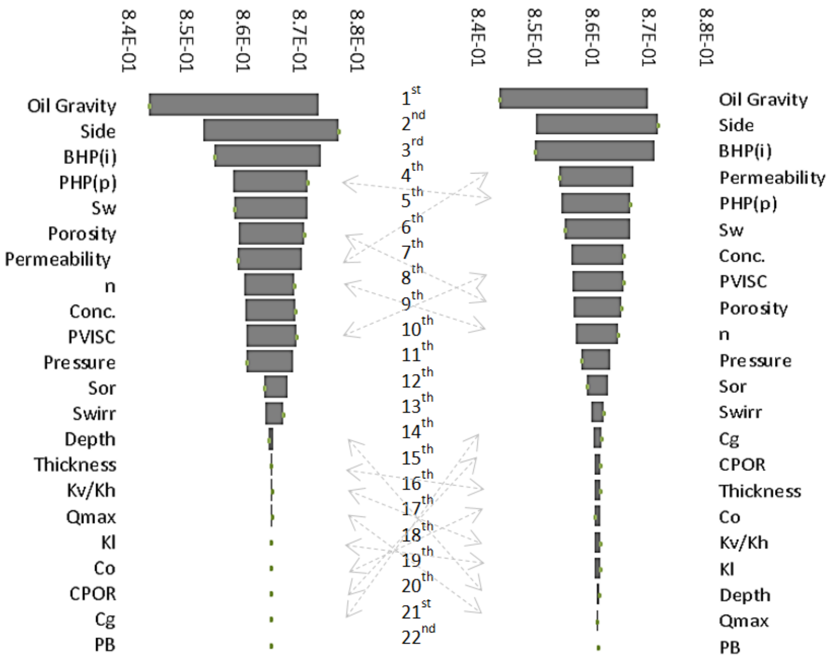

Figure 5.41. Parameter sensitivity of numerical model (left) and ANN model (right) to water cut for *8.yrs* polymer injection model.

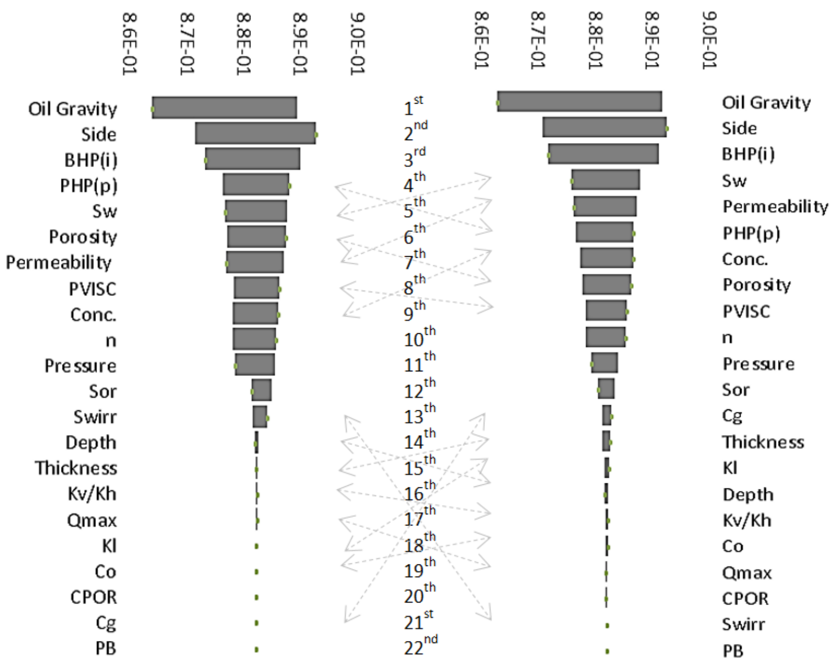

Figure 5.42. Parameter sensitivity of numerical model (left) and ANN model (right) to water cut for *10.yrs* polymer injection.

5.2.3 Real Field Implementation of Polymer Flooding Screening Tool

In this part of the study, two powerful implementation of data-driven screening model are presented. The primary objective of this implementations are to provide the robust evidence on how the data driven models can overcome the weaknesses of the numerical simulators. In order to examine the built data-driven polymer injection screening model, a real field data in which the polymer flooding is successfully implemented is used.

Daqing oil field as one of the largest oil reservoir is discovered in 1959 (Chauveteau et al., 1988). Laboratory studies to investigate the potential EOR method is initiated in 1960s and the polymer flooding is chosen to improve the sweep efficiency and mobility control (Wang et al., 2008). Today, the largest polymer flooding application is applied to Daqing oil field. Remarkably, by 2004, the polymer flooding contributed to 22.7% of the total oil production, enhancing the ultimate recovery of the field to more than 50% OOIP and producing 10% OOIP more than water flooding practice. To create a representative reservoir model for Daqing field using the data driven model, a 19 reservoir parameters are required. As a single detailed research describing the Daqing field not found, the reservoir rock and fluid properties are assembled from various published studies (Sheng et al., 2011;Wang et al., 2008; Wankui et al., 2000; Jingcun et al., 1995; Corlay et al., 1992; Chauveteau et al., 1988). In Table 5.6, the reservoir properties assigned for the model to represent the Daqing field is presented as "Implementation I". "Implementation I" is the uncertainty range defined for the second implementation. It should be mentioned the some parameters controlling the polymer adsorption, relative permeabilities and capillary pressures cannot be founded in literature, therefore, values are assigned in way that it can result in high efficient polymer flooding process.

Table 5.6. Daqing oil field reservoir properties.

Parameters	**Implementation I**	**Implementation II**
Well Spacing, *ft*	736	[663, 810]*
Layer Thickness, *ft*	10, 11, 12, 13, 14	[9 , 15]
Reservoir Depth (D), *ft*	4300	[3870 , 4730]
Permeability Anisotropy Ratio (k_V/k_H)	0.7	[0.63 , 0.77]
Average Porosity (ϕ)	0.27	[0.225 , 0.33]
Average Permeability (k), *mD*	342	[90 , 658]
Pore Compressibility (CPOR), psi^{-1}	$6.5 \, x \, 10^{-6}$	[$5.85 \, x \, 10^{-6}$, $7.15 \, x \, 10^{-6}$]
Oil Gravity (γ_o), *°API*	30	22.5, 30, 37.5
Bubble Point Pressure (P_b), *psi*	1300	[P , 1595]
Reservoir Pressure (P), *psi*	1450	[1305 , 1595]
Adsorption Coefficient (b)	10	[9 , 11]
Maximum Polymer Adsorption (a_{max})	0.15	[0.135 , 0.165]
Reference Polymer Solution Viscosity, *cp*	5	[4 , 5]
Irreducible Water Saturation (S_{wirr})	0.2	[0.18 , 0.22]
Residual Oil Saturation (S_{or})	0.3	[0.27 , 0.33]
Relative Permeability Coefficient (n)	4	[3.5 , 4]
Oil Capillary Pressure Coefficient (C_o)	2.25	[2.025 , 2.475]
Gas Capillary Pressure Coefficient (C_g)	0.2	[0.18 , 0.22]
Water Saturation (S_w)	0.2	[S_{wirr} , 0.22]
Polymer Concentration (C_p), $lb.STB^{-1}$	[0.05 , 1]	0.5
Injector Bottom Hole Pressure ($P_{bhp\ (inj.)}$), *psi*	[P+1,500 , P+3,000]	3200
Producer Bottom Hole Pressure ($P_{bhp\ (prod.)}$), *psi*	[0.05P , 0.95P]	1600

* [minimum , maximum] range of random values

First implementation objective is to optimize the performance of the polymer flooding process by selecting of proper values for the operational parameters, namely polymer concentration, injector and the producer bottom hole pressure. 10,000 production scenarios are generated for the modeled Daqing oil field, using different combination of the operational parameters which are changing within specified ranges. Assuming that the operational parameters are the uncertainty of the Daqing field's production scenarios, the Monte Carlo simulation is used to indicate the probability of the polymer efficiency. Figure 5.43 shows the probability of the water cut amount for two to ten years of injection. In Figure 5.44 and Figure 5.45 the efficiency and the economic efficiency probability of the production scenarios are presented. The economic efficiency probability is considering the uncertainty of the oil and polymer price of 20 to 100 $/bbl and 1 to 3 $/kg, respectively. The proved, probable and possible probability of the water cut, efficiency and economic efficiency values are summarized in Table 5.7.

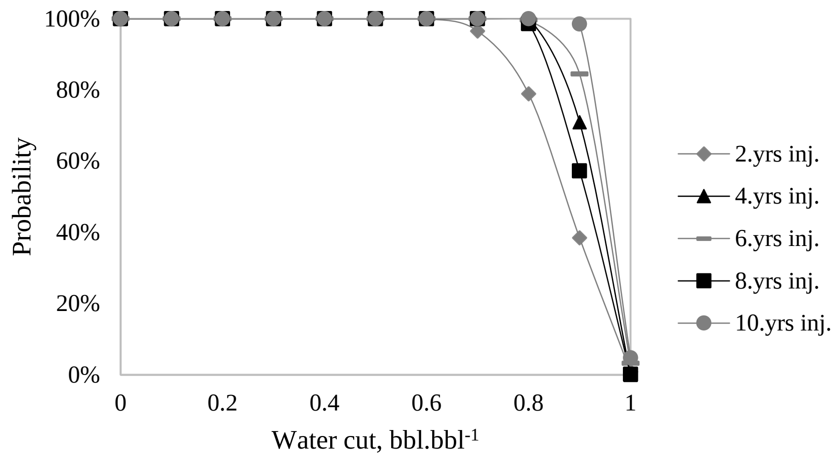

Figure 5.43. Implementation I water cut probability.

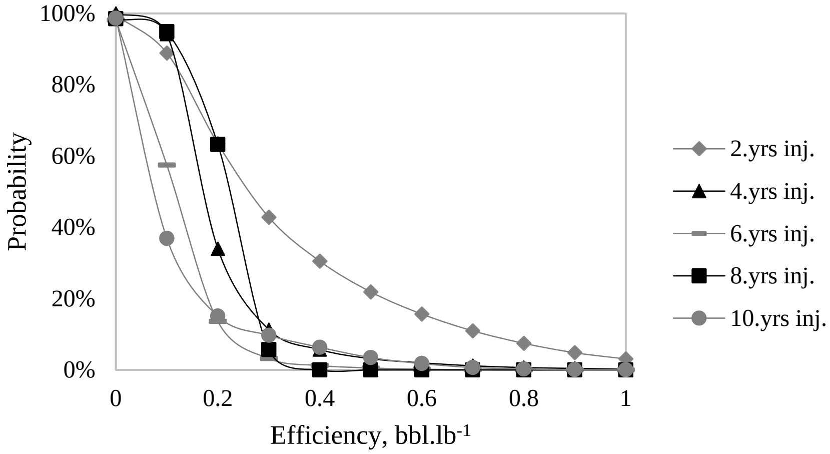

Figure 5.44. Implementation I efficiency value probability.

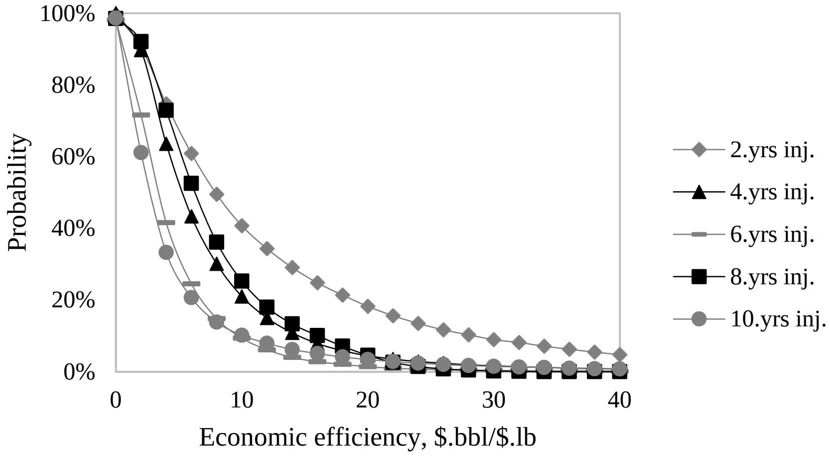

Figure 5.45. Implementation I economic efficiency value probability.

Table 5.7. Proved, probable, possible probability of Implementation I.

Injection Duration	Water cut, bbl.bbl^{-1}			Efficiency, bbl.lb^{-1}			Efficiency$_{eco}$, \$.bbl/\$.lb		
	90%	50%	10%	90%	50%	10%	90%	50%	10%
2 years	0.75	0.87	0.98	0.10	0.26	0.72	2	8	28
4 years	0.85	0.94	0.99	0.11	0.17	0.30	2	5.5	14
6 years	0.88	0.95	0.99	0.03	0.12	0.22	0.6	3.5	10
8 years	0.83	0.92	0.99	0.13	0.22	0.29	2	6.5	16
10 years	0.92	0.96	0.99	0.02	0.07	0.30	0.5	0.28	10

Second implementation is aiming for predicting the performance of polymer flooding process when there are uncertainties in the reservoir properties. Similar to the procedure followed in the first implementation, 10,000 scenarios are generated. However, this time the operational parameters are kept constant and the reservoir parameters are randomly selected around the base values used in the previous implementation. Figure 5.46, Figure 5.47 and Figure 5.48 provides the probability of the water cut, efficiency and the economic efficiency value for five different injection duration from two to ten years. The proved, probable and possible probability resulted from the graphs are shown in Table 5.8.

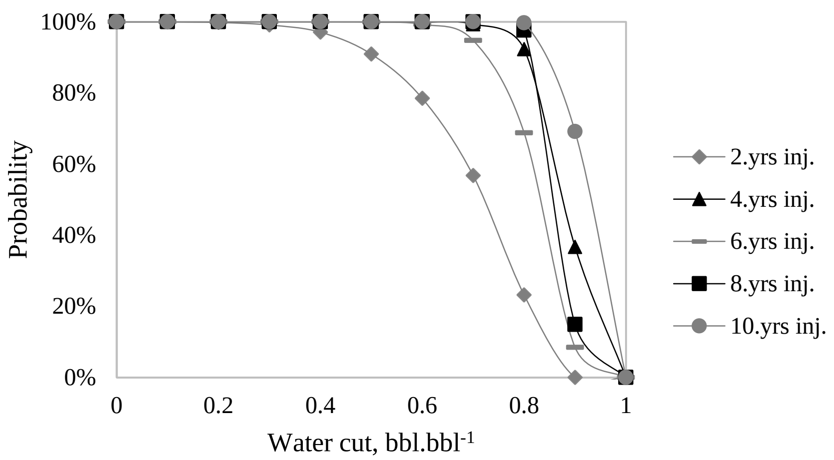

Figure 5.46. Implementation II water cut probability.

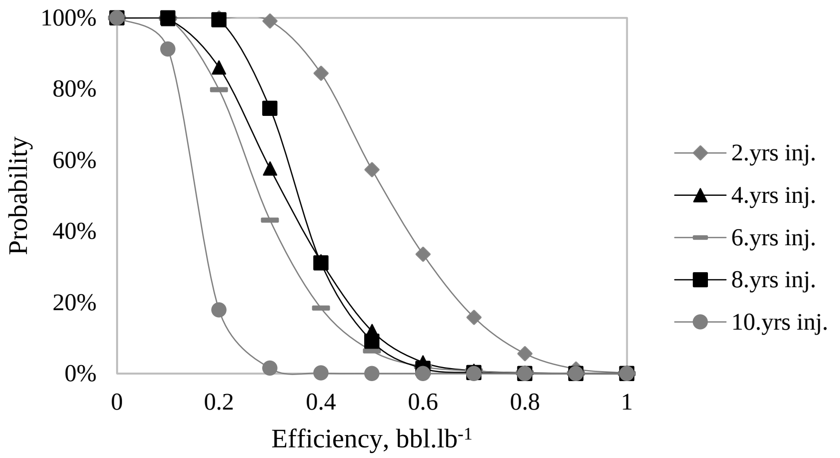

Figure 5.47. Implementation II efficiency value probability.

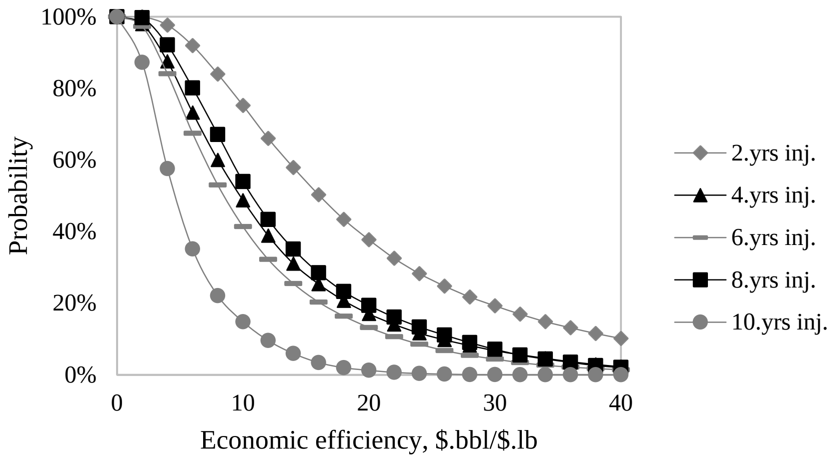

Figure 5.48. Implementation II economic efficiency value probability.

Table 5.8. Proved, probable, possible probability of Implementation II.

Injection Duration	Water cut, bbl.bbl^{-1}			Efficiency, bbl.lb^{-1}			Efficiency$_{eco}$, \$.bbl/\$.lb		
	90%	50%	10%	90%	50%	10%	90%	50%	10%
2 years	0.50	0.72	0.85	0.37	0.53	0.75	6.5	16	40
4 years	0.81	0.88	0.97	0.18	0.33	0.52	3.5	10	24
6 years	0.73	0.83	0.89	0.16	0.28	0.46	3.2	8.5	22
8 years	0.82	0.86	0.92	0.25	0.36	0.49	4.5	11	26
10 years	0.84	0.93	0.98	0.10	0.16	0.23	1.8	4.5	12

The obtained results from two implementations suggest that the simulated Daqing oil field with all uncertainties define for the reservoir properties, operational parameter and the polymer/oil prices, the field is strongly suitable for the polymer injection practice. The acceptable water cuts and the economic efficiencies of above one for most of the proved probabilities are the indication of this conclusion. It should be emphasized that aforementioned implementations of the data-driven polymer flooding screening model can predict these performances in fraction of seconds which is extremely time demanding if numerical models are to be used alone.

5.3 Graphical User Interface for Polymer Flooding Screening Tool

This part of the chapter is aiming for introducing the graphical user interface (GUI) for the polymer flooding screening tool built in this study. The transition from text-base environment to a user-friendly environment has a significant importance in terms of accessibility and usability of a tool for the end user. For the polymer flooding screening tool, the end users are the petroleum or more specifically reservoir engineers, who are not particularly specialized to use a text-base environment such as a neural network. Hence, to make the implementations of this screening tool straightforwardly usable, a GUI is built using Matlab tool box (Matlab, 2013).

The developed GUI can predict the performance of the polymer flooding application for both deterministic and probabilistic scenarios. Deterministic model can be used once no uncertainty exist in the reservoir and operational parameter. The main panel of the deterministic model is shown in Figure 5.49. A total of 25 inputs including the reservoir properties, operational parameters, oil and polymer price are to be defined for the model within a range specified beside each of the input cells. The outputs provided by the model are the efficiency, water cut and the economic efficiency which is the function of polymer and oil price defined for the time being. Once the input data are defined, “Run” button displays the output of the polymer flooding for the reservoir under appraisal. To indicate economic feasibility of the process for the defined reservoir, the economic efficiencies are indicate by green and red color representing feasible and unfeasible process, respectively. In order to ease the inputting data task, an “Import Excel” button can be selected by the user to transport the data into input cells of the panel. “Process” button is provided in case user prefer to manually input or if the Lorenz value is not known. This button calculates the Lorenz value, total thickness, thickness weighted porosity and permeability of the reservoir for the porosity, permeability and the thickness defined for each of the individual layer.

The probabilistic approach can be utilized if an uncertainty is exiting for any of the input parameters. A total of 50 input cells are generated for the probabilistic panel accounting for uncertainty range of each parameter within a minimum and maximum range according to the suggested intervals. The manually inputting the thickness, porosity and permeability of the layers in the probabilistic panel has two buttons of "Process Minimums" and "Process Maximums". The "Import excel" and the "Run" buttons are working similar to deterministic model panel. In the outputs, the proved (P 90%), probable (P 50%) and possible (P 10%) probabilities are appeared as outputs for efficiency, water cut and economic efficiency for different injection periods. In addition, probability distributions of the economic efficiency and the water cut can be appeared by selection of the "2 years" to "10 years" buttons to graphically observe the probability percentages.

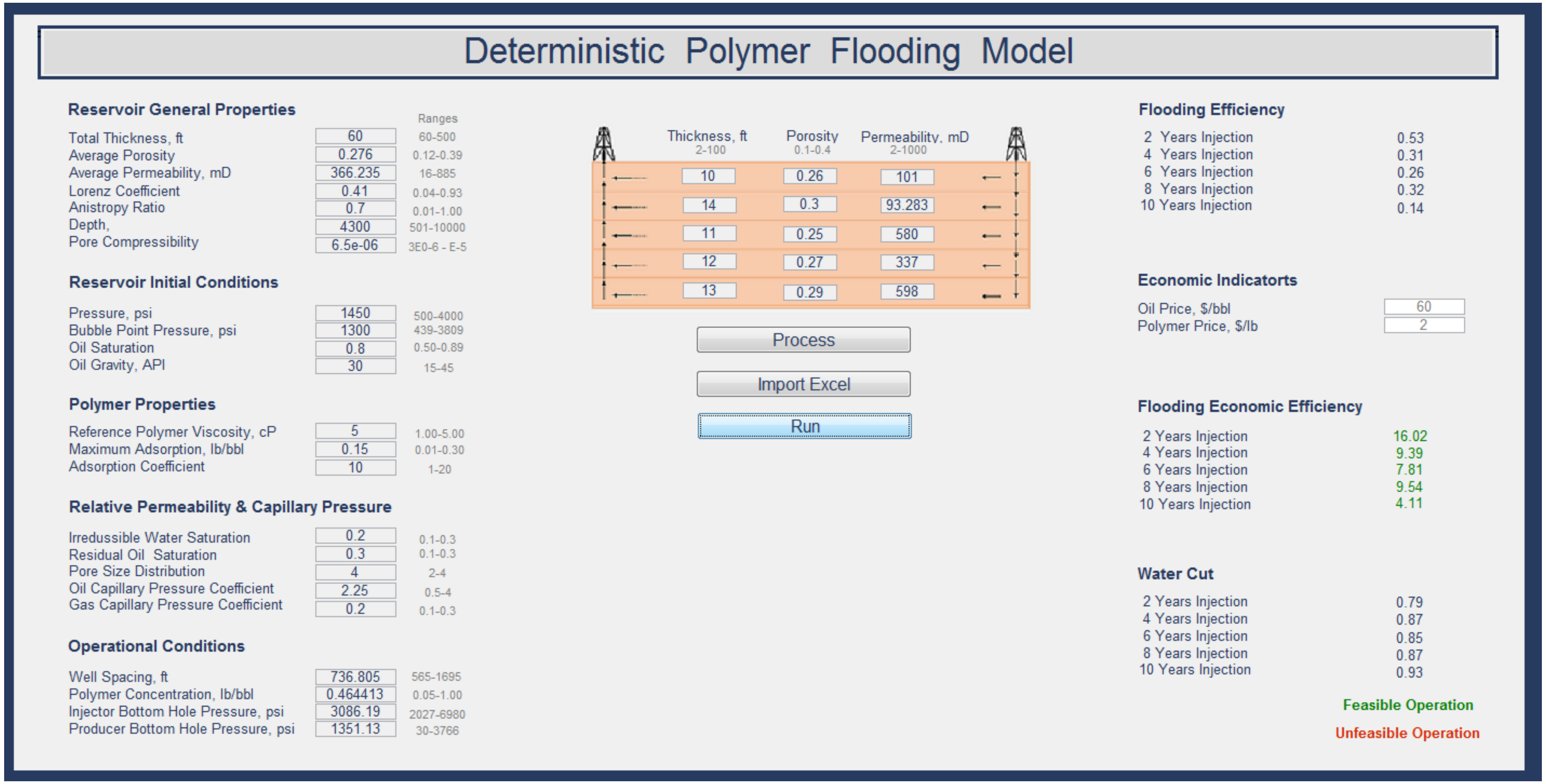

Figure 5.49. GUI for deterministic polymer flooding approach.

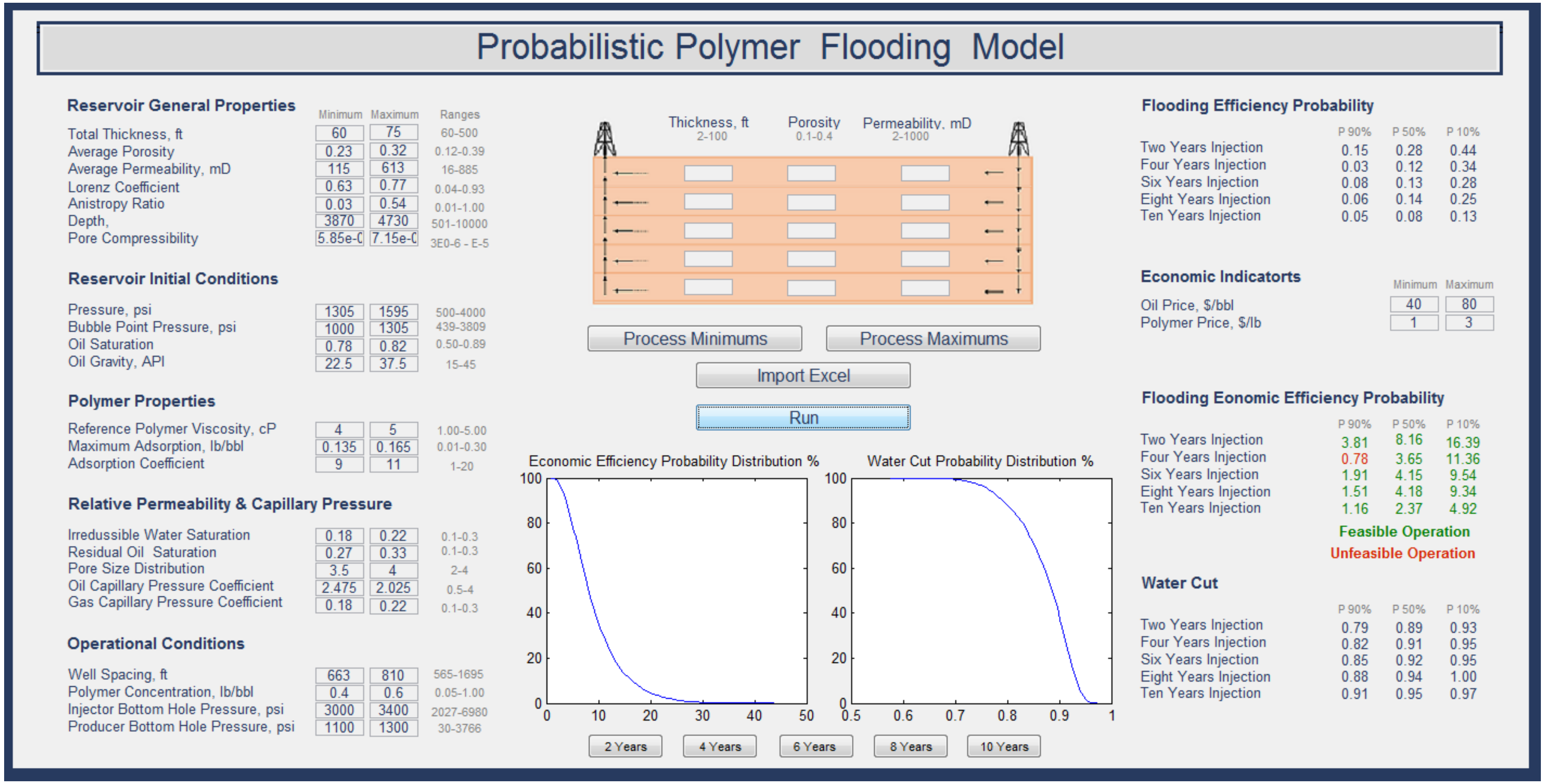

Figure 5.50. GUI for probabilistic polymer flooding approach.

CHAPTER 6

CONCLUSIONS

Although polymer flooding is the most abundantly implemented method among the chemical enhanced oil recovery techniques, it should be kept in mind that the chemical recovery methods are contributing to insignificant enhanced recoveries in comparison with other EOR methods. Low intention toward selection of polymer flooding is due to the fact that economic condition is a limiting factor for the use of high concentration or large bank of polymer. Consequently, the actual sweeping potential of polymer flooding is not observed and low additional oil production and small alteration in water cut amount are achieved comparing with response of water-only flooding projects. Two main objectives are accomplished in this research practice: First, it is aimed to have a better understanding of the polymer injection process and analyzing the effect of the different reservoir characteristics and operational conditions on the performance of the flooding operation. Second, a data-driven screening tool is developed to predict the performance of the polymer flooding operation in a time efficient manner in comparison with computational time of reservoir simulators. In the following part some of the properties and features of the used reservoir model and developed screening tool with their specific conclusions are discussed.

Polymer flooding reservoir model is generated in CMG black oil simulator for a multilayer heterogeneous system. A total of 10,000 injection/production scenarios are generated with combination of 34 reservoir and operational parameters, all uniformly (except for permeability) distributed within acceptable ranges decided upon available sources in literature. The sensitivity of the flooding process to different parameters [a] and the best performance cases [b] (high efficiency and low water cut) are investigated. Two set of conclusions can be expressed for this section of the study:

a) Sensitivity: The efficiency and water cut sensitivity to the parameters for two years injection is similar to sensitivities of longer injection durations, however, the orders of influences are slightly varying.

Five top most effecting parameters for the two outputs of the process (efficiency and water cut) are: initial water/oil saturation, oil gravity, well spacing and bottom hole pressures. The most influencing one for two years injection is initial water/oil saturation and for the longer injection periods is the oil gravity.

b) Best performance cases: In general, the behavior of the successful polymer scenarios which contribute to high efficiencies and low water cuts are suggesting for:

- High porosity
- High oil saturation
- High polymer viscosity
- High well spacing
- Well sorted pore size distribution
- Low permeability
- Low Lorenz coefficient (low heterogeneity)
- Low reservoir pressure
- Low bubble point pressure
- Low irreducible water saturation
- Low oil gravity
- Low residual oil saturation
- Low polymer concentration
- Low bottom hole pressure at injector well

High well spacing and low permeability are preferred by the polymer injection process as in the efficiency value defined in this study, the amount of water cut is taken into consideration. Hence, this outcome suggest that low well spacing and high permeability cause high water production.

Successes of low oil gravity scenarios indicates that, the light oils can effectively be produced without polymer injection. This is due to the efficiency value which accounts for incremental oil that can be produced by polymer injection in addition to no injection scenario.

Polymer flooding screening tool is developed using artificial neural networks. To enhance the performance of the tool, five models are generated representing two to ten years of flooding periods. Individual optimization based on the efficiency value for each model resulted in different network structures. The performance results [c], strengths [d] and limitations [e] of the tool can be listed as the following:

c) Performance results: Efficiency and water cut sensitivity to reservoir and operational parameters resulted from neural network models are in a good agreement with the simulator sensitivity output.

Efficiency and water cut are predicted by regression of more than 0.91 and 0.96, respectively.

Efficiency and water cut are predicted with less than ±0.06 bbl/lb and ±0.02 bbl/bbl errors, respectively.

d) Strengths: The numerical model errors and uncertainties are directly transported to the screening tool as the neural networks are trained with the outputs of the simulator.

The screening tool is capable of predicting polymer flooding performance only if the parameters are defined within the range they were trained for.

e) Limitations: Among a total of 10,000 cases run in the simulator, 6400 cases are converged. However, this screening tool is able to give outputs as it learned the flow dynamics of the polymer flooding process.

Probabilistic and deterministic performance estimation of the polymer flooding can be achieved within fraction of seconds.

CHAPTER 7

RECOMMENDATIONS FOR FUTURE WORK

This section of the thesis presents several recommendations that can be thought out if a further improvement is intended for the current study. As one of the main recommendations, in addition to comparing the polymer flooding operation with no injection scenario, comparison to water-only flooding can be considered. This comparison can strengthen the work by providing the amount of additional recovery that can be achieved if polymer flooding is used instead of water-only flooding operation. Moreover, the evaluation of model sensitivity analysis to different reservoir and operational parameters suggests that the parameters which do not significantly affect the flooding process can be eliminated. On the other hand, initial conditions of the reservoir can be improved in order to simulate the reservoir at saturated conditions. In addition, the polymer flooding model can be analyzed with different grid orientations, in order to consider the best orientation representing real polymer flow in the porous media from injector to producer well. Regarding the economic aspects of the polymer flooding operation, a more detailed economic parameter consideration can be supplemented. This consideration may include capital investments, operational and etc. costs of the polymer flooding. Lastly, the practicability of the developed GUI for polymer flooding can be improved by adding an operational optimization routine. This can be used for both deterministic and probabilistic approaches of model.

REFERENCES

Abidin, A., Puspasari, T., & Nugroho, W. (2012). Polymers for Enhanced Oil Recovery Technology. Procedia Chemistry, 4, 11-16. doi:10.1016/j.proche.2012.06.002

Abou-Kassem, J. H., Mattar, L., & Dranchuk, P. M. (1990, September 1). Computer Calculations of Compressibility of Natural Gas. Petroleum Society of Canada. doi:10.2118/90-05-10

Ahmed, T. H. (2010). Reservoir engineering handbook. Oxford: Gulf Professional.

Alghazal, M. (2015). Development and testing of artificial neural network based models for water flooding and polymer gel flooding in naturally fractured reservoirs. Master Thesis, The Pennsylvania State University.

Ali, J. K. (1994, January 1). Neural Networks: A New Tool for the Petroleum Industry? Society of Petroleum Engineers. doi:10.2118/27561-MS

Aniemena, C., (2013, April 22). Retrieved August 03, 2017, from https://www.mathworks.com/matlabcentral/fileexchange/37396-dak-equation-of-state?focused=3783933&tab=function

Artun, E. (2008). Optimized design of cyclic pressure pulsing in naturally fractured reservoirs using neural-network based proxy models. PhD Thesis, the Pennsylvania State University.

Artun, E. (2016). Characterizing interwell connectivity in waterflooded reservoirs using data-driven and reduced-physics models: a comparative study. Neural Computing and Applications, 28(7), 1729-1743. doi:10.1007/s00521-015-2152-0

Carcoana, A. (1992). Applied enhanced oil recovery. Englewood Cliffs: Prentice-Hall.

Center of Petroleum and geosystems Engineering. UTCHEM [Computer software]. Retrieved January 2, 2018, from http://www.cpge.utexas.edu/?q=iap_rsjip_simulators

Chang, H. (1978). Polymer Flooding Technology Yesterday, Today, and Tomorrow. Journal of Petroleum Technology, 30(08), 1113-1128. doi:10.2118/7043-pa

Chauveteau, G., Combe, J., & Dong, H. (1988, January 1). Preparation of Two Polymer Pilot Tests in Daqing Oil Field. Society of Petroleum Engineers. doi:10.2118/17632-MS

Computer Modeling Group Ltd. (2015). User's Guide IMEX: Three-Phase, Black Oil Reservoir Simulator. Calgary: Computer Mod.

Computer Modeling Group LTD. 2015. IMEX – Three-Phase, Black Oil Reservoir Simulator. http://www.cmgl.ca/software/imex2014 (accessed 15 November 2015)

Corey, A. T. (1954). The interrelation between gas and oil relative permeabilities. Producers Monthly. p. 38-41

Corlay, P., Lemouzy, P., Eschard, R., & Zhang, L. R. (1992, January 1). Fully Integrated Reservoir Study and Numerical Forecast Simulations of Two-Polymer Pilots in Daqing Field. Society of Petroleum Engineers. doi:10.2118/22364-MS

Dawson, R., & Lantz, R. B. (1972). Inaccessible Pore Volume in Polymer Flooding. Society of Petroleum Engineers Journal, 12(05), 448-452. doi:10.2118/3522-pa

Delamaide, E., Zaitoun, A., Renard, G., & Tabary, R. (2013). Pelican Lake Field: First Successful Application of Polymer Flooding in a Heavy Oil Reservoir. SPE Enhanced Oil Recovery Conference. doi:10.2118/165234-ms

Denney, D. (2009). Effect of Elasticity on Displacement Efficiency: High-Concentration-Polymer Flooding. Journal of Petroleum Technology, 61(01), 50-51. doi:10.2118/0109-0050-jpt

Donaldson, E. C., Chilingarian, G. V., & Yen, T. F. (1989). Enhanced oil recovery. Amsterdam: Elsevier.

Fausett, L. V. (2004). Fundamentals of neural networks: architectures, algorithms, and applications. Delhi, India: Pearson Education.

Gao, C.H. (2011). Scientific Research and Field Application of Polymer Flooding in Heavy Oil Recovery. Journal of Petroleum Exploration and Production Technology. 1:65. doi:10.1007/s13202-011-0014-6

Guo, W., Cheng, J., Yao, Y., Li, C., Li, W., Li, Q., … Wu, J. (2000, January 1). Commercial Pilot Test of Polymer Flooding in Daqing Oil field. Society of Petroleum Engineers. doi:10.2118/59275-MS

Hagan, M. T., Demuth, H. B., Beale, M. H., & Jesús, O. D. (2016). Neural network design. S. l.: S. n.

Hebb, D. O. (1949). The Organization of Behavior. New York: Wiley

Jewett, R., & Schurz, G. (1970). Polymer Flooding-A Current Appraisal. Journal of Petroleum Technology, 22(06), 675-684. doi:10.2118/2545-pa

Karambeigi, M., Zabihi, R., & Hekmat, Z. (2011). Neuro-simulation modeling of chemical flooding. Journal of Petroleum Science and Engineering, 78(2), 208-219. doi:10.1016/j.petrol.2011.07.012

Lee, A. L., Gonzalez, M. H., & Eakin, B. E. (1966, August 1). The Viscosity of Natural Gases. Society of Petroleum Engineers. doi:10.2118/1340-PA

Mabkhout M. Al-Dousari, Ali A. Garrouch, An artificial neural network model for predicting the recovery performance of surfactant polymer floods, Journal of Petroleum Science and Engineering, Volume 109, 2013, Pages 51-62, ISSN 0920-4105,

Manrique, E., Muci, V., & Gurfinkel, M. (2006). EOR Field Experiences in Carbonate Reservoirs in the United States. Proceedings of SPE/DOE Symposium on Improved Oil Recovery. doi:10.2523/100063-ms

Matlab Neural Network Toolbox (Version 8.1.0.604) [Computer software]. (2013). MathWorks, Inc.

Matlab R2013a (Version 8.1.0.604) [Computer software]. (2013). MathWorks, Inc.

McCulloch, W., & Pitts, W. (1943). A logical calculus of the ideas immanent in nervous activity. Bulletin of Mathematical Biophysics. Vol. 5, pp. 115–133

Mohaghegh, S. (2000, September 1). Virtual-Intelligence Applications in Petroleum Engineering: Part 1—Artificial Neural Networks. Society of Petroleum Engineers. doi:10.2118/58046-JPT

Mohaghegh, S. D. (2017). Shale Analytics. doi:10.1007/978-3-319-48753-3

Morel, D. C., Vert, M., Jouenne, S., Gauchet, R., & Bouger, Y. (2012, April 1). First Polymer Injection in Deep Offshore Field Angola: Recent Advances in the Dalia/Camelia Field Case. Society of Petroleum Engineers. doi:10.2118/135735-PA

Mungan, N. (1969). Rheology and Adsorption of Aqueous Polymer Solutions. Journal of Canadian Petroleum Technology, 8(02), 45-50. doi:10.2118/69-02-01

MWV. (n.d.). Average annual OPEC crude oil price from 1960 to 2017 (in U.S. dollars per barrel). In Statista - The Statistics Portal. Retrieved July 15, 2017, from https://www.statista.com/statistics/262858/change-in-opec-crude-oil-prices-since-1960/.

Needham, R. B., & Doe, P. H. (1987). Polymer Flooding Review. Journal of Petroleum Technology, 39(12), 1503-1507. doi:10.2118/17140-pa

Neuroshel (1998). Neuroshell 2 Tutorial. Ward Systems, Inc., Frederick, Maryland.

Oloo, E., & Chon, B. H. (2017). Prediction of Polymer Flooding Performance with an Artificial Neural Network: A Two-Polymer-Slug Case. Energies 10, no. 7: 844.

Örs, O. (2017). Candidate Selection Process for Polymer Gel Application by Using Artificial Neural Networks (Unpublished master's thesis). Middle East Technical University, Turkey.

Polymer Flooding Predictive Model (PFPM) (Version 1986) [Computer software]. (1986). Oklahoma: Department of Energy - United States of America.

Pye, D. J. (1964). Improved Secondary Recovery by Control of Water Mobility. Journal of Petroleum Technology, 16(08), 911-916. doi:10.2118/845-pa

Rosenblatt, F. (1958). The perceptron: A probabilistic model for information storage and organization in the brain. Psychological Review, 65(6), 386-408. doi:10.1037/h0042519

Saleh, L. D., Wei, M., & Bai, B. (2014, February 1). Data Analysis and Updated Screening Criteria for Polymer Flooding Based on Oilfield Data. Society of Petroleum Engineers. doi:10.2118/168220-PA

Sandiford, B. (1964). Laboratory and Field Studies of Water Floods Using Polymer Solutions to Increase Oil Recoveries. Journal of Petroleum Technology, 16(08), 917-922. doi:10.2118/844-pa

Schneider, F., & Owens, W. (1982). Steady-State Measurements of Relative Permeability for Polymer/Oil Systems. Society of Petroleum Engineers Journal, 22(01), 79-86. doi:10.2118/9408-pa

Seright, R. (2010, August 1). Potential for Polymer Flooding Reservoirs with Viscous Oils. Society of Petroleum Engineers. doi:10.2118/129899-PA

Sharqawy, M. H., V, J. H., & Zubair, S. M. (2012). Erratum to Thermophysical properties of seawater: A review of existing correlations and data [Desalination and Water Treatment, Volume 16 (2010) 354–380]. Desalination and Water Treatment, 44(1-3), 361-361. doi:10.1080/19443994.2012.691709

Sheng, J. J. (2011). Polymer Flooding. Modern Chemical Enhanced Oil Recovery, 101-206. doi:10.1016/b978-1-85617-745-0.00005-x

Sheng, J. J., Leonhardt, B., & Azri, N. (2015, March 1). Status of Polymer-Flooding Technology. Society of Petroleum Engineers. doi:10.2118/174541-PA

Sieberer, M., Jamek, K., & Clemens, T. (2017, April 1). Polymer-Flooding Economics, From Pilot to Field Implementation. Society of Petroleum Engineers. doi:10.2118/179603-PA

Sorbie, K. S. (1991). Polymer-Improved Oil Recovery. doi:10.1007/978-94-011-3044-8

Sun, Q., & Ertekin, T. (2017). Structuring an artificial intelligence based decision making tool for cyclic steam stimulation processes. Journal of Petroleum Science and Engineering, 154, 564-575. doi:10.1016/j.petrol.2016.10.042

Sutton, R. P. (1985, January 1). Compressibility Factors for High-Molecular-Weight Reservoir Gases. Society of Petroleum Engineers. doi:10.2118/14265-MS

Taber, J., Martin, F., & Seright, R. (1997). EOR Screening Criteria Revisited - Part 1: Introduction to Screening Criteria and Enhanced Recovery Field Projects. SPE Reservoir Engineering, 12(03), 189-198. doi:10.2118/35385-pa

Vazquez, M., & Beggs, H. D. (1980, June 1). Correlations for Fluid Physical Property Prediction. Society of Petroleum Engineers. doi:10.2118/6719-PA

Wang, D., Dong, H., Lv, C., Fu, X., & Nie, J. (2009). Review of Practical Experience by Polymer Flooding at Daqing. SPE Reservoir Evaluation & Engineering, 12(03), 470-476. doi:10.2118/114342-pa

Wang, D., Li, Q., Gong, X., & Wang, Y. (2000). The Engineering and Technical Aspects of Polymer Flooding in Daqing Oil Field. Proceedings of International Oil and Gas Conference and Exhibition in China. doi:10.2523/64722-ms

Wang, D., Liu, H., Niu, J., & Chen, F. (1998). Application Results and Understanding of Several Problems of Industrial Scale Polymer Flooding in Daqing Oil Field. Proceedings of SPE International Oil and Gas Conference and Exhibition in China. doi:10.2523/50928-ms

Wang, D., Zhang, J., Meng, F., Liu, H., Li, L., Han, B., & Qi, L. (1995, January 1). Commercial Test of Polymer Flooding in Daqing Oil Field Daqing petroleum Administrative Bureau. Society of Petroleum Engineers. doi:10.2118/29902-MS

Wassmuth, F. R., Green, K., Hodgins, L., & Turta, A. T. (2007, January 1). Polymer Flood Technology For Heavy Oil Recovery. Petroleum Society of Canada. doi:10.2118/2007-182

Widrow, B., & Hoff, M. E. (1960). Adaptive switching circuits. New York: IRE WESCON. Convention Record. IRE Part 4, pp. 96–104

Willhite, G. P. (1986). Waterflooding. Richardson, TX: Society of Petroleum Engineers.

Yang, F., Wang, D., Wu, W., Wu, J., Liu, W., Kan, C., & Chen, Q. (2006, January 1). A Pilot Test of High-Concentration Polymer Flooding to Further Enhance Oil Recovery. Society of Petroleum Engineers. doi:10.2118/99354-MS

APPENDIX A

CMG TEMPLATE FOR POLYMER FLOOD PROCESS

```
RESULTS SIMULATOR IMEX
******************  I/O Control Section  ******************
*TITLE1
"Polymer Test Problem"
*TITLE2
"3d Polymer Test Case in a 25x25x5 grid configuration."
*INUNIT *FIELD
*WPRN   *WELL 10
*WPRN   *GRID 10
*WPRN   *ITER    *ALL
*OUTPRN *WELL    *ALL
*OUTPRN *TABLES  *NONE
*OUTPRN *RES     *NONE
*OUTPRN *GRID    *EXCEPT  *OILPOT  *DATUMPRES
 *WSRF   *GRID    *TIME
 *OUTSRF *GRID    *EXCEPT  *OILPOT  *DATUMPRES
*************  Reservoir Description Section  *************
 *GRID *CART 25 25 5
 *DI *CON
 41.00
 *DJ *CON
 41.00
 *KDIR *DOWN
 *Dk *KVAR
  20.5   98.8   94.8   56.2   25.2
*DEPTH 1 1 1 5487.4
 *POR *KVAR
 0.356   0.280   0.192   0.237   0.209
 *PRPOR    14.7
 *CPOR     7.46e-06
 *PERMI *KVAR
      37.56   257.06   144.85    11.28   710.70
 *PERMJ *KVAR
      37.56   257.06   144.85    11.28   710.70
 *PERMK *KVAR
      36.87   252.34   142.19    11.07   697.66
**************  Component Property Section  ***************
 *MODEL *POLY
 *PVT
 **  p       rs      bo       eg      viso    visg
    14.7     1.1    1.020       4.998   87.343   0.011
   264.7    26.8    1.032       93.935   61.704   0.011
   514.7    55.5    1.045      190.899   45.027   0.012
   764.7    85.5    1.058      296.658   34.273   0.013
   1014.7   116.5    1.072      411.285   27.033   0.014
```

```
  1264.7   148.2    1.086      533.905   21.950   0.015
  1514.7   180.6    1.101      661.501   18.249   0.016
  1764.7   213.4    1.115      790.003   15.470   0.017
  2014.7   246.7    1.130      914.561   13.328   0.019
  2514.7   314.3    1.160      1138.194   10.283   0.023
  3014.7   383.3    1.191      1321.346   8.258   0.026
  3514.7   453.3    1.223      1467.746   6.835   0.029
  4014.7   524.3    1.254      1585.507   5.792   0.033
  4514.7   596.1    1.286      1682.314   5.001   0.035
  5014.7   668.7    1.319      1763.638   4.384   0.038
  5514.7   742.0    1.352      1833.133   3.892   0.040
  6014.7   815.9    1.385      1893.688   3.492   0.042
  6514.7   890.3    1.418      1947.328   3.161   0.045
  7014.7   965.3    1.452      1995.293   2.884   0.046
  7500.0   1038.6    1.484      2037.519   2.655   0.048
 *DENSITY *OIL    60.27
 *DENSITY *GAS    6.470000e-02
 *DENSITY *WATER  62.238000
 *CO     1.37e-05
 *CVO    4.60e-05
 *BWI    1.04
 *CW     3.04e-06
 *REFPW  14.7
 *VWI    0.31
 *CVW    0.00
 *PADSORP
 **  p_con        adsop_level
     0         0.00
     1.000000e-01        0.01
     2.000000e-01        0.01
     3.000000e-01        0.02
     4.000000e-01        0.02
     5.000000e-01        0.02
     6.000000e-01        0.03
     7.000000e-01        0.03
     8.000000e-01        0.03
     9.000000e-01        0.03
 *PMIX *LINEAR
 *PVISC     3.318047
 *PREFCONC  1.000000
 *PPERM
 **  perm   max_ad   res_ad   p_pore   rrf
    10.0   0.30      0.15    0.95     1.20
    1000.0 0.20      0.10    1.00     1.20
*************  Rock-fluid Property Component  *************
 *ROCKFLUID
 *RPT
 *SWT
** Sw     krw       krow      Pcow
 0.19 0.0000000 1.0000000 3.6836725
 0.25 0.0004559 0.7365446 2.9368518
 0.30 0.0042139 0.5252842 2.0766678
 0.36 0.0154752 0.3599820 1.6955921
 0.41 0.0389476 0.2345438 1.4684259
```

```
  0.46 0.0796890 0.1430334 1.3134000
  0.52 0.1430334 0.0796890 1.1989647
  0.57 0.2345438 0.0389476 1.1100256
  0.63 0.3599820 0.0154752 1.0383339
  0.68 0.5252842 0.0042139 0.9789506
  0.73 0.7365446 0.0004559 0.9287141
  0.79 1.0000000 0.0000000 0.8854941
*SLT
** Sl     krg       krog      Pcog
  0.19 1.0000000 0.0000000 1.0257886
  0.24 0.8129707 0.0001370 0.9035042
  0.29 0.6515433 0.0012665 0.6388739
  0.35 0.5136704 0.0046511 0.5216384
  0.40 0.3973348 0.0117057 0.4517521
  0.45 0.3005514 0.0239507 0.4040593
  0.50 0.2213695 0.0429889 0.3688540
  0.55 0.1578749 0.0704925 0.3414925
  0.60 0.1081931 0.1081931 0.3194370
  0.65 0.0704925 0.1578749 0.3011681
  0.70 0.0429889 0.2213695 0.2857131
  0.75 0.0239507 0.3005514 0.2724168
  0.80 0.0117057 0.3973348 0.2608192
  0.85 0.0046511 0.5136704 0.2505870
  0.90 0.0012665 0.6515433 0.2414716
  0.95 0.0001370 0.8129707 0.2332838
  1.00 0.0000000 1.0000000 0.2258760
***************  Initial Condition Section  ***************
 *INITIAL
 *USER_INPUT
 *PRES *CON 2350.6
 *PB   *CON 1915.7
 *SO   *CON     0.676
 *SW   *CON     0.324
***********  Numerical Methods Control Section  ***********
 *NUMERICAL
 *DTMAX  62
******************  Well Data Section  *******************
 *RUN
 *DATE  2017 03 13
 *AIMSET   *CON  1
 *DTWELL      1.0
 *WELL 1    "WATER INJECTOR"
 *WELL 2    "PRODUCER"
 *INJECTOR  *MOBWEIGHT  1
 *INCOMP  *WATER  4.66e-01
 *OPERATE   *MAX       *STW    100000
 *OPERATE   *MAX       *BHP    4846 *CONT
 **           rad    geofac  wfrac   skin
 *GEOMETRY  *K  0.25   1    1   0
 *PERF *GEO  1
 ** UBA      ff      Status      Connection
    1 1 1      1      OPEN     FLOW-FROM     "SURFACE"   REFLAYER
    1 1 2      1      OPEN     FLOW-FROM     1
    1 1 3      1      OPEN     FLOW-FROM     2
```

```
   1 1 4     1     OPEN    FLOW-FROM    3
   1 1 5     1     OPEN    FLOW-FROM    4
*PRODUCER  2
*OPERATE   *MAX      *STO    100000
*OPERATE   *MIN      *BHP    1793
**          rad    geofac  wfrac   skin
*GEOMETRY  *K  0.25   1    1   0
*PERF *GEO  2
** UBA      ff      Status      Connection
   25 25 1     1     OPEN    FLOW-FROM    "SURFACE"   REFLAYER
   25 25 2     1     OPEN    FLOW-FROM    1
   25 25 3     1     OPEN    FLOW-FROM    2
   25 25 4     1     OPEN    FLOW-FROM    3
   25 25 5     1     OPEN    FLOW-FROM    4
*TIME     3650
*DTWELL    5
*TIME 3650.1
*STOP
```

APPENDIX B

ANN MODEL FOR TWO YEARS POLYMER INJECTION

```
clc; clear all;
% Inporting the Input and Output Data
data_in = xlsread('NPV-Eff poly removed.xlsx', 'B4:AS6342'); %%7494conc btw 0.1 & 1
data_out1 = xlsread('NPV-Eff poly removed.xlsx', 'GM4:GM6342'); %% WOR
data_out2 = xlsread('NPV-Eff poly removed.xlsx', 'GH4:GH6342'); %% Np/Pi

P(1,:)=data_in(:,1)';                                        %Side
P(2,:)=data_in(:,7)';                                        %Depth
P(3,:)=data_in(:,14)';                                       %CPOR
P(4,:)=data_in(:,20)';                                       %Kv/Kh
P(5,:)=data_in(:,21)';                                       %Pres
P(6,:)=data_in(:,22)';                                       %BP
P(7,:)=data_in(:,23)';                                       %API
P(8,:)=data_in(:,25)';                                       %Kl
P(9,:)=data_in(:,26)';                                       %Qmax
P(10,:)=data_in(:,27)';                                      %Pvisc
P(11,:)=data_in(:,28)';                                      %Swirr
P(12,:)=data_in(:,29)';                                      %Sor
P(13,:)=data_in(:,30)';                                      %n
P(14,:)=data_in(:,31)';                                      %Co
P(15,:)=data_in(:,32)';                                      %Cg
P(16,:)=data_in(:,33)';                                      %Sw
P(17,:)=data_in(:,34)';                                      %Conc
P(18,:)=data_in(:,35)';                                      %BHP(i)
P(19,:)=data_in(:,36)';                                      %BHP(p)
P(20,:)=data_in(:,37)';                                      %avg. Premeability
P(21,:)=data_in(:,38)';                                      %Total thickness
P(22,:)=data_in(:,39)';                                      %avg. Porosity
P(23,:)=data_in(:,40)';                                      %Lorenz
% Functions %
P(24,:) = 8829.6 ./ (131.5 + P(7,:));                        %Oil Density
P(25,:) = 70 + P(2,:)./100 ;                                 %Temperature
P(26,:) = (P(1,:).^2).*P(21,:).*(1-P(16,:)).* P(22,:)./5.615; %OOIP
P(27,:) = P(17,:)./P(16,:);                                  %conc/Sw
P(28,:) = P(5,:)./P(18,:);                                    %Press/BHP(i)
P(29,:) = P(5,:)./P(19,:);                                    %Press/BHP(p)
P(30,:) = (P(1,:).^2).*P(21,:);                               %Reservoir Volume
P(31,:) = 1- P(16,:);                                         %So
P(32,:) = P(17,:)./P(18,:);                                   %conc/BHP(i)

T(1,:)=data_out1(:,1)';   % Water Cut
T(2,:)=data_out2(:,1)';   % Np/Pi

[NLin,NP] = size(P);     %size of input
[NLout,Nt] = size(T);    %size of output layer
```

```
% NORMALIZATION OF DATA
for i= 1:NLin
    Pminimum(i,:)= min(P(i,:));
    Pmaximum(i,:)= max(P(i,:));
    Pn(i,:)= (2*(P(i,:)-Pminimum(i,:))/(Pmaximum(i,:)-Pminimum(i,:))) - 1;
end

for i= 1:NLout
    Tminimum(i,:)= min(T(i,:));
    Tmaximum(i,:)= max(T(i,:));
    Tn(i,:)= (2*(T(i,:)-Tminimum(i,:))/(Tmaximum(i,:)-Tminimum(i,:))) - 1;
end

rand('state',0);
%BACKPROPAGATION ALGORITHM - CREATING THE NETWORK
net = fitnet([60 35]);
% SEPARATE TRAINING, TESTING AND VALIDATION
NP=NP;
ntrain=ceil(NP*0.70);
nval= floor((NP-ntrain)*0.5);
ntest= floor((NP-ntrain)*0.5);
% Division of data set for training, validation, testing
net.divideFcn = 'divideind';
net.divideParam.trainInd = 1:ntrain;
net.divideParam.valInd = ntrain+1:ntrain+nval;
net.divideParam.testInd = ntrain+nval+1:ntrain+nval+ntest;
% Adjustment of training parameters
net.trainParam.goal = 0.00001;         %Accuracy check
net.trainParam.epochs = 15000;         %# of iterations check
net.trainParam.show = 1;
net.trainParam.max_fail = 5;           %# of validation check
net.efficiency.memoryReduction = 2;    %Reduction of memory requirements
net.trainParam.showWindow = true;

% Network Training
[net,tr]=train(net,Pn,Tn);

% SIMULATION OF THE NETWORK WITH THE TRAINING DATA
for i=1:ntrain
    Pn_train(:,i) = Pn(:,i);
    Tn_train(:,i) = Tn(:,i); %nomalized
    T_train(:,i) = T(:,i);   %not Normalized
end
tn_train_ann = sim(net,Pn_train);
% SIMULATION OF THE NETWORK WITH THE VALIDATION DATA
for i=1:nval
    Pn_val(:,i) = Pn(:,i+ntrain);
    Tn_val(:,i) = Tn(:,i+ntrain);   %nomalized
    T_val(:,i) = T(:,i+ntrain);     %not Normalized
end
tn_val_ann = sim(net,Pn_val);
% PREDICTIONS-NEW DATA-SETS THE NETWORK HAS NOT SEEN BEFORE
for i=1:ntest
```

```
    Pn_test(:,i) = Pn(:,i+ntrain+nval);
    Tn_test(:,i) = Tn(:,i+ntrain+nval);
    T_test(:,i) = T(:,i+ntrain+nval);
end
tn_test_ann = sim(net, Pn_test);
% DENORMALIZATION OF THE SIMULATION
for i= 1:NLout
    t_train_ann(i,:)= (Tmaximum(i,:)-Tminimum(i,:)).*((tn_train_ann(i,:)+1)./2)+Tminimum(i,:);
end
for i= 1:NLout
    t_val_ann(i,:)=(Tmaximum(i,:)- (i,:)).*((tn_val_ann(i,:)+1)./2)+Tminimum(i,:);
end
for i= 1:NLout
    t_test_ann(i,:)=(Tmaximum(i,:)- (i,:)).*((tn_test_ann(i,:)+1)./2)+Tminimum(i,:);
end
Tn_ann = [tn_train_ann,tn_val_ann,tn_test_ann];
T_ann = [t_train_ann,t_val_ann,t_test_ann];
T=T(:,1:(nval+ntest+ntrain));
Tn=Tn(:,1:(nval+ntest+ntrain));
```